The Dissertation Committee for James Andrew Bynum Jr. Certifies that this is the approved version of the following dissertation:

A Systems Pharmacology Approach to Discovery of Drugs to Ameliorate Oxidant Stress in Human Endothelial Cells

Committee:

Salomon Stavchansky, Supervisor

Phillip D. Bowman

Sean M. Kerwin

Zhengrong Cui

Robert O. Williams III

A Systems Pharmacology Approach to Discovery of Drugs to Ameliorate Oxidant Stress in Human Endothelial Cells

by

James Andrew Bynum Jr., B.S.

Dissertation

Presented to the Faculty of the Graduate School of

The University of Texas at Austin

in Partial Fulfillment

of the Requirements

for the Degree of

Doctor of Philosophy

The University of Texas at Austin

May 2015

Dedication

I would like to dedicate this dissertation to my wife, Jamie, and our two boys, Chase and Colton, for all your support and encouragement through this time. Thank you with all of my heart,

Jim

Acknowledgements

I would like to thank and acknowledge my advising professor Dr. Salomon Stavchansky for his advice and guidance as a mentor. I am grateful to Dr. Phillip Bowman for his friendship and mentorship that has enabled me to grow as a scientist throughout the years. I would also like to thank the members of my dissertation committee, Dr. Robert O. Williams III, Dr. Sean Kerwin and Dr. Zhengrong Cui for their advice and review of this dissertation. In addition, I am grateful to College of Pharmacy staff members, Stephanie Crouch and Yolanda Camacho, for all their assistance in various matters throughout my graduate studies. I am thankful for the advice and friendship of Ashish Rastogi. Thanks to Adam Meledeo for support and advice throughout the years. Finally, I would like to thank my family for all their encouragement and love.

A Systems Pharmacology Approach to Discovery of Drugs to Ameliorate Oxidant Stress in Human Endothelial Cells

James Andrew Bynum Jr., Ph.D.

The University of Texas at Austin, 2015

Supervisor: Salomon Stavchansky

Ischemia is characterized by reduced blood flow to an area of the body which can then cause cellular injury through the generation of reactive oxygen species (ROS), activation of inflammation, and induction of apoptosis. Although rapid reestablishment of flow is required to prevent organ death, the reperfusion phase of this injury can cause its own deleterious effects often exacerbating the initial insult. The combined action of the two injuries is termed ischemia/reperfusion (I/R) injury. Oxidative stress that results from ischemia/reperfusion injury is a common pathological condition that accompanies many human diseases including stroke, heart attack and traumatic injury. In addition, neurodegenerative diseases including Parkinson's, Alzheimer's, and Huntington's disease appear to involve oxidative stress.

Although actively investigated by the medical and pharmaceutical industry; limited progress has been made to ameliorate I/R injury and to date there is no drug approved for treatment for I/R injury. Therapeutic approaches to treat I/R injury have

included the administration of compounds to scavenge ROS or induce protective pathways or genetic responses. It was previously reported that caffeic acid phenethyl ester (CAPE), a plant-derived polyphenol, displayed cytoprotective effects against menadione (MD)-induced oxidative stress in human umbilical vein endothelial cells (HUVEC), and the induction of heme oxygenase-1 (HMOX1), a phase II enzyme, played an important role for CAPE cytoprotection.

In an effort to improve this cytoprotection, other phase II enzyme inducers were investigated and, 2-cyano-3,12 dioxooleana-1,9 dien-28-imidazolide (CDDO-Im) and 2-cyano-3,12-dioxooleana-1,9-dien-28-oyl methyl ester (CDDO-Me), were found to be potent inducers with a rapid onset of action. CDDO-Im and CDDO-Me, synthetic olenane triterpenoids, developed as anticancer agents were compared to CAPE revealing that CDDO-Im was a more potent inducer of Phase II enzymes including HMOX1 and provided better cytoprotection than CAPE. Gene expression profiling showed that CDDO-Im was more potent inducer of protective genes like HMOX1 than CAPE and additionally induced heat shock proteins. To better understand the mechanism of action of CDDO-IM, a gene expression time-course was undertaken to identify early initiators of the transcriptional response preceding cytoprotection. Application of systems pharmacology identified molecular networks of cell mediating processes.

Table of Contents

List of Tables

List of Figures

STATEMENT OF OBJECTIVES AND SIGNIFICANCE OF RESEARCH

This dissertation is the result of efforts directed towards drug discovery to ameliorate the oxidative stress that accompanies ischemia/reperfusion (I/R) injury. Derivatives of CDDO were chosen as they are potent and rapid phase II enzyme inducers. It was established that they are potent cytoprotective agents and the mechanisms of action was investigated by a systems biology and network analysis approach to better understand the mechanism of cytoprotection and form a basis for further reduction in the sequelae of oxidative stress.

The following objectives were followed during the course of this research project:

1. Establish an *in vitro* cytoprotection assay of CDDO derivatives against oxidative stress-induced injury in human umbilical endothelial cells that simulates I/R injury;

2. Compare cytoprotection and gene expression profiles between CAPE and CDDO-Im;

3. Evaluate the role of HMOX1 induction in cytoprotection provided by CDDO derivatives;

4. Compare structure activity relationships from a cytoprotection and gene expression approach between CDDO-Me and CDDO-Im;

5. Investigate transcriptional kinetics of CDDO-Im by utilizing time course gene expression;
6. Integrate a systems pharmacology approach combined with gene expression and network analysis to investigate the mechanisms of action in a drug discovery model using CDDO-Im;
7. Integrate systems pharmacology with pharmacokinetics and pharmacodynamics in drug discovery and development.

Ischemia reperfusion injury (I/R) has been hypothesized to be caused by an initial reduction in oxygen and nutrients to tissues and the subsequent damage caused by reintroduction of blood flow to affected tissues. Ischemia, initially a blockage or reduction of blood flow results in damage to tissues. Paradoxically, the reintroduction of blood flow to the affected tissues initiates a cascade of events that often cause increased damage. Reperfusion of blood and oxygen to previously ischemic tissues or organs has been shown to cause increases in cellular damage and accelerate damaging free radical generation. Reactive oxygen species (ROS) have been implicated in wide array of I/R related injuries including organ transplantation, traumatic injury, and heart disease. Studies have shown that I/R injury initiate inflammatory processes on the endothelial surface of the vasculature through production of ROS. *In vitro* and *in vivo* studies have shown that endothelial cells exposed to hypoxia/oxygenation generates ROS and causes up-regulation of genes such as E-selectin, ICAM-1 and leukocyte adhesion molecules and additionally causes neutrophil adherence. During I/R injury endogenous mechanisms that provide cellular protection against free radical damage become depleted and overwhelmed.

Several studies support the claim that oxidant stress accompanies I/R injury and that administration of antioxidants and compounds that ameliorate oxidant stress reduces the degree of injury and aids in overall recovery and protection of such damage. Caffeic Acid Phenethyl Acid (CAPE) is one such compound that has been shown to have beneficial effects in reducing damage associated with I/R injury in cellular models as well as rabbits and rats models of I/R injury. Studies, including our own, have shown that induction of the gene, heme oxygenase-1 (HMOX1), plays a critical role in the cytoprotection provided by CAPE [1, 2].

This dissertation is a result of research aimed at discovering compounds that protect against oxidant stress. Based on the correlation that induction of HMOX1 is associated with cytoprotection, other compounds have been screened for induction of HMOX1 and two such compounds, 1[2-Cyano-3,12-dioxooleana-1,9(11)-dien-28-oyl]imidazole (CDDO-Im) and the C28 methyl ester derivative (CDDO-Me), are the subjects of the current research presented here. CDDO-Im and CDDO-Me are synthetic derivatives of oleanolic acid that have recently been shown to possess potent anti-inflammatory properties as well inhibit proliferation and induce differentiation in various cancer cells. CDDO-Im and CDDO-Me additionally have been shown to be strong activators of the gene, nuclear factor (erythroid-derived 2)-like 2 (Nrf2) that is involved in an antioxidant induced pathway. The hypothesis was tested that better inducers of cytoprotective genes such as HMOX1, through the Nrf2 pathway, would offer extended protection against oxidant stress-induced damage. A comprehensive study of potent inducers of protective genes by compounds such as CDDO derivatives could provide a better understanding of underlying mechanisms of action and offer a model for future drug screening and drug design from an integrated systems biology approach.

CHAPTER 1

Background and Literature Review

1.1 ISCHEMIA, REPERFUSION, AND ISCHEMIA/REPERFUSION INJURY

Ischemia/reperfusion (I/R) injury plays a role in several conditions such as cardiovascular disease including myocardial infarction and stroke and contribute to the leading causes of death worldwide [3-5]. The ischemia aspect of this injury is largely defined by a reduction of oxygen supply either to a whole organ or in specific tissue areas which also results in loss of nutrients and the inability to remove waste products leading to irreversible cellular damage. In the case of cardiovascular disease the interruption of blood flow due to arterial occlusion can cause ischemia to affected vessels or can be caused by insufficient ability to pump appropriate volumes of blood [6].

1.2 MECHANISM OF ISCHEMIA/REPERFUSION INJURY

Mammalian cells are constantly exposed to reactive oxygen species (ROS) generated from oxidase systems, mitochondria metabolism, and external sources (e.g. UV irradiation, xenobiotics) [7, 8]. ROS at low concentrations serve as important signaling messengers in the processes of cell division, inflammation, and stress response [9]. Under normal conditions, cells can neutralize extra ROS through redox reactions with intracellular antioxidants. These self-defense mechanisms help protect cells from oxidative damage and maintain a redox homeostasis of the cell. However, sustained production of oxidants (pro-oxidants or ROS) rather than counter balancing cellular

reductants (antioxidants) leads to oxidative stress. ROS can attack cellular components causing oxidative damage to constituents of cell membranes, lipids, proteins, and DNA. Damage to lipids and proteins will lead to lipid peroxidation, protein degradation, fragmentation, modification, and inactivation. Although DNA is relatively protected and stable, it can still be attacked by ROS resulting in modification of DNA bases, single- and double-strand breaks, and damage to DNA repair system [10]. The oxidative damage generated by ROS overproduction exacerbates cardiovascular diseases, cancer, diabetes, chronic inflammation, stroke, septic shock, and neurodegenerative diseases [8, 11]. In addition, the theory of free radicals remains a major contributor to aging [12].

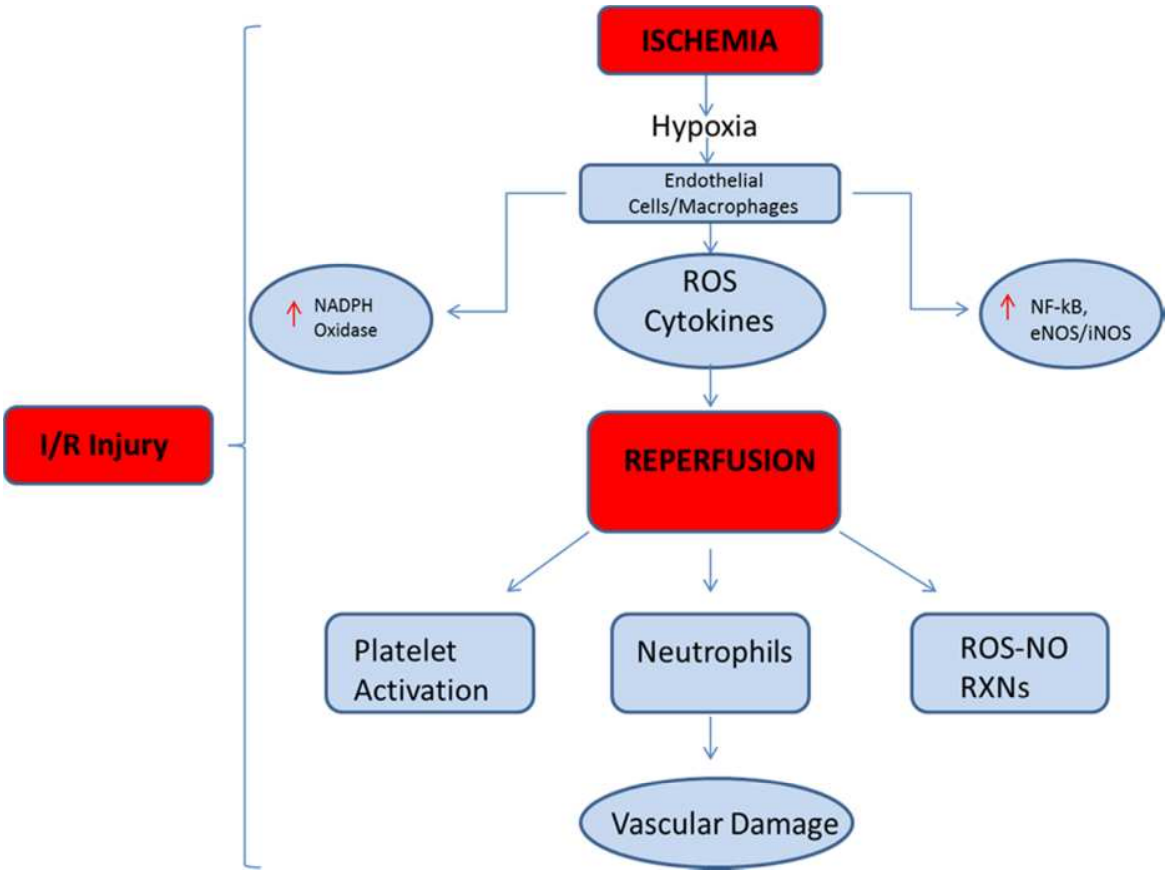

Figure 1.1: Proposed mechanism of I/R injury, modified [13].

1.3 MODEL CELL TYPE FOR CYTOPROTECTION

Endothelial cells (EC) are an active component of the vessel wall and play a critical role in maintaining structure and function. Additionally, EC are key modulators in response to I/R injury [14, 15]. EC have been shown to be an active source of ROS in response to I/R injury [16]; in addition to expressing pro-inflammatory properties they also play a role in the recruitment of neutrophils which are known to cause cellular damage [17]. Studies have shown that EC exposed to periods of hypoxia and reoxygenation generates an oxidative stress that simulates *in vivo* conditions of I/R injury [18]. EC are one of the first cell types to be affected during I/R injury and for that reason provide a relevant *in vitro* model for the study of treatments against I/R injury.

Endothelial cells form the inner lining of all blood vessels, and at the level of the capillary individual cells form tubes that allows for the movement of blood to all tissues. No cell in a mammalian organ is more than 100 microns from a capillary. The total number of endothelial cells is estimated to be 1 kg in an average-sized human covering a total surface area of 4000–7000 m^2 [19]. The endothelium was long thought to provide only an inert cell layer but is has turned out to be a highly metabolically active cell, participating in many homeostatic processes, including control of vasomotor tone, trafficking of cells and nutrients, maintenance of blood fluidity, regulation of permeability, and formation of new blood vessels [20]. However, the endothelium is a highly distributed tissue and efforts to understand endothelial specific characteristics have largely relied on isolation and study of endothelial cells from specific organs.

The human umbilical vein endothelial cell (HUVEC), exhibits many of the general properties of human endothelial cells, is readily available and is the best studied of human endothelial cells.

Menadione (MD), a synthetic quinone, belongs to the vitamin K family and has extensively been used as a means for evaluating the cellular effects of oxidative stress in endothelial cells [21, 22]. The primary mechanism of menadione-induced cytotoxicity is through the stimulation of ROS generation by redox cycling, largely dependent on the single electron reduction of O_2 that generates superoxide. The superoxide anion produced by this process is dismutated and forms hydrogen peroxide primarily through the enzymatic reaction with superoxide dismutase which further participates in Fenton reactions to produce hydroxyl radicals [23]. Studies done in our lab demonstrate the effects of cell damage induced by MD toxicity compared to normal HUVEC cultures and are shown in Figure 1.2.

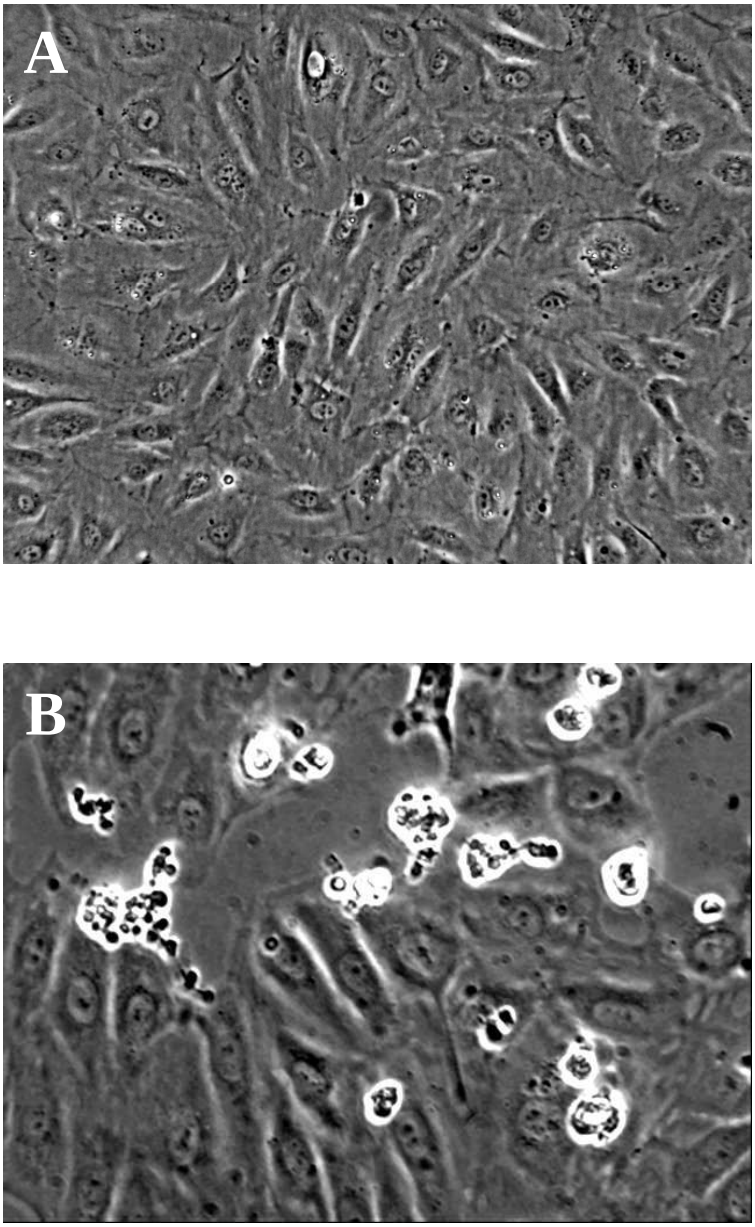

Figure 1.2: Oxidative stress-induced cytotoxicity in HUVEC after 24 h MD treatment. (A) Confluent HUVEC treated with control (DMSO). (B) HUVEC treated with 25 µM MD; rounded up cells demonstrate apoptosis of the cells.

1.4 ROLE OF ANTIOXIDANTS IN I/R INJURY TREATMENT

Proposed treatments of I/R injury have largely involved blocking the formation of ROS or scavenging ROS after they have been formed. The pathology of I/R injury has been defined by ROS-induced oxidative stress; the use of compounds with antioxidant activity have extensively been studied to ameliorate I/R injury [24, 25]. Over the last 25 years numerous types of interventions have been studied for the treatment of I/R injury, however, to date there is no approved treatment for I/R injury except restoring flow to hypoperfused vascular beds [26-28].

Glutathione is a molecule comprised of glycine, glutamine, and cysteine and is an essential part of cellular antioxidant defense systems. Glutathione is the substrate used by the enzyme glutathione peroxidase and has been tested as a potential therapeutic against I/R injury. Glutathione has been reported to have antioxidant properties and may act as a metal chelator (including iron, copper, mercury, and cadmium) and hydroxyl radical scavenger. Studies have shown that when glutathione is given exogenously it cannot penetrate cell membranes [29]. Endogenous production of glutathione is limited by the amino acid cysteine. N-acetylcysteine (NAC) has been reported to allow continued production of glutathione [30, 31]. NAC, a low molecular weight thiol antioxidant, also reacts with hydrogen peroxide and decreases production of hydroxyl radicals. Reported protective effects of NAC include radiation-induced injury, lung injury caused by toxic gas, and cardiac protection during ischemia [32-34].

Vitamin C, ascorbic acid, is a water-soluble vitamin that allows for regeneration of Vitamin E and provides antioxidant effects. While vitamin C has been shown to attenuate endothelial dysfunction in humans through its ability to act as a superoxide scavenger, it appears that vitamin C must be given in very high concentrations to be

effective [35]. Additionally, vitamin C has been shown to act as a pro-oxidant during ischemic conditions by providing more ferrous iron for the generation of hydroxyl radicals [36]. However, clinical trials with vitamin E and C have not yielded a reduction in mortality from heart disease [37, 38].

Recently, there has been a renewed interest in the use of plant-derived products that exhibit antioxidant activity. Curcumin is the active ingredient of turmeric; the Indian spice has been used to treat inflammatory disorders for hundreds of years [39]. Curcumin is one of the most studied natural compounds to date and reports show a wide variety of actions including anti-inflammatory, antibacterial and antioxidant [40]. The anti-inflammatory/antioxidant mechanisms have been shown to work by inhibiting pro-inflammatory signaling cascades such as Nuclear Factor of Kappa Light Polypeptide Gene Enhancer in B-Cells (NFκB).

NFκB and mitogen-activated protein kinase (MAPK) act through the induction of several genes such as tumor necrosis factor alpha (TNF-α), interleukin-1 beta (IL-1β), and intercellular adhesion molecule 1 (ICAM-1); although several studies indicate that curcumin, like many plant-derived compounds, work through multiple modes to provide protection [41, 42]. Resveratrol possesses similar multiple modes of actions as curcumin such as anti-inflammatory, antioxidant and chemoprevention.

Resveratrol can be found in a number of plants and red wine and has been shown to similarly involve the NFκB pathway as well as the sirtuin 1 (SIRT1) gene [43]. While resveratrol has been shown to have poor bioavailability there are a number of groups working to improve its performance [44, 45]. Quercetin, a flavonoid found in many fruits and vegetables, has also shown initial promise in providing anti-inflammatory benefits including protection against I/R related pathologies in cerebral and cardiac tissues [46].

While these compounds are active; *in vitro* studies with cultured cells and bioavailability, in particular by the oral route, appear to suggest limits to the potential benefit offered by this class of compounds [47]. In general, reports of reduction in I/R injury of such compounds have been through IP or IV injection. Understanding the role of potential therapeutic agents for the treatment of I/R injury needs to take into account not only the action of the compound of interest, but a more complete understanding of the I/R injury process [48]. The study of these types of compounds through an integrated systems biology approach will allow for more focused treatments of I/R injury as well as management of other diseases.

1.5 CAFFEIC ACID PHENETHYL ESTER (CAPE)

Previous work in our laboratories has investigated the cytoprotective activity of caffeic acid phenethyl ester (CAPE) and chemical modifications to improve this activity [1, 49, 50]. CAPE has been cited numerous times in the literature as a protectant against I/R induced injuries [51, 52]. CAPE is a polyphenolic plant-derived compound that is naturally concentrated in honeybee propolis (Figure 1.3A). Propolis has been used in folk medicine in many cultures to treat various diseases and has been reported to possess antifungal, antioxidant, antibacterial and other benefits. Flavonoids extracted from propolis have been shown to protect against various models of I/R injury; CAPE has been tested in numerous models of I/R injury in various tissues and organs [53-55]. Sud'ina *et al.* report that when 10 µmol of CAPE was administered to human neutrophils it completely blocked production of ROS [56]. Another study reports that CAPE provided beneficial effects against I/R induced injuries in rat skeletal muscle [55]. When 50

μmol/kg of CAPE was given to rats with an occluded coronary artery 10 minutes before initiation of ischemia, CAPE was shown to protect against I/R injury through potent scavenging of free radicals in the heart [57]. Additional studies have demonstrated the ability of CAPE to ameliorate I/R injury in spinal cord, testes, and kidneys [52, 58, 59].

CAPE has also been shown to affect transcriptional activity in a manner similar to other phytochemicals such as resveratrol and curcumin [60, 61]. Several mechanisms have been proposed for the different beneficial effects that have been reported. In an anticancer or tumor model CAPE has been used either to reduce or induce oxidative stress largely through the alteration of redox balance in these cells[62]. In these models the dose dependency was shown to be important [63, 64]. Reports have shown that CAPE can inhibit angiogenic activity of metalloproteinases in different cancer cells [65]. In the anticancer field it has also been demonstrated that it inhibits the transcription factor NFκB and Fas. Other reports show that activation of kinases such as ERK and MAPK by CAPE are involved in tumor suppression [66, 67].

Anti-inflammatory and antioxidant properties of CAPE have largely been shown to function through transcriptional signaling and involvement of multiple pathways. Involvement of the NFκB, like the anticancer mechanism, seems to be the main mechanism responsible for anti-inflammatory properties of CAPE [68, 69]. NFκB transcriptionally mediates the expression of proinflammatory cytokines, adhesion molecules, chemokines and enzymes such as inducible nitric oxide synthase. Mediators of the proinflammatory response such as IL-1β and TNF-α are regulated by NFκB and through regulatory feedback loop can directly activate the NFκB pathway, further exacerbating inflammation and its response. Many other inflammatory diseases are associated with NFκB activation including inflammatory bowel disease and rheumatoid arthritis [70, 71].

Studies have shown that CAPE and similar derivatives such as caffeic acid phenethyl amide (CAPA-Figure 1.3B) provides inhibition of NFκB activation in a variety of different models [50, 72-74]. Berger *et al.* showed reported that CAPE exhibit beneficial effects in B-lymphoma cell lines as well as non-B-cell lines through its ability to inhibit the NFκB pathway by specific binding to targets of NFκB [75]. Inhibition of NFκB activation by CAPE has also been confirmed in studies with U937 cells, rat macrophages and peptidoglycan polysaccharide-induced colitis in rats [76-78].

The direct antioxidant capacity of CAPE was compared by Son *et al.* against seven other potential antioxidants including caffeic acid and trolox and revealed that CAPE exhibited the highest antioxidative activity as well as exhibiting high scavenging activity [79]. The group performed structure-activity studies and revealed that antioxidant activity of the tested compounds was directly correlated by both the number of hydroxyl groups and catechol rings as well as the hydrophobicity of the compounds; the structure of CAPE is shown in (Figure 1.3). Recent work by our own group with CAPE treated human umbilical vein endothelial cells (HUVEC) confirms the direct antioxidant ability of CAPE as one possible mechanism for cytoprotection [1, 49].

While CAPE has widely been reported to have direct antioxidant capacity recent studies also implicate a more indirect antioxidant effect. Studies have shown that CAPE and other compounds like it induce antioxidant or detoxifying phase II enzymes [61, 80]. The phase II system is a well-known response to oxidative stress such as those incurred during an I/R injury; the phase II system functions through activation of a key set of enzymes such as NAD(P)H dehydrogenase, quinone 1 (NQO1) which is located on chromosome 16, and heme oxygenase-1 (HMOX1) on chromosome 22. This set of enzymes/genes has been reported to be activated through transcriptional factor Nuclear Factor, erythroid derived 2 (Nrf2) located on chromosome 2 and antioxidant-responsive

element (ARE) signaling pathways [81, 82]. CAPE and other natural compounds often are eliminated through metabolism *in vivo*; the compounds may only offer minimal concentrations of active ingredients and possibly limit the scavenging or direct antioxidant abilities. Mechanisms of such compounds that additionally function through more indirect antioxidant effects such as transcriptional activation might provide better cytoprotective profiles.

Recently, CAPE has been identified as a proficient inducer of heme oxygenase-1 (HMOX1) by our lab; confirming other groups findings that demonstrate that CAPE provides significant protection against oxidative stress-induced damage through cellular signaling functions [2]. These results establish the basis for use of novel therapeutic treatments with potent inducers of cytoprotective genes such as HMOX1.

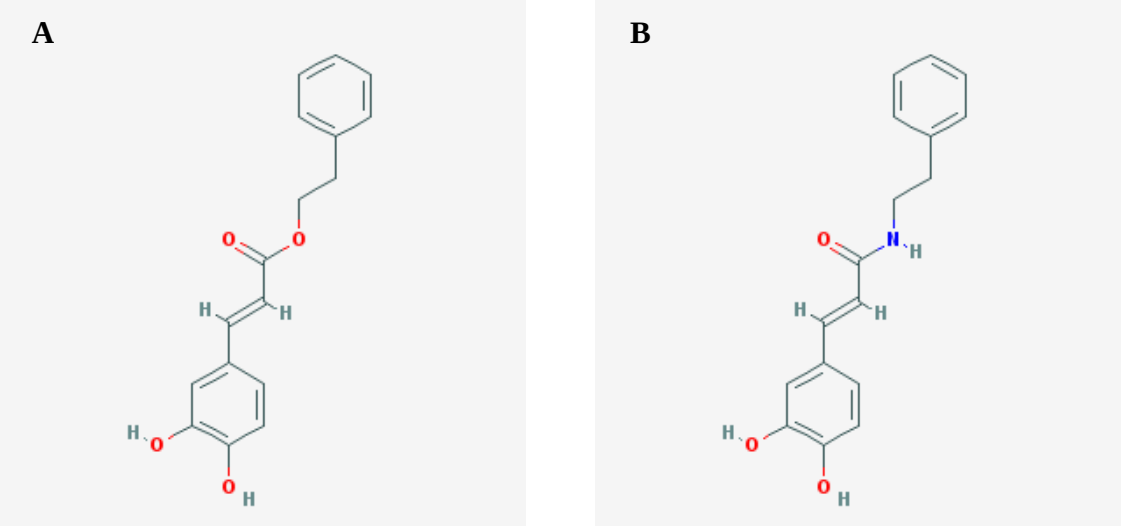

Figure 1.3: A) Structure of Caffeic Acid Phenethyl Ester (CAPE) showing two hydroxyl groups on the catecholic ring. B) Structure of Caffeic Acid Phenethyl Amide (CAPA) an amide group addition.

1.6 HEME OXYGENASE-1 (HMOX1)

Heme oxygenase-1 (HMOX1) is a stress-responsive enzyme that degrades free heme into carbon monoxide. Equimolar amounts of three products are yielded through the heme degradation: carbon monoxide (CO), iron, which further induces the expression of heavy-chain (H-) ferritin (iron-sequestering protein), and biliverdin which is converted by biliverdin reductase to bilirubin. While HMOX1 contributes to several aspects that provide its broad effects in protection against a varying amount of disease models, the main biological function seems to be modulating the accumulation of deleterious free heme [83].

HMOX1 expression is induced by a wide variety of stimuli including the stress response [84]. The induction of HMOX1 by a variety of stimuli is related to the variety of DNA binding sites in the promoter region of the HMOX1 gene [85]. The heme degradation products produced by HMOX1 activity, CO, iron and biliverdin, additionally provide beneficial effects alone or in combination through their respective anti-inflammatory and antioxidant properties [86].

Three distinct isoforms of heme oxygenase (HO):HMOX1, HO-2 and HO-3 have been identified. Along with the inducible HMOX1 form, HO-2 is the constitutive isoform that is present in relatively small amounts in most tissues. HO-3 has recently been identified, but only in rats and its biological role still remains unclear [87]. The role of HMOX1 in I/R injury has been studied and reports indicate that the HMOX1 system may play a role in the I/R response and could provide a new target for new treatments of this condition [53, 88].

Issan *et al.* reported that HMOX1 induction improved cardiac function following myocardial ischemia by reducing oxidative stress [89]. Studies have also shown that 24 h

ischemic post conditioning can protect an organ from I/R injury; furthermore, inhibition by commonly used HMOX1 inhibitors such as zinc protoporphyrin confirmed the importance of HMOX1 in protection against rat hepatic I/R injury as protection was seen to be negated when HMOX1 expression was inhibited [90]. HMOX1 has further been shown to protect against I/R related injuries in many other models such as protection of rat kidney transplants from I/R injury [91], cerebral ischemia models [92, 93], acute pancreatitis[94], amelioration of HIV-1 via HMOX1 induction [95] and several forms of I/R induced hypertension [96-98].

1.7 1[2-CYANO-3,12-DIOXOOLEANA-1,9(11)-DIEN-28-OYL] (CDDO) AND ITS DERIVATIVES

Naturally-derived products have been an invaluable source of novel compounds for treatment of many diseases including I/R injury. Naturally occurring substances are created by complex reactions and thus contain chemical structures that are difficult to synthesize in the laboratory; for this reason they represent an invaluable source of starting materials for drug development [99, 100]. Triterpenoids represent an example of such compounds [101]. Widely present in many foods and plants, including olive oil and garlic, oleanolic acid (OA) is a naturally occurring triterpenoid formed by the cyclization of squalene. Oleanolic acid has been used in traditional medicine for years and reports of its anti-inflammatory and anti-proliferative properties, while weak, have been known to be beneficial [102]. Researchers became interested in these properties and began to test whether these activities could be optimized by further modifications to their structures; in

1996 Michael Sporn and colleagues at Dartmouth College began to synthesize novel compounds for the purposes of prevention and treatment of cancer [103].

Over the last 18 years hundreds of derivatives have been synthesized from oleanolic acid as well as similar compounds such as ursolic and betulinic acids [103-106]. 2-cyano-3,12-dixooleana1,9(11)-dien-28-oic acid (CDDO), a synthetic derivative of oleanolic acid, was first synthesized in 1998 by Tadashi Honda in the Chemistry Department at Dartmouth College. The synthesis of this molecule represented a significant advance towards the optimization of triterpenoids in providing potent anti-inflammatory and growth suppressive properties. Initially designed for use in cancer treatment it was shown that for inhibition of *de novo* iNOS expression which produces nitric oxide as a defensive mechanism in IFN-γ stimulated primary mouse macrophages, CDDO was determined to be 100,000 times more potent than oleanolic acid [107].

From the synthesis of the original set of molecules by Sporn *et al.* by modifications of oleanolic acid, it was determined that the conversion of OA from the 3-OH alcohol group to a 1-ene-3-one resulted in the increased inhibition of iNOS induction. Continued derivitization resulted in creation of a di-enone, increasing the potency by 30 and 10-fold respectively. Finally, two intermediate compounds were combined to create the final molecule in the synthesis, also called CDDO. From the starting material of OA to the creation of CDDO 11 steps were involved [104].

In an effort to maximize the pharmacokinetic profile of the synthetic triterpenoids and further increase potency a series of C28 derivatives of CDDO were synthesized and tested [104]. Two of these compounds, the C28 imidazolide of CDDO 1[2-Cyano-3,12-dioxooleana-1,9(11)-dien-28-oyl]imidazole (CDDO-Im) and the C28 methyl ester derivative (CDDO-Me), have demonstrated increased activity to CDDO in a variety of assays and models [108-110]. The design of these two compounds had the goal of

providing additional protection to the C28 carboxylic acid (COOH) group and to potentially optimize the pharmacokinetics of the molecule partially through the formation of compounds that were capable of acetylating a protein target. The addition of the imidazole and later the methyl ester form were done so as to act as a leaving group when reacting with protein targets, potentially forming a covalent bond between the target and the triterpenoid. This approach has been performed before with beneficial results, such as in the generation of retinoyl imidazolide [111]. The imidazolide addition is generally an intermediate step in the synthesis of ester forms because the imidazole can act as a leaving group in reactions with alcohols [112, 113]. Structures of CDDO, CDDO-Im, and CDDO-Me are shown in Figure 1.4 (A-C).

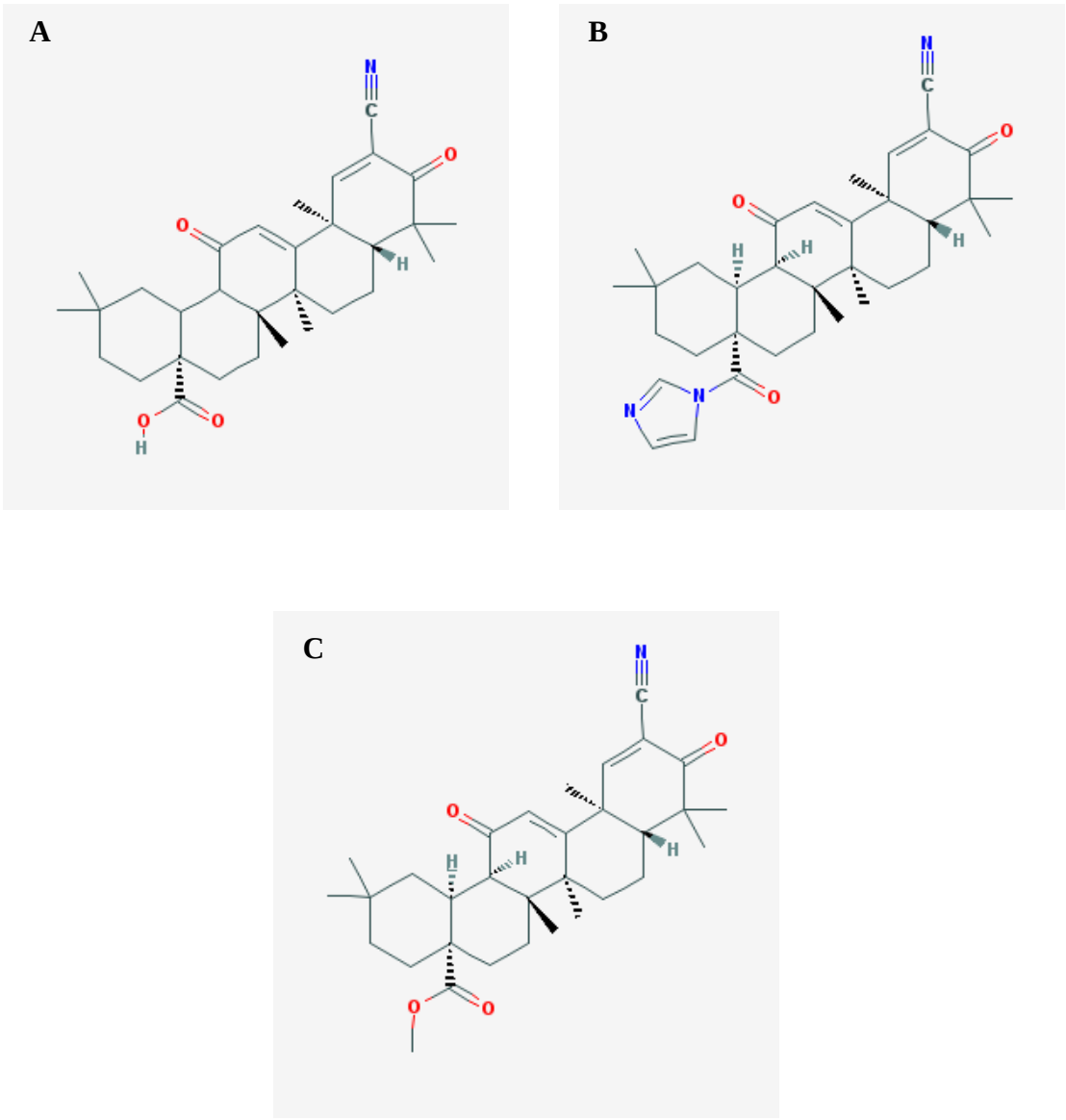

Figure 1.4: Structures of A) CDDO, B) CDDO-Im, and C) CDDO-Me.

The high potency of CDDO and its derivatives have enabled their use in a number of diverse studies, many of which have been focused on determining the mechanism of action. One of the first published studies involving CDDO and it mechanism of action was done by Wang *et al.* who used 3T3-L1 cells to show that CDDO induced adipocytic differentiation and establish that both CDDO and CDDO-Me were ligands for the peroxisome proliferator-activated receptor γ (PPARγ) [110]. While CDDO and CDDO-Me had similar affinity for the receptor it was shown that CDDO was a partial agonist for the PPARγ receptor, but CDDO-Me was an antagonist; this difference was hypothesized to be the reason for the difference in observed effect. CDDO-Me potentially had a better ability to recruit the coactivator CREB-binding protein to PPARγ; a known protective pathway involved in inflammation [114].

CDDO and many of its derivatives have been used in numerous disease models. Specific use of these potent compounds relies heavily on the desired effect one is hoping to achieve and appears to be both time and concentration dependent. When these compounds are used in cancer treatment higher doses have been shown to induce apoptosis and differentiation [109, 115-117]. CDDO has further been tested in Phase I studies in advanced solid tumors [118] with seven patients receiving CDDO from dose ranges of 0.6 to 38.4 mg/m^2/h. One patient at the highest dose level experienced grade 2 mucositis, nausea and vomiting while four other patients developed thromboembolic events subsequently considered as dose-limiting toxicity. Additionally, no antitumor activity was noted; this study highlights the importance of dose range when using such drugs. In contrast, studies have also shown promising results with the use of these synthetic triterpenoids including inhibition of tumor cell growth in chordoma [119], suppression of liver metastasis [120], use for solid cancer prevention [121] and treatment, pancreatic cancer treatment [122] and breast cancer [123].

Along with use of synthetic triterpenoids in cancer treatment several studies have utilized the compounds in novel areas of treatment such as the use of CDDO-Im for the improvement of platelet production [124]. In this study it was shown that CDDO-Im induces megakaryocytic differentiation of normal progenitor cells and could potentially be used to increase platelets in patients with such deficiencies. In another study Reddy *et al.* showed that CDDO-Im given to mice orally at a dose of 30 μM/kg body weight during hyperoxic exposure was sufficient to attenuate hyperoxia-induced acute lung injury and was related to up-regulation of Nrf2-regulated cytoprotection [125]. CDDO-Im has also been reported to attenuate cigarette-induced emphysema and cardiac dysfunction in mice, again through mediation of Nrf2 [126] while CDDO-Me has recently been shown to protect against space radiation-induced transformation of human colon epithelial cells [127].

CDDO-Me was recently tested for its ability to mitigate moderate-to-severe chronic kidney disease. Pergola *et al*. showed that oral treatment of patients with CDDO-Me over several weeks saw a significant increase in glomerular filtration rate when compared to baseline [128, 129]. The group attributed elevated glomerular filtration rate to a decrease in inflammation and oxidative stress. However, a follow-up clinical trial was recently stopped due to adverse outcomes in the long-term CDDO-Me treated patients. In more acute treatments with CDDO-Me other groups have shown more promising results including protection against ischemic acute kidney disease [130]. Recently Liu *et al*. showed the CDDO-Im protects kidneys from ischemia-reperfusion injury in mice and protection was achieved through activation of the Nrf2 pathway [131]. Furthermore, the group showed that protection against acute kidney ischemia was lost in Nrf2-deficient mice, implying that the mechanism of CDDO-Im action in that specific model was primarily modulated through Nrf2. Others studies, including our own recent

work, have shown that while Nrf2 is a major contributor to cytoprotection, other cellular processes contribute in an Nrf2-independent fashion to confer cytoprotection in various models [132-134]. While some of the above mentioned studies have convincingly shown that both CDDO-Me and CDDO-Im offer better protection than CDDO, the mechanism and differences between CDDO-Im and CDDO-Me are still unclear and is investigated in this dissertation. In particular the study of these compounds in an oxidative stress-induced model from a systems pharmacology standpoint may provide insights into mechanisms of action and compare these synthetic triterpenoids with other compounds in an effort to find a treatment that can maximize the cytoprotective effect in a relevant model for the benefit of I/R injury treatment and furthermore, screen for compounds that initiate their protective effects rapidly to maximize their potential benefits post-injury.

1.8 SYSTEMS PHARMACOLOGY

"Systems biology...is about putting together rather than taking apart, integration rather than reduction. It requires that we develop ways of thinking about integration that are as rigorous as our reductionist programmes, but different....It means changing our philosophy, in the full sense of the term" -Denis Noble, The Music of Life [135]

The conceptual framework of the scientific method has been continuously evolving and this can be seen by considering the history of science. In the 17th century the idea of reductionism was presented by Rene Descartes (1596-1650). Descartes proposed that complex situations could be analyzed by reducing them to manageable pieces and studying each in turn; further he asserted that by reassembling the whole from the

behavior of the pieces was an appropriate way of handling such complex matters [136]. While Descartes' principles were developed in a time when biology was in its infancy the reductionist concepts were applied to mathematics and physics including Isaac Newton's work describing planetary movements and gravity which helped strengthen the reductionist theories. Reductionist approaches in the biological sciences in the 20th century formed the basis for major advances in our understanding of biology and are still much used today; however, it is subject to significant limitations. Jan Smuts (1870-1950) revived Aristotle's views that "the whole is something over and above its parts and not just the sum of them all" [137]. Smuts, a naturalist and philosopher, coined the term holism. He established that whole systems including cells, tissues, and organisms were proposed to have emergent and unique properties. Smuts' theories laid the groundwork for the idea that it was impractical to try and reassemble the behavior of the whole from individual components and that new technologies must be explored to describe and understand the complexity of biological systems.

While aspects of systems biology have been utilized in part for hundreds of years; it's not until the completion of the Human Genome Project in 2003 that biology entered a profound new era. This revolution in science led to the development of high-throughput technologies that were capable of generating massive amounts of data about complex systems [138, 139]. While these and other molecular biology technologies have uncovered vast numbers of biological data such as novel genome sequences and proteins; by themselves they are insufficient for interpreting biological systems.

The decoding of the human genome in 2003 and development of genomic technology such as microarrays and RNA-seq have provided an opportunity to look at the activity of virtually every gene in response to a perturbation. Specifically, gene expression profiling by whole genome microarray or RNA-seq can interrogate all genes

that might be changing following a perturbation. Proteomic techniques to analyze large numbers of proteins simultaneously are also being developed using high performance liquid chromatography with tandem mass spectrometry to similarly determine the proteome. The goal of systems biology is to combine this experimentally-derived data with computational biology. The amalgamation of the two provides the framework for generating hypothesis and prediction-based *in silico* simulation of biological systems across time scale and multiple distances of an organism.

Efforts to ameliorate I/R injury have been ongoing for more than 50 years; the lack of an approved therapeutic drug for treatment may be a result of an incomplete understanding of the problem [140-143]. I/R injury is a complex disease that involves multiple pathophysiologies including oxidant stress [144]. A system that involves such a dynamic response to an injury must take into account the global response to adequately understand the whole issue in hopes of designing better drugs that provide improved outcomes of such an injury.

Biological systems are complex and dynamic; systems biology is an approach that aims to understand the complexity of biological systems in order to develop predictive models that focus on the most important aspects of the system that may be used to treat human disease [145]. Systems biology is the integration of information that quantifies behaviors of interactions between components from data obtained from technologies such as genomics, proteomics, and metabolomics through the use of mathematical and computational modeling to describe and predict complex biological systems. Additionally, this integration of computational and experimental research that forms the basis of systems biology seeks to further explore these interactions to explain the global and dynamic nature of complex behavior in biological systems.

Systems pharmacology is an emerging discipline that combines systems biology with pharmacology in an attempt to understand the actions of drugs on a global scale [146]. The drug becomes the perturbation of the system that is quantified to better understand the system and the consequences of the drug on that system [147, 148]. Systems pharmacology combines high-throughput genomics and proteomics of drugs in cellular models with computation and modeling software that enables a more complete analysis of drug action and known biological networks [149].

1.9 NETWORK ANALYSES IN DRUG ACTION STUDIES

Network analysis is utilized in systems biology to represent molecular interactions as networks depicting integrated data with graph analysis for biological interaction studies. Network analysis allows for predictive modeling of novel gene, protein, and functional interactions based on a vast network of prior knowledge. In drug action studies these approaches are often combined with specific drug data such as structure, pharmacokinetic, and pharmacodynamics (PK/PD) studies to accelerate the drug discovery process as well as increasing the overall chances of drug success. Incorporation of network analyses has become an emerging tool for increasing the understanding of relationships between disease susceptibility genes and drug action [150].

A network is a way of representing highly dimensional biological data by emphasizing the relationships between entities termed nodes [151]. Combining network and pathway analyses along with data from pharmacokinetic and pharmacodynamics studies enables advanced modeling for the study of new drugs, potential adverse effects, and increased data on therapeutic efficacy. The integration of network analysis with

systems pharmacology offers profound implications in drug discovery; mainly instead of the classical approach of searching for single “effector” genes, systems pharmacology allows for identification of changes from a global “effector-causing network” (Figure 1.5).

Nodes can represent objects such as genes, proteins, small molecules, disease, or any other entity capable of being modeled in a complex system. Nodes in a network can have various attributes and connotations; furthermore, they can have exist as different states in the system such as active or inactive or be combined with differential equations to be used in modeling pharmacokinetic and pharmacodynamics data of a system.

In a complex system nodes are connected to each other through what is termed edges. Edges represent the interactions between the nodes and can represent interactions such as drug-target interactions, protein-protein interactions, and transcriptional regulation [152]. Edges can have weight, direction, and other meaning to provide information in the network in a hierarchical perspective. The flexibility of the varied types of complex interactions that can be modeled in network analyses allows for explicit tracking of drug affects in a system. The edges in any given network can further be directed, for example, a source node that causes an effect on a target node that only exists in one direction. An example of such a network is the activation of a transcription factor by a protein kinase and the regulation of a target gene by that transcription factor. In contrast, edges can also exist as undirected in which interactions occur in multiple directions. Examples of undirected edge networks are interactions between proteins and their scaffolds.

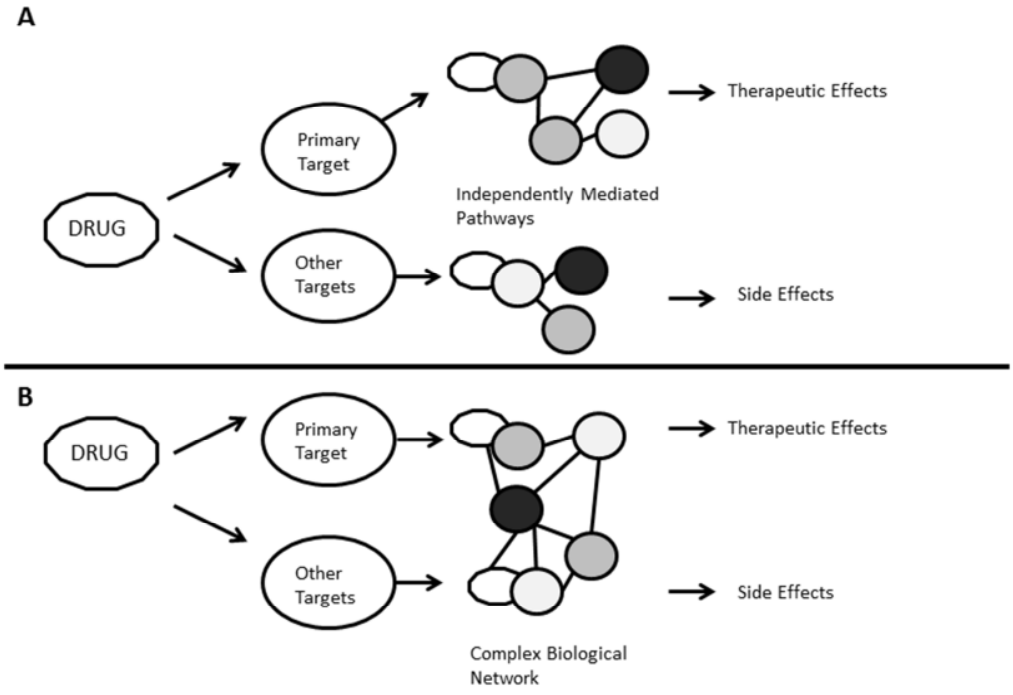

Figure 1.5: Evolution of network studies. (A) Classical view of drug action studies depicting separate pathways affecting therapeutic and side effects of a system after treatment with a drug. (B) Systems pharmacology approach towards drug action showing the dependence on a complex network that mediates the response of a drug (Modified [153]).

1.10 BRIDGING PK/PD WITH SYSTEMS PHARMACOLOGY

Lack of predictable clinical efficacy and safety is an increasing problem facing the pharmaceutical industry today. Pharmacokinetic-pharmacodynamic (PK/PD) modelling approaches have played a crucial role in clinical research and development for decades. In more recent years, the integration of PK/PD and model-based drug development and drug discovery has been advocated by both the pharmaceutical industry and regulatory agencies [154]. This integrated approach links mechanistic PK/PD data from the exposure of a drug to physiological pathways, modulation of pharmacological targets, and disease systems to better develop unified data of drug action at different stages of drug discovery and development, thus providing a more robust framework for translational drug research. Attrition in Phase II clinical trials is a serious concern facing successful development of new innovative therapies today and has largely been attributed the lack of translation of efficacy and safety from preclinical studies to actual human physiology; implementation of strategies such as combining PK/PD data and systems pharmacology could have significant impact on the overall success and efficiency of pharmaceutical research [155].

Conventional PK/PD approaches rely largely on empirical, descriptive models that can have limited predictive capabilities, especially in evolving therapeutics such as biologics [156]. A key difference between classical PK/PD approaches and more mechanism-based approaches is the incorporation of specific data pertaining to processes from drug administration to actual effect as well as methods for defining distinct data obtained from drug-specific and system-specific sources. PK/PD parameters obtained from system-specific sources include cell life-span, target and biomarker abundance, organ and tissue blood flow rates, and feed-back mechanisms. Sources for system related

data of a drug are commonly mined from the literature or prior experimentation and through advanced bioinformatic software incorporated into the model containing corresponding PK/PD data. In contrast, drug-specific sources of data integrated into this mechanism-based approach include PK parameters such as clearance, and volume of distribution as well as pharmacological data such as affinity and efficacy.

In 2011 the NIH published a white paper discussing the results of two NIH initiated workshops comprised of academia, industry, and government experts for the purpose of determining the best way to integrate advanced systems biology principles and pharmacology [157]. The goal of the workshops and the white paper was to determine whether a merger of pharmacology and systems biology could advance the development, discovery, and clinical use of therapeutic drugs. The initiative defined the process as a discipline termed “quantitative and systems pharmacology” (QSP).

QSP was further defined as an integrated approach to translational medicine that combines experimental and computational methods to elucidate, validate, and apply new pharmacological concepts for determining mechanism of action, creating knowledge needed for complex systems to improve therapeutic benefits while reducing toxicity, and implement a “precision medicine” approach to improve overall health of patients.

The findings by the group identified an urgent need for change in classical pharmacology approaches and suggested the integration of concepts, methods, and investigators from computational biology, systems biology, systems engineering, and genomics. Furthermore, the panel identified a need for advanced training and academic programs for the training of students in systems pharmacology to meet the expected growth in the field. Finally, the group predicted that integration of advanced systems biology with pharmacology could revitalize pharmacology and revolutionize practical drug discovery. The value and interest in this integrated approach to drug development

and discovery has rapidly grown; the pharmaceutical industry is beginning to incorporate these ideas into their classical approaches with success [146]. QSP is based on the idea that quantitative experiments and mathematical modeling incorporating biological networks in health and disease will lead to better understanding of the multiplicity of factors influencing drug effects; this process will allow for new ways to therapeutically intervene while limiting adverse effects.

1.11 GRAPH THEORY

Graph theory is a field of mathematics that has largely been applied and developed through the fields of computer science and sociology; recently the field has evolved and now forms the backbone of network analysis and systems biology by utilizing the theory to analyze regulatory networks within biological systems [158, 159]. The preceding discussion of nodes and edges provides the basis for the resulting networks that integrates different algorithms to provide information in an organized fashion about a system.

In addition to the variations in representation of nodes and edges through directed or undirected graphs; more advanced mathematics provides powerful options for expressing more in-depth interactions. A bipartite graph is an undirected graph G = (V, E) where V is a set of vertices that represent the nodes and E is a set of edges that represent the connections between those nodes. Bipartite graphs are commonly used to express biological networks, pathways, or ontologies and will be highlighted in following chapters comparing gene expression profiles of drug treatments [160]. In an undirected graph the degree of a node is an important measure for any particular node. Degree of a

node is the number of edges (connections) that a particular node has to other nodes, mathematically defined as deg(i) =k(i) = [N(i)] where [N(i)] = number of neighbors of the node (i). In contrast, in a directed graph each node has two degrees, the in-degree deg_{in} (i) which is the number of edges that are incoming to the node and the out-degree deg_{out} (out) which is the number of outgoing edges leaving the node (i). Thus, total connectivity of any network can be defined as C = E/N(N-1) where E = number of edges and N = total number of nodes where $N \neq 1$. The value of measuring connectivity can provide information in a biological network such as importance of single genes or interplay of a gene as well as groups of genes that potentially are responsible for efficacious effects or even adverse events [161].

Biological networks are often governed by subsets of genes or molecules that are linked and together affect cellular processes. Centralization is the measure that relates this effect and provides means for evaluating connectivity of a set of molecules (i.e. genes) in a network [162]. The degree of centrality measures the importance of a node by its number of interactions calculated by $C_{d(i)}$ = deg(i), where $C_{d(i)}$ is the degree of centrality and deg(i) is the degree of interactions. Nodes with large values of degree centrality are called hubs due to the high amount of connections to many neighbors. It has been shown that removal of such hubs has great impact on the topology of a network; demonstrating the importance of such interactions in a biological system. Similarly, closeness centrality is another applied graph theory measure that evaluates the importance of a node by measuring how quickly one node can communicate with another node in a network. Closeness centrality has been used in studies to identify the top central metabolites in whole genome-based studies and to rank pathways by providing a value of distance between pathways in a system. Betweenness centrality defines the importance of

nodes that are intermediate between other neighbors and provide communication between each other.

The leading cause of drugs failing to reach the market is lack of efficacy and unanticipated adverse events in phase II and III trials [163, 164]. This costly aspect of the drug development process could greatly be benefitted by integration of systems pharmacology including data on mechanism of action, drug safety, and target/pathway interactions [165]. The current study utilizes this approach by integrating genomics over time to study dynamic changes of genes in response to drugs with advanced bioinformatics to evaluate mechanistic information of drug response. Combined with network and pathway analysis, this integration highlights an alternative approach towards treatment of oxidative stress and potentially outlines future paths of drug discovery that will allow for a more complete understanding of drug response and processes in a more global context.

1.12 EXPERIMENTAL APPROACHES IN SYSTEMS PHARMACOLOGY

When analyzing the action of a drug, there are a wide variety of network based approaches that can incorporate different types of interactions, thus allowing networks to transcend multiple levels of complex systems biology [166]. In biological systems, interaction networks provide the foundation for representing interactions of highly specified systems. Interaction networks typically use edges that have the same weight and have relatively the same connectivity. This type of network is often considered one of the simplest forms of networks and allows for the least amount of knowledge regarding

nodes and edges. This design allows for interaction networks to easily be constructed and applied to a wide variety of data.

Interaction networks are the most common type of network used in analyzing “omic” data (e.g. proteomic, genomic, and metabolomic) [167, 168]. The utilization of such a network allows for the rapid assessment of potential downstream and upstream initiators of any particular node providing valuable information on signaling pathways and regulatory motifs of a system. For example, an interaction network designed to study transcriptional regulation before and after drug treatment could be expanded by connecting affected genes to their physiological function and in doing so, drug-to-physiological function data could be obtained. Further analysis of known protein-protein, kinase, phosphorylation, acetylation interactions could be combined to provide a global map of a particular drug action in a system. Interaction networks combine large numbers of variables and output in response to perturbations of a system such as drug treatments and form the basis of the systems biology and data handling incorporated in succeeding chapters.

CHAPTER 2

Cytoprotection of human endothelial cells against oxidative stress: Comparison of 2-cyano-3,12-dioxooleana-1,9-dien-28-imidazolide (CDDO-Im) and caffeic acid phenethyl ester (CAPE)

2.1 INTRODUCTION

In a continuing effort to find drugs to ameliorate oxidative stress-mediated ischemia-reperfusion injury, we identified a natural polyphenolic compound, caffeic acid phenethyl ester (CAPE), as a potential cytoprotectant. Our previous studies showed that pretreatment with CAPE protected human umbilical vein endothelial cells (HUVEC) against menadione-induced oxidative stress and that this protection was highly correlated with a cytoprotective gene, heme oxygenase-1 (HMOX1), by CAPE [2, 49]. The protein product of HMOX1, usually known to be the rate-limiting enzyme for heme degradation, is now considered as a phase 2 detoxification enzyme [169]. Classical phase 2 enzymes such as glutathione S-transferases and UDP-glucuronosyltransferases are used to conjugate xenobiotics with endogenous ligands like glutathione and glucuronic acid. This conjugation reaction leads to more easily excretable products. Currently, the list of phase 2 enzymes has been expanded to include enzymes regulated through the antioxidant responsive element (ARE) and include enzymes that lead to cytoprotection against oxidative stress [169]. To further improve cytoprotection of human endothelial cells, we investigated a recently described inducer of phase 2 enzymes, 1[2-cyano-3,12-dioxooleana-1,9(11)-dien-28-oyl] imidazole (CDDO-Im), a new synthetic triterpenoid [170].

CDDO-Im is the imidazolide derivative of its parent compound, 2-cyano-3,12-dioxooleana-1,9-dien-28-oic acid (CDDO). CDDO, a synthetic oleanane triterpenoid, was identified through an attempt to design new anti-inflammatory agents from the natural products oleanolic acid and ursolic acid [103, 171]. CDDO, CDDO-Im, and methyl ester derivative of CDDO (CDDO-Me) also showed antitumor activities *in vitro* and in animals [170, 172, 173]. A recent study found that CDDO and CDDO-Im induced HO-1 both *in vitro* and *in vivo*, and the imidazolide derivative was more potent [108]. This induction was possibly through the activation of a signaling pathway regulated by transcriptional factor nuclear factor, erythroid 2-like 2 (Nrf2). Upon activation, Nrf2 translocates from the cytoplasm to the nucleus and binds to ARE to initiate transcription of an array of drug metabolism and antioxidant genes. Activation of this Nrf2/ARE pathway leads to an increased elimination of xenobiotics and thus increased resistance to oxidative stress [174].

The purpose of our present research was to 1) identify more potent cytoprotectants against oxidative stress than CAPE and 2) obtain insight into potential mechanisms of this cytoprotection through a genome-wide approach. In this study, we examined the cytoprotective effect of CDDO-Im against oxidative stress in HUVEC and compared it to CAPE. A microarray analysis was conducted on HUVEC after a 6-h treatment with either CDDO-Im or CAPE to look for induction of cytoprotective genes. Data were analyzed through the use of Ingenuity Pathway Analysis (IPA, Ingenuity Systems, www.ingenuity.com) for functional enrichment and pathway analysis of microarray data to identify potential involvement of cellular functions and canonical pathways mediating oxidative stress.

2.2 MATERIALS AND METHODS

2.2.1 Materials

CAPE was purchased from Cayman Chemicals (Ann Arbor, MI, USA). CDDO-Im was kindly provided by Dr. Michael Sporn (Dartmouth Medical School, Hanover, NH). Menadione sodium bisulfite (menadione) and dimethyl sulfoxide (DMSO) were obtained from Sigma-Aldrich (Saint Louis, MO, USA).

2.2.2 Cell Culture

HUVEC (Life Technologies, Carlsbad, CA) were cultivated on 1% gelatin-coated 75-cm2 culture flasks (Corning Incorporated, Corning, NY, USA) in Medium 200 supplemented with 2% fetal calf serum, penicillin (100 units/ml), streptomycin (100 units/ml), and fungizone (0.25µg/ml) supplied by Life Technologies [2]. Stock cultures were maintained at 37ºC in a humidified atmosphere of 95% air and 5% CO2 with medium changes every 2 days until confluent. Prior to an experiment, HUVEC were subcultivated with trypsin/EDTA onto 1% gelatin-coated 48-or 96-well Costar® multiplates (Corning Incorporated, Corning, NY, USA) at 10,000 or 5,000 cells/well respectively, grown to confluence, and kept for 72 h to produce a quiescent cell layer. On the day prior to the experiment, the medium was changed. Only the second through fifth population doubling levels of cells were used.

2.2.3 Cell viability and toxicity assay

Cell viability was estimated in HUVEC using Alamar Blue™ (Life Technologies, Carlsbad, CA), which utilizes metabolic conversion of resazurin to fluorescent resorufin by viable cells. As previously described [2], menadione was used to induce oxidative injury in HUVEC. Briefly, HUVEC were exposed to a 60 μM dose of menadione, causing 80-90% cell death, for 24 h. The cells were then incubated with culture medium containing 10% Alamar Blue™ for an additional two hours. Fluorescence was measured at 545 nm excitation and 590 nm emission with a SpectraMAX® M2 microplate reader (Molecular Devices, Sunnyvale, CA, USA). Nontoxic doses of CDDO-Im in HUVEC were determined as follows. A series of doses of CDDO-Im (50 ~ 1000 nM) were incubated with HUVEC for 24 h followed by cell viability assay. Doses of CDDO-Im causing more than 90% cell viability were considered not toxic to HUVEC and used in the following cytoprotection assay.

2.2.4 Cell protection assay

CDDO-Im and CAPE were dissolved in DMSO and diluted 1000-fold with medium (final concentration of DMSO no more than 0.1%). Confluent HUVEC in 48-well plates were pretreated with CDDO-Im and CAPE at nontoxic doses for 6 h. They were then exposed to the preselected dose of menadione for an additional 24 h. Cell viability was measured using the Alamar Blue™ assay.

2.2.5 mRNA-based microarray expression profiling

HUVEC were incubated with CDDO-Im at 200 nM or CAPE at 20 μM for 6 h. Total RNA was extracted from treated HUVEC grown in 6-well plates with TRI™ reagent according to the manufacturer's protocol (Molecular Research Center, Cincinnati, OH, USA). The amount of isolated RNA samples was quantified using a NanoDrop® ND-1000 Spectrophotometer (NanoDrop Technologies, Wilmington, DE, USA). The integrity of isolated RNA samples was assessed using an Agilent Bioanalyzer 2100 (Agilent Technologies, Palo Alto, CA, USA).

Gene expression profiling of HUVEC treated with CDDO-Im or CAPE compared to vehicle control (DMSO, 0.1%) was performed using Agilent 60-mer Whole Human Genome Microarrays (Agilent Technologies. Inc.,Santa Clara, CA). Statistical analysis for differences among treatment groups was performed using BRB Array Tools (Biometric Research Branch, National Cancer Institute, USA). Genes were determined to be statistically altered in their expression with both p value < 0.001 and false discovery rate (FDR) < 0.001 after class comparison between treated and control groups. In addition, the significant gene lists from both CDDO-Im and CAPE treatment were intersected through BRB (Biometric Research Database) Array Tools to identify common genes significantly altered by compounds.

2.2.6 Ingenuity Pathway Analysis

The lists of significant genes from microarray data analysis were submitted to Ingenuity Pathway Analysis (IPA) for gene function and canonical pathway analyses (Ingenuity® Systems, www.ingenuity.com). IPA maintains a large knowledge database

of modeled relationships among proteins, genes, complexes, cells, tissues, drugs, pathways, and diseases generated from published reports. When a date set containing gene identifiers and corresponding expression values such as fold change were uploaded into IPA application, each gene identifier was mapped to its corresponding gene object in this Ingenuity Pathway Knowledge Base (IPKB). A p-value and FDR cutoff of 0.001 was previously applied to the gene sets before submitting to IPA. A fold change cutoff of 2 for both up- and down-regulated genes was applied. These selected genes, called Focus Genes in IPA, were overlaid onto a global molecular network developed from information contained in the IPKB. Networks of Focus Genes were then generated based on their connectivity. IPA calculated a significant score for each network. The higher the score, the more interconnected among those genes within that network. The scores for networks represent the negative log of the P value. Therefore, scores of 2 or higher provide at least 99% confidence of not being generated by chance alone. Genes are represented as single nodes in the network.

A functional analysis of the network was done to identify the biological functions that were most significant to the genes in the network. A right-tailed Fisher's exact test was used to calculate a p value to determine the probability that each biological function assigned to that network would be due to chance alone. The smaller the p-value, the less likely the association is random and the more significant the association. In addition, a functional analysis of the entire data set was done to identify the biological functions that were most significant to the data set. The same right-tailed Fisher's exact test was used to calculate a p value to determine the probability that each biological function assigned to the entire data set is random. A canonical pathway analysis of the submitted data set was also performed to identify the pathways from the IPA library of canonical pathways that were most significant to the data set. The significance of the association between the data

set and the canonical pathway was also measured using right-tailed Fisher's exact test. The p-value calculated was used to determine the probability that the association between the genes in the data set and the canonical pathway is explained by chance alone.

2.2.7 Quantitative real-time RT-PCR

One μg of total RNA from the same samples used for microarray analysis was converted to cDNA using random primers and Superscript III reverse transcriptase according to the manufacture's instruction (Invitrogen, Carlsbad, CA, USA). Real-time PCR was performed on a LightCycler^{TM} thermal cycler (Idaho Technology, Salt Lake City, UT, USA). Roche LightCycler® TaqMan Master was used for reverse-transcription (Roche Diagnostics, Indianapolis, IN, USA) and HMOX1 and 18S primer sets were from TaqMan® Gene Expression Assays (Applied Biosystems, Foster City, CA, USA). HMOX1 was normalized to the expression level of 18S for each sample. Relative quantification was acquired by comparative CT (crossing threshold) method.

2.2.8 Polyacrylamide gel electrophoresis and western blotting

Protein was extracted from HUVEC grown on gelatin-coated 12-well multiplates after incubation with CDDO-Im (200 nM), CAPE (20 μM) or 0.1% DMSO for 6 h by addition of 50 μl of lysis buffer (NOVEX, San Diego, CA, USA) containing 10 mM tris (carboxyethyl) phosphine hydrochloride (Sigma, St Louis, MO, USA). Fifteen microliters, containing approximately 5 μg of protein, were run on NuPage 4-12% bis-tris gels (Invitrogen) and then transferred to a nitrocellulose membrane (Invitrogen). After blocking in 0.2% I-Block (Tropix, Bedford, MA, USA), 0.1% Tween-20 (Sigma) and

0.1% thimerosal (Sigma) in PBS, the blots were incubated with a rabbit anti-human HO-1 antibody (Stressgen Biotechnologies Inc., Vancouver, BC, USA; 1:5000) for 2 h. Rabbit ABC alkaline phosphatase reagents (Vector Laboratories, Burlingame, CA, USA) were used to label the bands and the alkaline phosphatase visualization was accomplished with nitro blue tetrazolium chloride (NBT) and 5-Bromo-4-chloro-3-indolyl phosphate (BCIP) (Invitrogen) until the bands developed. Quantitative analysis was performed with NIH Images (NIH, USA) on blots scanned into the computer.

2.2.9 Statistical analysis

Data are presented as the mean plus standard deviation. Differences among groups were analyzed using one-way analysis of variance (ANOVA) followed by post hoc tests of Tukey (equal variances assumed) or Games-Howell (equal variances not assumed) for multiple comparisons through SPSS statistical software. A difference of p value < 0.05 was considered significant. All experiments were performed at least 3 times and a representative experiment is presented.

2.3 RESULTS

2.3.1 Cytoprotection of CDDO-Im compared to CAPE against oxidative stress in HUVEC

To evaluate the effects of CDDO-Im on cytoprotection against oxidative stress, a model of oxidative stress induced by menadione-generated reactive oxygen species was developed as previously described [2]. Cytotoxicity of CDDO-Im in HUVEC is shown in (Figure 2.1). Because 750 nM of CDDO-Im resulted in more than 10% cell death, the

maximum doses of CDDO-Im used for cytoprotection testing were 500 nM. It was determined that a dose of 60 μM of menadione reduced viability to about 20%. CDDO-Im protected HUVEC against menadione-induced oxidant injury in a dose-dependent manner (Figure 2.2 A). To compare the cytoprotective effect of CAPE to CDDO-Im, HUVEC was treated with various doses of CAPE under the same extent of oxidative insult (60 μM menadione). The results showed that CAPE provided some cytoprotection to HUVEC in a dose-dependent manner (Figure 2.2 B). CAPE at 20 μM exhibited maximum protection of HUVEC with only about 30% recovery. On the other hand, CDDO-Im at 200 nM protected HUVEC leading to about 80% and at 400 nM about 90% cell recovery from menadione toxicity. This result indicated that CDDO-Im on a molar basis was about one hundred times more potent cytoprotectant than CAPE.

2.3.2 Identification of potential cytoprotective targets through microarray analysis

To investigate the mechanism of action and identify common molecular targets involved in the cytoprotective effect of CDDO-Im and CAPE in HUVEC, gene expression profiling with microarray analysis was used to monitor alterations in gene expression. For this analysis, triplicate HUVEC cultures were treated with CDDO-Im at an optimal cytoprotective dose of 200 nM and CAPE at 20 μM for 6 h, respectively and compared to vehicle controls. After processing microarray experiments; BRB Array Tool, an integrated software package for the visualization and statistical analysis of DNA, was used to analyze microarray data. Advantages of the BRB Array Tool software include: free excel add-in, flexible data import, excellent statistical tools, sophisticated visualization tools, and integratable gene lists with biological data. After filtering and normalization of gene expression data, class comparison of CDDO-Im or CAPE to the

vehicle treated control group was performed. Upon the activation of 200 nM CDDO-Im, the expression of 2229 genes was found to be significantly regulated ($p < 0.001$ and FDR ≤ 0.001) within 6 h. In addition, the expression of 1186 genes was found to be significantly changed ($p < 0.001$ and FDR ≤ 0.001) due to the treatment of 20 μM CAPE for 6 h.

To explore common pattern of gene expression altered in HUVEC under the action of CDDO-Im and CAPE, both gene lists were intersected and 339 genes were commonly altered in their expression. Among them, HMOX1, a well-known cytoprotective gene, was induced to about 9 fold by 20 μM CAPE similar to our previous finding [2]. However, 200 nM CDDO-Im, a dose hundred times lower than CAPE, triggered the induction of HMOX1 up to 43 fold. To validate this particular result from microarray screening, quantitative real-time RT-PCR and western blotting were performed for HMOX1 at 6 h. The results confirmed the induction of HMOX1 gene at transcriptional and translational levels (Figure 2.3 A/B). Interestingly, a number of molecular chaperone genes were highly up regulated by CDDO-Im. These genes were heat shock protein (HSP) and DNAJ related. To take a close look at the transcriptional activation of these chaperone genes by both compounds, we selected and listed all those genes in (Table 2.1). Sixteen chaperone genes were found to be induced by CDDO-Im. Among them, HSP genes HSPA1 (HSPA1A/HSPA1B) and HSPA6 were highly induced up to 150 and 100 fold at 6 h, and DNAJA4 was up regulated to around 80 fold. In comparison, CAPE up regulated 5 chaperone genes including 3 DNAJ genes and 2 HSP genes.

2.3.3 Functional enrichment and pathway analysis by IPA

To better understand the cytoprotective effects of CDDO-Im and CAPE in HUVEC, we used IPA to analyze microarray data sets for enrichment of transcriptional networks, functions, and pathways. The list of 339 common genes was first submitted to IPA to look for common pattern in functions and pathways. Results of network analysis indicate that the most relevant network to our list of genes was enriched in regulatory functions of cell death and survival, cellular development, and cellular growth and proliferation. The corresponding interactions of genes involved in this network were shown in (Figure 2.4 A). In addition, functional analysis found that these functions are among top ten molecular and cellular functions (p value ≤ 0.0001) most related to the list of common genes submitted, which was shown in (Figure 2.4 B). Results of pathway analysis identified one top canonical pathway of particular interest to us, Nrf2-mediated oxidative stress response, which was highly affected by both compounds (p value = 2.54E-04). Nrf2, a transcription factor, is known to play an important role in cellular defense system against oxidative stress through activation of an array of antioxidant and detoxification enzymes. The activation of this pathway may provide a possible mechanism for the cytoprotective effects of both compounds against oxidant insult in HUVEC as described above.

To explain the difference in cytoprotective effects, we submitted the lists of genes significantly altered by CDDO-Im and CAPE individually and compared their enrichments in cellular function and involvement in canonical pathways. Both compounds affected major cellular functions significantly without notable discrepancies as shown in (Figure 2.5). When focusing on canonical pathways, in particular Nrf2-mediated oxidative stress response, more related genes and genes with higher up-

regulation were found in CDDO-Im than CAPE treatment as shown in (Table 2.2). The canonical pathway representing Nrf2-mediated oxidative stress response from CDDO-Im treatment was shown in (Figure 2.6).

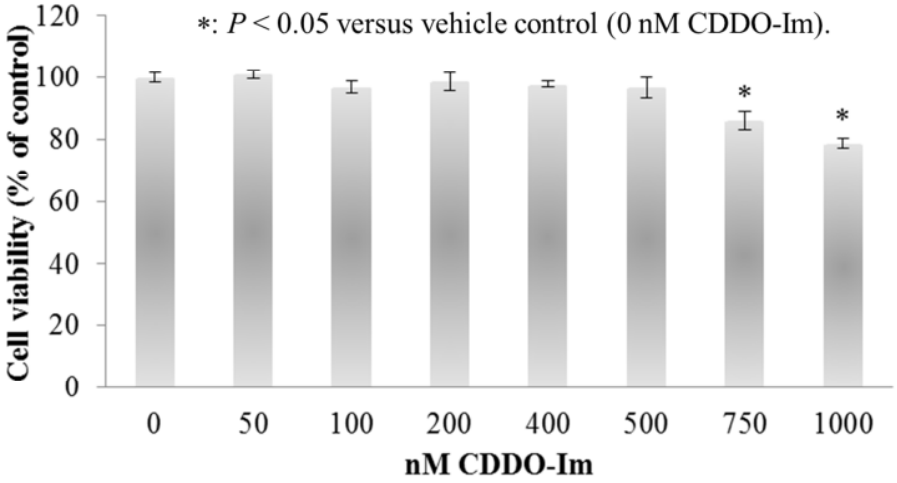

Figure 2.1: Cytotoxicity of CDDO-Im to HUVEC. Cell viability shown as percent of vehicle control and values presented as means ± standard deviations (n=3). Cell viability less than 90% was considered toxic. CDDO-Im at 750 and 1000 nM were considered toxic.

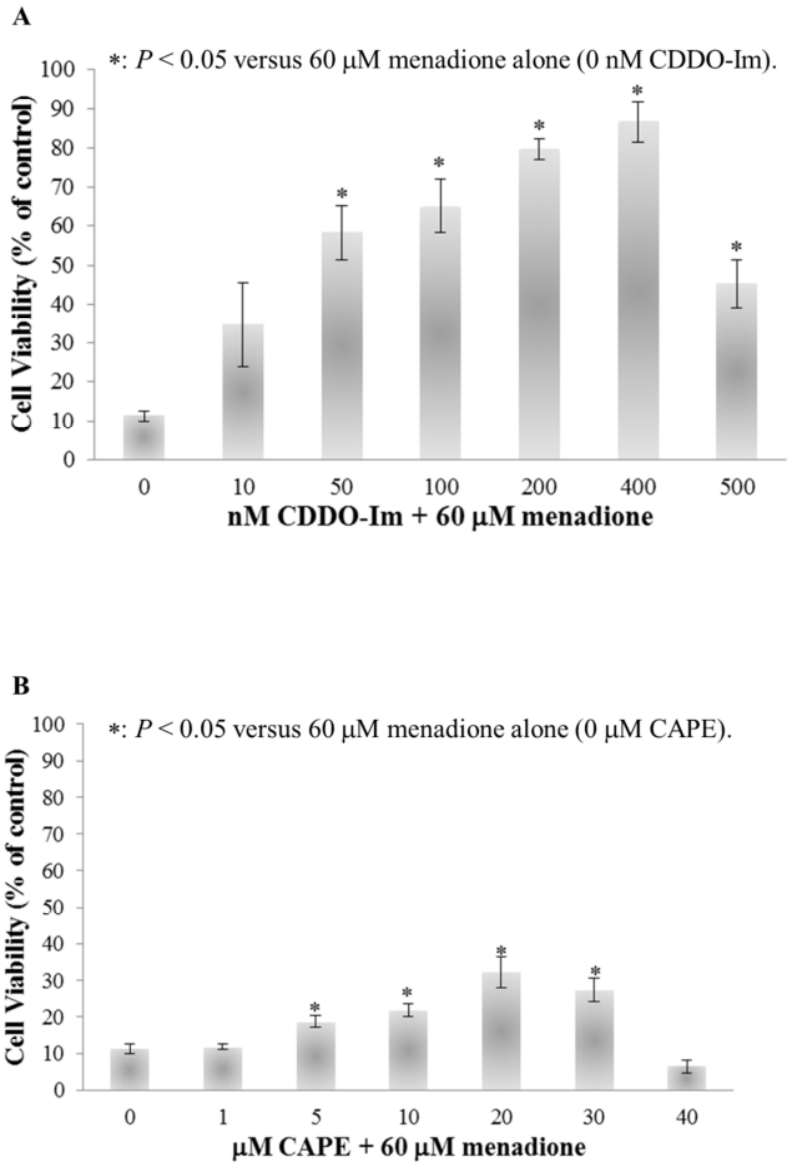

Figure 2.2: Cytoprotection of CDDO-Im (A) and CAPE (B) against menadione-induced cytotoxicity in HUVEC. Cell viability is shown as percent of vehicle control and values presented as means ± standard deviations (n=3). CDDO-Im and CAPE showed a dose-dependent cytoprotection of HUVEC from 60 μM menadione-induced oxidative stress. CDDO-Im at 200 nM recovered HUVEC significantly to about 80%, whereas CAPE at 20 μM only salvaged around 30% HUVEC compared to control group.

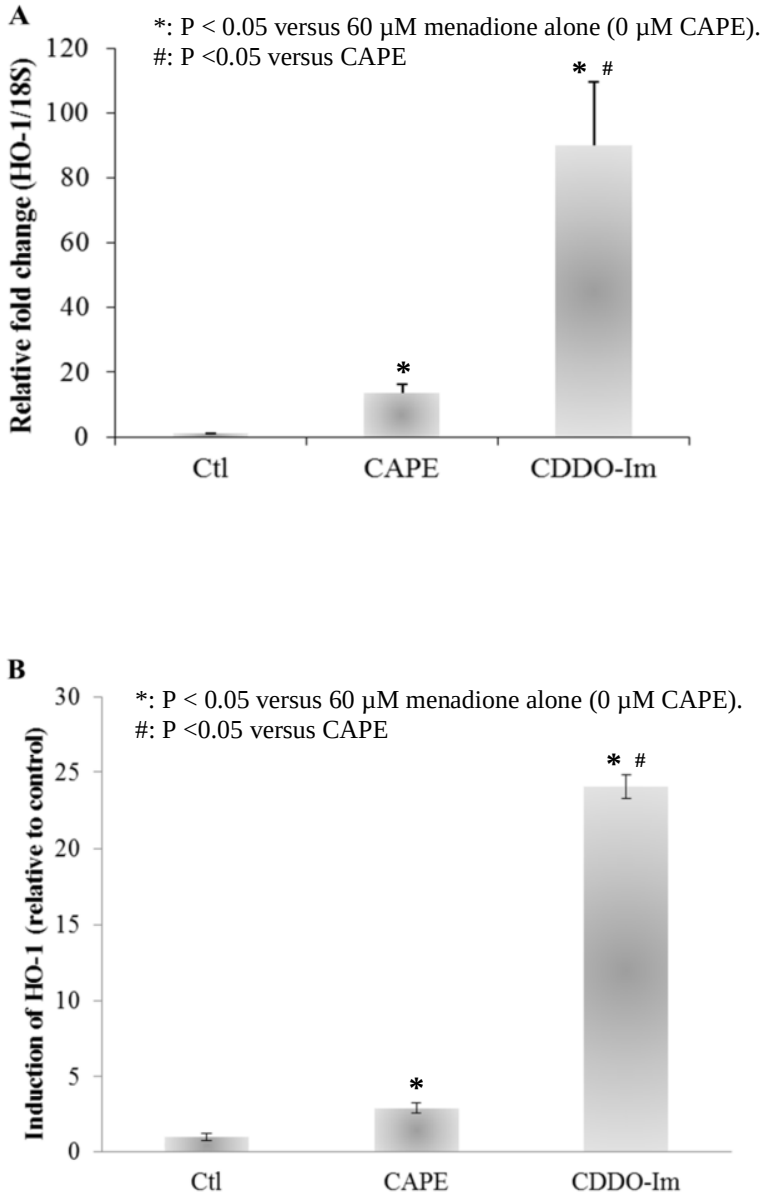

Figure 2.3: Comparison of HMOX1 induction in HUVEC at transcriptional level (A) and translational level (B) by CAPE and CDDO-Im. HMOX1 mRNA was induced up to 90 fold by 200 nM CDDO-Im within 6 h compared to a 13-fold increase following 20 µM CAPE treatment. In addition, HO-1 protein was induced up to 24 fold by 200 nM CDDO-Im within 6 h compared to a 3-fold increase following 20 µM CAPE treatment (n=3).

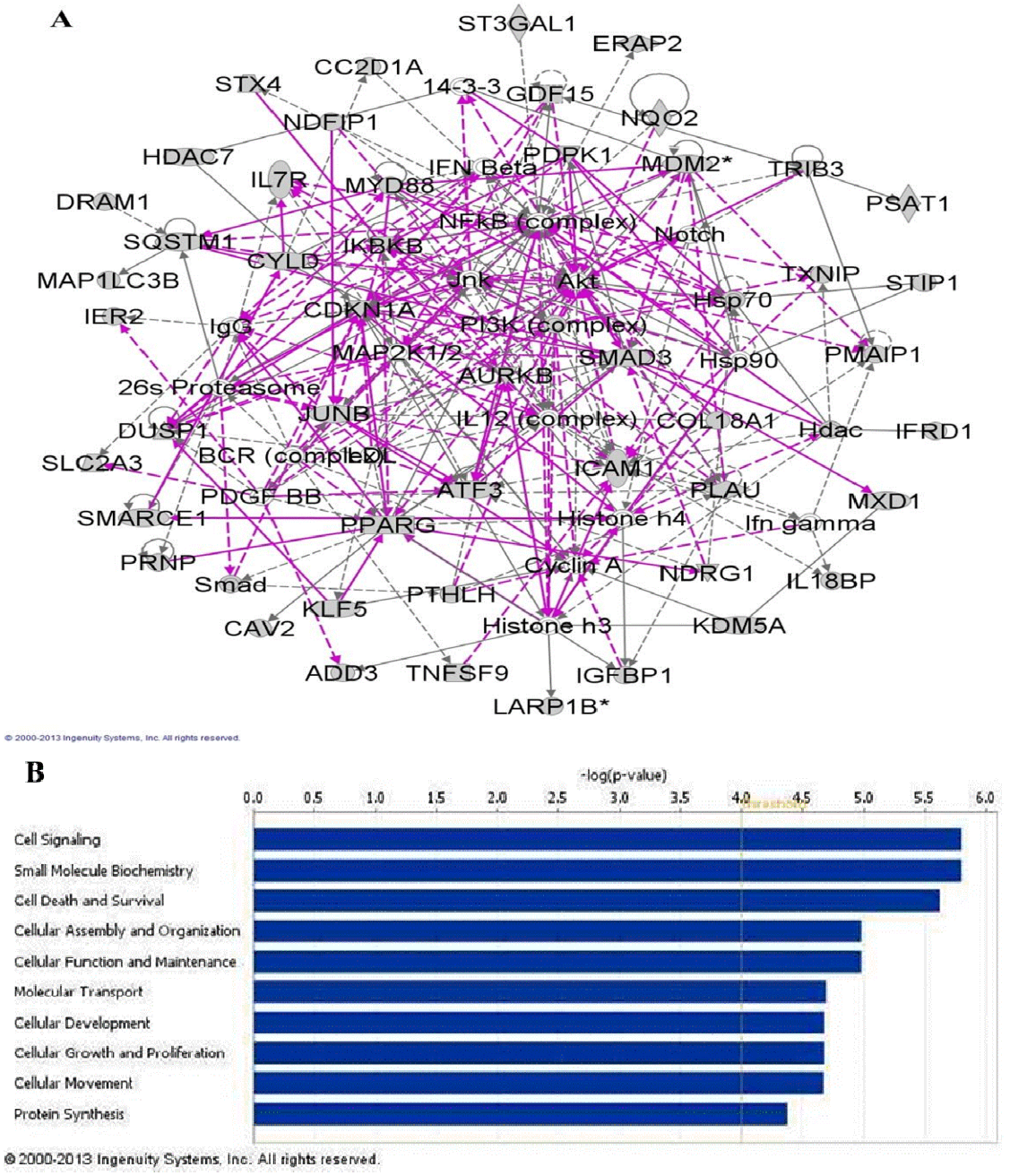

Figure 2.4: Top scored network (A) and functions (B) of genes commonly altered by CDDO-Im and CAPE. Network associated functions involve cell death and survival, cellular development, and cellular growth and proliferation, which are among top ten molecular and cellular functions commonly regulated by both compounds.

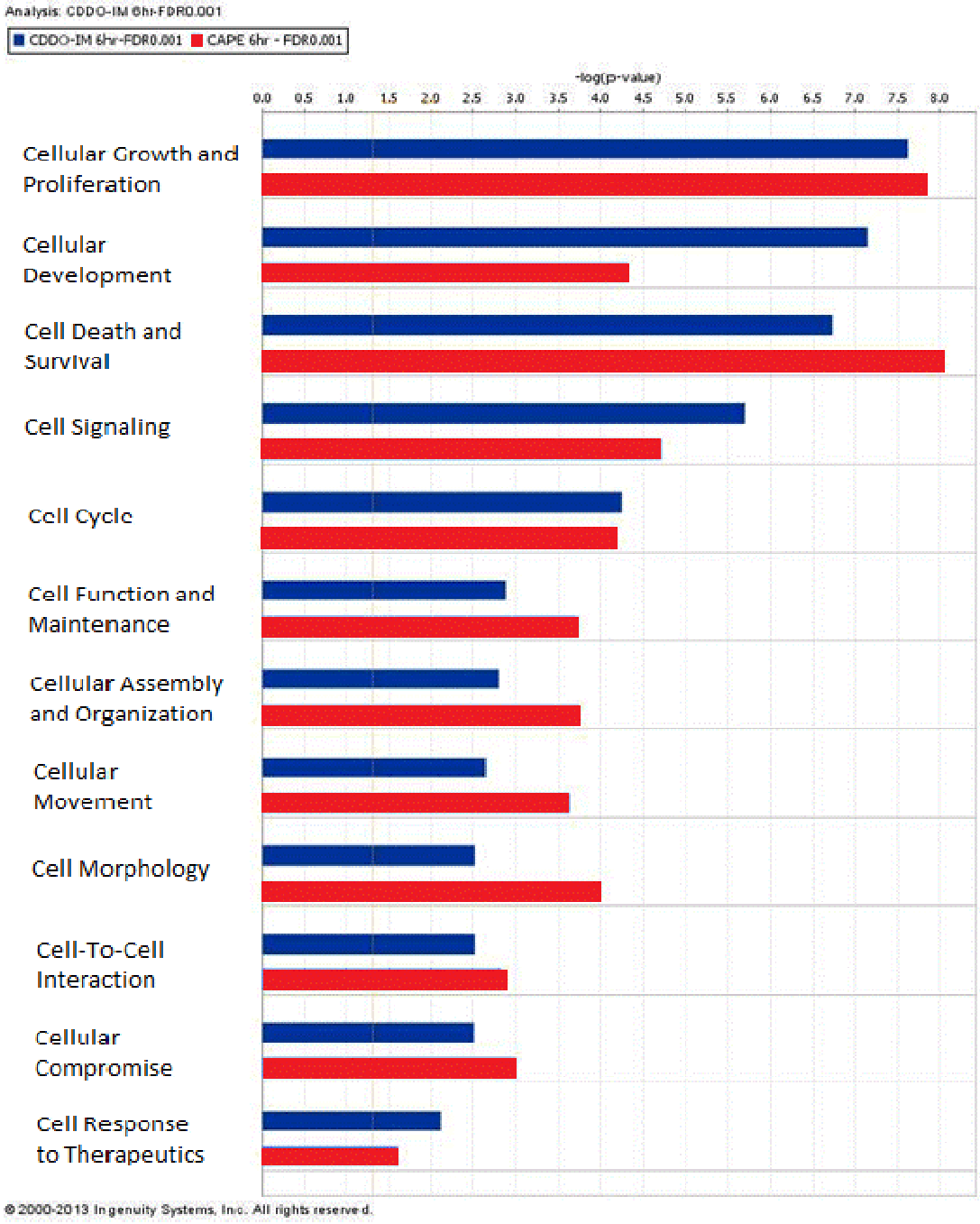

Figure 2.5: Comparison of cellular functions most highly enriched in the gene sets altered by CDDO-Im and CAPE.

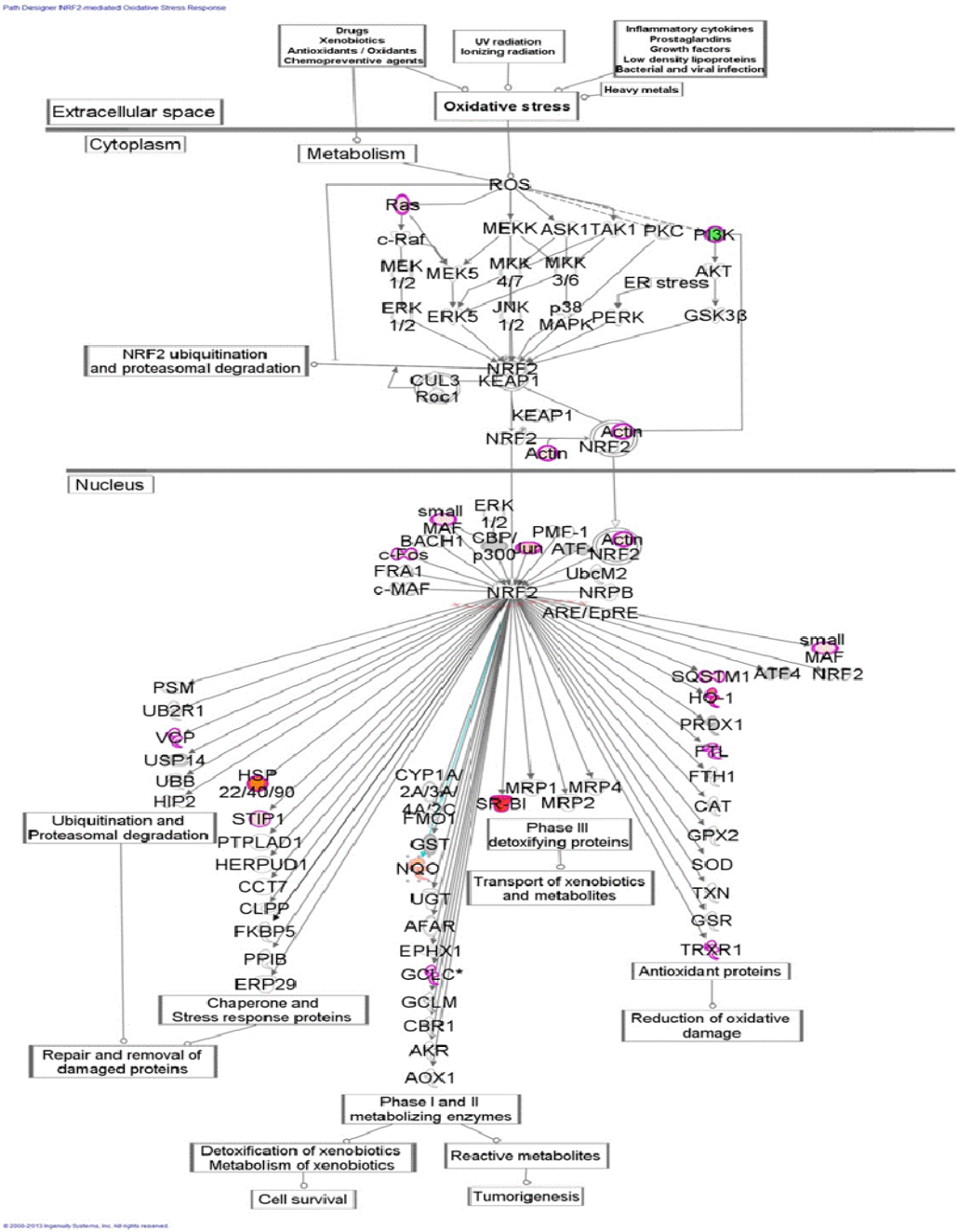

Figure 2.6: Nrf2-mediated oxidative stress response pathway from IPA analysis of CDDO-Im gene set. Genes up- and down-regulated are in red and green, respectively.

.

Symbol	Entrez Gene Name	CDDO-Im (200 nM)	CAPE (20 μM)
HSPA1A/HSPA1B	heat shock 70kDa protein 1A	152.85	2.3
HSPA6	heat shock 70kDa protein 6 (HSP70B')	103.07	
DNAJA4	DnaJ (Hsp40) homolog, subfamily A, member 4	83.56	
DNAJB1	DnaJ (Hsp40) homolog, subfamily B, member 1	20.3	
HSPH1	heat shock 105kDa/110kDa protein 1	12.1	
HSPB8	heat shock 22kDa protein 8	8.86	
HSP90AA1	heat shock protein 90kDa alpha (cytosolic), class A member 1	4.74	
DNAJB4	DnaJ (Hsp40) homolog, subfamily B, member 4	4.21	
DNAJB9	DnaJ (Hsp40) homolog, subfamily B, member 9	4.19	10.46
HSPA8	heat shock 70kDa protein 8	3.44	
DNAJB6	DnaJ (Hsp40) homolog, subfamily B, member 6	3.27	24.13
HSPD1	heat shock 60kDa protein 1 (chaperonin)	2.99	
HSP90AB1	heat shock protein 90kDa alpha (cytosolic), class B member 1	2.28	
DNAJC21	DnaJ (Hsp40) homolog, subfamily C, member 21	2.24	
HSPA9	heat shock 70kDa protein 9 (mortalin)	2.2	
DNAJC3	DnaJ (Hsp40) homolog, subfamily C, member 3	1.91	4.05
HSP90B1	heat shock protein 90kDa beta (Grp94), member 1		4.49

Table 2.1: Molecular chaperone genes significantly altered (6 h, fold change > 2) by CDDO-Im and CAPE treatment in HUVEC

Symbol	Entrez Gene Name	CDDO-Im (200nM)	CAPE (20μM)
DNAJA4	DnaJ (Hsp40) homolog, subfamily A, member 4	83.66	
SCARB1	scavenger receptor class B, member 1	59.59	
HMOX1	heme oxygenase (decycling) 1	42.62	9.38
DNAJB1	DnaJ (Hsp40) homolog, subfamily B, member 1	20.3	
JUNB	jun B proto-oncogene	17.77	3.85
SQSTM1	sequestosome 1	10.3	3.02
HSPB8	heat shock 22kDa protein 8	8.66	
NQO2	NAD(P)H dehydrogenase, quinone 2	6.89	2.02
FOS	FBJ murine osteosarcoma viral oncogene homolog	6.82	16.34
GCLC	glutamate-cysteine ligase, catalytic subunit	6.78	
VCP	valosin containing protein	6.17	
NQO1	NAD(P)H dehydrogenase, quinone 1	4.48	
MAFG	v-maf musculoaponeurotic fibrosarcoma oncogene homolog G (avian)	4.26	
DNAJB4	DnaJ (Hsp40) homolog, subfamily B, member 4	4.21	
DNAJB9	DnaJ (Hsp40) homolog, subfamily B, member 9	4.19	10.46
ACTG1	actin, gamma 1	3.34	
DNAJB6	DnaJ (Hsp40) homolog, subfamily B, member 6	3.27	24.13
STIP1	stress-induced-phosphoprotein 1	3.08	4.44
TXNRD1	thioredoxin reductase 1	3.06	
FTL	ferritin, light polypeptide	2.88	2.62
SOD1	superoxide dismutase 1, soluble	2.35	
DNAJC21	DnaJ (Hsp40) homolog, subfamily C, member 21	2.24	
MRAS	muscle RAS oncogene homolog	2.04	
DNAJC3	DnaJ (Hsp40) homolog, subfamily C, member 3	1.91	4.05
PIK3C2B	phosphatidylinositol-4-phosphate 3-kinase, catalytic subunit type 2 beta	-4.167	-1.981
ACTA2	actin, alpha 2, smooth muscle, aorta		2.22
BACH1	BTB and CNC homology 1, basic leucine zipper transcription factor 1		2.44
EIF2AK3	eukaryotic translation initiation factor 2-alpha kinase 3		3.75
RRAS2	related RAS viral (r-ras) oncogene homolog 2		3.1

Table 2.2: Genes involved in Nrf2-mediated oxidative stress response pathway and modulated by CDDO-Im and CAPE in HUVEC.

2.4 DISCUSSION AND CONCLUSIONS

Redox homeostasis within cells refers to a well-controlled balance between cellular antioxidant system and ROS generation. Maintenance of the cellular redox homeostasis is important for a number of biological processes since ROS at physiological level have been reported to serve as potential signaling molecules mediating cellular proliferation, differentiation, and apoptosis [175]. However, when this balance is disturbed as a result of oxidative stress where the overproduced ROS failed to be eliminated by the antioxidant system, the accumulation of excessive ROS may result in severe damage to cellular components and eventually involve in various diseases including ischemia/reperfusion injury, cardiovascular diseases, neurodegenerative diseases, and cancer [176-179].

In a continuing effort to identify potential agents for ameliorating oxidative stress, we compared a synthetic triterpenoid compound, CDDO-Im to CAPE, and tested their ability to protect human endothelial cells from oxidative stress. Nanomolar concentrations of CDDO-Im were sufficient to keep HUVEC viability close to 80% to oxidative stress induced by menadione. The cytoprotection provided by CDDO-Im was more potent than that of CAPE, a natural polyphenolic compound we previously found cytoprotective [2, 49]. Under the same degree of oxidative stress, CAPE at micromolar concentrations only improved survival of HUVEC to 30%. We then explored mechanisms of this cytoprotection by looking for any common cytoprotective factors shared by both CAPE and new cytoprotective mediators induced by CDDO-Im, which may provide a possible explanation for the different cytoprotective effects observed.

We investigated the alteration of global gene expression using microarrays to identify the principal genes mediating HUVEC cytoprotection following the treatment of

CDDO-Im and CAPE. We found 2229 and 1186 genes were statistically significantly regulated in HUVEC after 6 h treatment of CDDO-Im and CAPE at optimal cytoprotective dose of 200 nM and 20 μM, respectively. Out of those genes, 339 genes were found commonly altered by both compounds, which may lead to a common mechanism of cytoprotection both compounds have employed. Out of these 339 genes, HMOX1 (heme oxygenase (decycling) 1) was found to be one of them. CDDO-Im was reported to be a strong inducer of HMOX1 in different cell lines at a similar range of nanomolar concentrations [108, 180, 181]. Our result confirmed and found HMOX1 was highly up-regulated by CDDO-Im up to 43 fold in HUVEC which is much higher than HMOX1 induction by CAPE (9 fold). This result from microarray analysis was confirmed at both transcriptional and translational levels. Much higher expression of HMOX1 mRNA and protein was observed in CDDO-Im group compared to the group of CAPE treatment. Our previous study showed that HMOX1 was induced by CAPE, which plays a very important role in its cytoprotection of HUVEC. The much higher up-regulation of HMOX1 by CDDO-Im may contribute, at least, in part to its greater cytoprotective effect than CAPE.

In addition to the up-regulation of HMOX1, CDDO-Im was found, for the first time to our knowledge, to strongly induce genes of HSP family, especially HSPA1, HSPA6, and DNAJA4. Heat shock proteins, a highly conserved class of stress response proteins, function as molecular chaperones to prevent protein aggregations, correct protein misfolding, and promote protein refolding. These functions of HSPs are crucial to the maintenance of cellular homeostasis by controlling cellular stress such as endoplasmic reticulum (ER) stress and oxidative stress [182, 183]. During ER stress, HSPs are expressed through activation of pathways called unfolded protein response (UPR). UPR can also trigger downstream antioxidant response, which provides a line of

defense against oxidative stress. When cells are exposed to oxidative stress, a cascade of events occurs including change of cellular redox balance, oxidation of cell lipid proteins, and protein aggregation and misfolding. As a consequence, inflammation and apoptosis pathways are activated, eventually leading to the failure of normal cell function and cell death. However, the induction of HSP can effectively interact with these events and rescue cells from stress induced programmed death. For example, heat shock protein Hsp33 was activated due to a change in redox state within bacteria cells [184]. Its homologue in eukaryotic cells, Hsp32, was reported to be induced through redox-sensitive transcription factors in response to redox change [185]. Interestingly Hsp32 is also referred to as HO-1. Therefore, HO-1 is considered one of the HSPs, which enhances the cytoprotective potential of heat shock proteins against oxidative stress. In addition, some HSPs such as Hsp70 can bind to apoptosis mediators such as apoptosis protease activating factor-1 and therefore prevent cell death to occur [186]. This anti-apoptotic effect of HSPs appears to be independent of their function as molecular chaperones. Up-regulation of Hsp70 was also found to reduce inflammatory response possibly through interaction with a transcriptional factor, nuclear factor kappa B [187].Since inflammatory response is one of the events that occurs following oxidative stress, anti-inflammatory property can contribute to the overall cytoprotective capacity of HSP against oxidative stress. Compared to CDDO-Im, CAPE induced not only less number of HSPs but also to a less extent. For example, HSPA1 was up-regulated to 150 fold upon action of CDDO-Im but only to 2 fold under CAPE treatment. The potential cytoprotective role of HSPs against oxidative stress could be added as another contributor to explain why CDDO-Im, a more potent HSP inducer, protected HUVEC against oxidant insult much better than CAPE.

To identify the cellular phenotypes most significant to the alteration of our gene expression profiles and further understand the corresponding impact of these changes in the content of well-characterized pathways, IPA was used to analyze the microarray data. For the purpose of extracting common pattern between CDDO-Im and CAPE, 339 “in common” genes were analyzed. The results indicate that top cellular functions include cell signaling, cell death and survival, cellular function and maintenance, cellular development, cellular growth and proliferation and protein synthesis, which is in agreement with the major functions of top network generated out of the set of common genes. In addition, canonical pathway analysis pointed out that Nrf2-mediated oxidative stress response pathway was highly regulated. This Nrf2 pathway mediates the expression of an array of genes involved in drug metabolism and transport, antioxidant defense, and oxidant signaling [174]. It is considered a useful strategy of detoxification that cells apply to response to the challenges from endogenous and exogenous oxidants, electrophiles, and toxicants. Activation of this pathway was reported to facilitate the induction of HMOX1 [108, 180, 181]. In a continuing effort to address the different cytoprotective ability of CDDO-Im and CAPE, a core analysis of individual data set and follow-up comparison were performed in IPA. The significance of top cellular functions was found similar between groups of CDDO-Im and CAPE. However, Nrf2-mediated oxidative stress response pathway was much more significantly activated in the case of CDDO-Im with more genes involved and higher level of gene up-regulation.

In summary, CDDO-Im was identified as a more potent cytoprotectant than CAPE protecting human endothelial cells from oxidative stress. Both compounds were found to induce HMOX1, affect similar cellular functions, and regulate Nrf2-mediated oxidative stress response pathway, which may provide a common mechanism behind this cytoprotection. Results suggest that the higher potential and greater cytoprotection

observed in CDDO-Im could possibly due to 1) stronger induction of HMOX1; 2) more intensive activation of Nrf2 –mediated oxidative stress response pathway; and 3) up-regulation of molecule chaperone HSP family [188]. This is a first report that CDDO-Im was found to induce HSPs to our knowledge, which is useful in further understanding of the beneficial effects of this compound. Based on current knowledge in the field and our results, we extrapolate that CDDO-Im may serve as a potent inducer of preconditioning endoplasmic reticulum (ER) and oxidative stresses to activate unfolded protein response, which in turn induces the expression of HSPs and triggers Nrf2-mediated antioxidant response in particular the up-regulation of HMOX1. While CDDO-Im has previously been shown to not have significant direct antioxidant abilities, the next series of studies presented here will evaluate CDDO-Im and CDDO-Me as potential post-treatments against oxidant stress in human endothelial cells to determine if the compounds could confer cytoprotection through rapid initiation of protective genes such as HMOX1.

CHAPTER 3

Cytoprotection of Human Endothelial Cells from Oxidant Stress by Post-Treatment with CDDO-Im and CDDO-Me:Network Analysis of Genes Responsible for Cytoprotection and Differences in Mechanism of Action

3.1 INTRODUCTION

Oxidative stress is commonly encountered in neurodegenerative diseases such as Parkinson's, Alzheimer's, and Huntington's, vascular disorders including strokes and heart attacks, as well as traumatic injuries. Oxidative stress results from the disproportion between antioxidant and prooxidant defense processes of the body. The endothelial cells that line the blood vessel wall are very responsive to injury caused by oxidative stress. Endothelial cells play a crucial role in maintaining hemostasis; any injury or abnormality in the endothelial cell structure and function such as that caused by oxidative stress can contribute to blood vessel diseases including thrombosis, vasculitis, and atherosclerosis.

The imidazole (CDDO-Im) and the C-28 methyl ester (CDDO-Me) derivative of 2-cyano-3,12-dioxooleana-1,9-dien-28-oic acid (CDDO), synthetic oleanane triterpenoids, have been shown to protect against oxidative stress in various cell and animal models [127, 134, 181, 189-191] and exhibit anti-inflammatory properties. In addition, they have been shown to provide a chemopreventative effect against certain tumors, largely by reducing the viability of these cells [192-194]. How drugs can be cytoprotective in normal cells and cytotoxic in tumors and tumor-derived cells is not

immediately clear. Understanding this paradox will require a better understanding of the specific response of different cell types to drugs.

We recently determined that CDDO-Im was 100X more potent as a cytoprotectant than caffeic acid phenethyl ester (CAPE) [188] against menadione-induced oxidant stress when given as a pre-treatment prior to subjecting HUVEC to oxidant stress and that induction of heme oxygenase-1 was required for cytoprotection. Most *in vitro* studies with CDDO derivatives showing cytoprotection have used a pre-treatment of 4 to 24 hrs [127, 195-197]. Here we asked if cytoprotection of endothelial cells was obtained if CDDO-Im and CDDO-Me were given at the initiation of oxidant stress. Endothelial cells line vessel walls and are one of the first cell types exposed to drugs and I/R injury or oxidative stress injury and appear to be an important target for cytoprotection. They have also been shown to be active in response to inflammatory stimuli and their transcriptional response to such stimuli has been well documented in the literature [198-200]. Previous studies have utilized HUVEC to demonstrate protection against oxidative stress-induced injury by treatment with CAPE, a plant-derived polyphenolic compound [1, 2, 49]. The injury induced by menadione, a well-known agent for inducing oxidative stress, was reduced by cytoprotective agents and this cytoprotection was highly correlated with HMOX1 induction [201]. The oxidant stress produced by appropriate doses of menadione results from intracellular production of reactive oxygen species (ROS) by redox cycling [202]. In this study, menadione-induced endothelial injury was used as an *in vitro* model to simulate I/R injury and for screening compounds that could provide protection against oxidative stress injury by inducing cytoprotective genes such as HMOX1. The purpose of

the present study was to determine if post-treatment by CDDO-Im and CDDO-Me was cytoprotective, to further investigate the precise mechanisms of the cytoprotective response of HUVEC to these agents, and to evaluate if gene expression profiling could determine which agent was more likely to be most efficacious in cytoprotection.

3.2 MATERIALS AND METHODS

3.2.1 Materials and Reagents

CDDO-Im and CDDO-Me (95% and 96% purity respectively) were purchased from Toronto Research Chemicals Inc. (Toronto, Ontario, Canada). Menadione sodium bisulfite (menadione) and DMSO were from Sigma-Aldrich (Saint Louis, MO, USA). Sn(IV) protoporphyrin IX dichloride (SnPPIX) was purchased from Frontier Scientific (Logan, UT, USA).

3.2.2 Cell Culture

Stock cultures of gender-mixed HUVEC (Lifeline Cell Technology, Walkersville, MD) pooled from 10 different donors were cultivated on T75 flasks (Sigma-Aldrich,Saint Louis, MO, USA) in MCDB 131 medium at 37 °C in a humidified atmosphere of 92% nitrogen and 3% oxygen 5% CO2 with medium changes every 2 days until confluent [203, 204]. MCDB 131 Medium, Trypsin/EDTA, antibiotic/antimycotic was obtained

from Life Technologies (Carlsbad, CA). Endothelial supplements were obtained from ATCC. Prior to an experiment, HUVEC were subcultivated with Trypsin/EDTA onto Costar® 96-well multiplates (Corning Incorporated, Corning, NY, USA) at 5000 cells/cm2, grown to confluence in 95% air, 5% CO2, and kept for 72 h to produce a quiescent cell layer. Only the second through fifth population doublings of cells were used as described in [2].

3.2.3 *In vitro* cytotoxicity assay

CDDO-Im and CDDO-Me were dissolved in DMSO and diluted 1000-fold with medium (0.1% final concentration of DMSO) before addition of serial dilutions to the 96-well culture plates. To assess the compound's toxicity, confluent HUVEC were initially pretreated with CDDO-Im and CDDO-Me at various concentrations (0-3000 nM) for 6 h. Cell viability was assessed at 24 h after initiation of injury by replacing medium with fresh medium containing resazurin (44 M final in medium; Sigma-Aldrich, Saint Louis, MO, USA), which is converted irreversibly to fluorescent resorufin by viable cells [205]. The cells were incubated for 2 h at 37 °C and fluorescence was measured at 545 nm excitation and 590 nm emissions using SpectraMAX M2 microplate reader (Molecular Devices, Sunnyvale, CA, USA). HUVEC were regularly observed under phase contrast microscopy for confirmation of viability results.

3.2.4 Menadione cytotoxicity and cell viability assays

Menadione bisulfite (0.5 M) was dissolved in phosphate buffered saline (PBS) and diluted with medium before being added to the plate wells [206]. Due to differences in cellular responses to menadione, each group of pooled HUVEC was initially assessed for a dose of menadione which resulted in 80–90% cell death. A dose of 70 µM menadione was chosen for cell viability comparisons between CDDO-Im and CDDO-Me.

For cell viability measurements CDDO-Im and CDDO-Me (200 nM) were given at the initiation of injury (with 70 µM menadione). Cell viability assays were assessed 24 h after initiation of injury. Cytotoxicity and cell viability were measured using the same methods as described above (Section 3.2.3). Additionally, propidium iodide was used as described by [207]. Briefly, propidium iodide was added during the last hour of the 24 h incubation, and similar results were obtained as those described here with the resazurin assays.

3.2.5 Total RNA isolation and gene expression analysis

Total RNA was extracted from cultured HUVEC grown in 12-well multiplates with TRI™ reagent according to the manufacturer's instructions (Molecular Research Center, Cincinnati, OH, USA). RNA yield was quantified using NanoDrop® ND-1000 Spectrophotometer (NanoDrop Technologies, Wilmington, DE, USA), and its quality

was assessed by electrophoresis on 1% agarose gels containing 1:1000 SYBR Gold in the loading buffer (Invitrogen, Carlsbad, CA, USA).

RNA (500 ng) from four biological replicates from each group (DMSO, CDDO-Im, and CDDO-Me) were labeled through the use of Agilent's Low RNA Input Linear Amplification Kit (Agilent, Santa Clara, CA). All sample-labeling, hybridization, washing, and scanning steps were conducted according to the manufacturer's specifications. For each group, 200 ng of cRNA (anti-sense labeled sample obtained from Agilent low RNA input linear amplification kit) from each labeling reaction was hybridized to the Agilent Whole Human Genome Oligo Microarray (Agilent, Santa Clara, CA). The Whole Human Genome Oligo Microarray is in an 8 X 60k slide format and microarray interrogates all known genes. After hybridization, the slides were washed and then scanned with the Agilent G2505C Microarray Scanner System (Agilent, Santa Clara, CA). The fluorescence intensities on scanned images were extracted and preprocessed by Agilent Feature Extraction Software.

3.2.6 Polyacrylamide gel electrophoresis and western blotting

Protein was extracted from the HUVEC after incubation for 6 h with 200 nM CDDO-Im or CDDO-Me, the same dose as used for gene expression studies, by addition of 50 μl of lysis buffer (Life Technologies, Grand Island, NY) containing 10 mM tris (carboxyethyl) phosphine hydrochloride (Sigma, St Louis, MO, USA). Fifteen microliters, containing approximately 5 μg of protein, from each treatment were run on E-PAGE 96-well 6% gels (Life Technologies, Grand Island, NY) and then transferred to a nitrocellulose membrane (Life Technologies, Grand Island, NY). After incubating in

blocking buffer (LICOR, Lincoln, Nebraska USA), individual blots were incubated with rabbit HMOX1 (Assay Designs Inc., Ann Arbor, MI, USA; 1:5000) and rabbit NQO1 (Abcam, Cambridge, MA; 1:5000) primary antibodies for 1 h. The blots were washed three times with 0.1% Tween 20 in PBS incubated with donkey anti-rabbit secondary antibody (LICOR, Lincoln, Nebraska USA) for 30 minutes, washed again, and allowed to dry. Visualization was performed using the Odyssey imaging system (LICOR, Lincoln, Nebraska USA) that allowed for dual labeling of two different proteins. Mouse monoclonal anti-human β-actin antibody (Sigma, St Louis, MO, USA) was used for normalization and labeled on the same blots with donkey anti-mouse secondary antibody (LICOR, Lincoln, Nebraska USA).

3.2.7 Quantitative real-time RT-PCR

One μg of total RNA from the same samples used for microarray analysis was converted to cDNA using the high capacity cDNA Archive Kit (Life Technologies, Grand Island, NY). Real-time PCR was performed on a Roche LightCycler® 480 thermal cycler (Roche Diagnostics, Indianapolis, IN, USA) with Roche LightCycler® TaqMan Master Kit (Roche Diagnostics, Indianapolis, IN, USA) for confirmation of microarray results. 18S primer/probe was used as an endogenous control for each sample and measured simultaneously with each labeled sample for purposes of normalization; relative quantification was acquired by the comparative CT method [208] . Primer/probes of interest (HMOX1, HSP1A1, OSGIN1, RASD1, NDUFA4L2, SPON2, NQO1, BBC3,

and COL1A1) and 18S primer sets were purchased from TaqMan® Gene Expression Assays (Applied Biosystems, Foster City, CA, USA).

3.2.8 Heme oxygenase-1 inhibition with SnPPIX

To measure the role of HMOX1 in cytoprotection, HUVEC were treated with 200 nM CDDO-Im at various doses of HMOX1 inhibitor SnPPIX (0-60 μM) for 6 h before exposing each group to menadione for 24 h. SnPPIX was dissolved in 0.1 M NaOH and diluted 1000-fold with medium before being added to the 96-well culture plates. Cell viability was measured using the resazurin assay.

3.2.9 Statistical analysis

Data are presented as the mean±standard deviation. Differences between or among the groups were analyzed using the independent samples T test or one-way analysis of variance combined with Tukey (equal variances assumed) or Games-Howell (equal variances not assumed) post hoc analysis using SPSS (IBM, Armonk, NY). Statistical significance was set at p value < 0.05. Each cytoprotection experiment was repeated at least 3 times and a representative experiment is presented.

3.2.10 Microarray analysis with BRB Array Tools

First a two-class comparison was performed to identify genes that were differentially expressed using a random-variance t-test (http://linus.nci.nih.gov/BRB-ArrayTools.html;version 4.4) [209]. Genes were considered significantly altered in their expression if the false discovery rate was less than 10%.

Clustering based on Cluster [210] and dendrogram generation with Treeview [211] were performed with Cluster 3.0 (http://bonsai.hgc.jp/~mdehoon/software/cluster/). Significantly altered genes were submitted to GeneMANIA (http://genemania.org/) software for network analysis [212-214].

3.3 RESULTS

3.3.1 CDDO-Me was more cytotoxic than CDDO-Im

The cytotoxicity of CDDO-Im and CDDO-Me was examined from 0 to 3000 nM and are shown in (Figure 3.1). Equimolar CDDO-Me doses between 2000 nM and 3000 nM were more cytotoxic than CDDO-Im. The dose used for subsequent testing in the cytoprotection assays was 200 nM for both compounds as this dose by itself had no effect on viability.

3.3.2 CDDO-Im was more cytoprotective against oxidant stress than CDDO-Me

In contrast to other studies in which cells were treated for 6-24 h prior to injury [127, 195-197]; CDDO-Im and CDDO-Me protected HUVEC against menadione-induced oxidative stress when given at the initiation of injury with menadione. Seventy

μM menadione reduced the viability of HUVEC by 90% and CDDO-Me improved survival to 40% ±1.7 while CDDO-Im improved survival to 50% ±2.6 (Figure 3.2). This result indicated this class of compounds can stimulate the cytoprotective response more rapidly than has been reported for other inducers of cytoprotection, although greater cytoprotection was provided with a preincubation of 6 h [188].

3.3.3 CDDO-Im and CDDO-Me have different gene expression profiles

Gene expression profiling of CDDO-Im and CDDO-Me in HUVEC treated for 6 hours was compared to the vehicle control using Agilent Whole Human Genome microarrays. Of the 44,000 probes interrogated on the microarray, 14,000 were present and detected by BRB-Array Tools, which performed a univariate T-test to determine significance of differentially induced genes. Twenty-three significantly up- or down-regulated genes were found to be in common with both compounds, however, 382 additional genes were altered in their expression by CDDO-Im only (Figure 3.4). A heat map of genes statistically altered in their expression (up- or down-regulated more than 8-fold) following clustering is shown in (Figure 3.3). Both CDDO derivatives highly induced HMOX1, (39-fold by CDDO-Im) and 26-fold (CDDO-Me) compared to the DMSO control, but CDDO-Im induced the expression to a greater extent ($P<0.005$). Similarly, greater increases in gene expression resulting from CDDO-Im treatment were seen in other genes including HSP1A1, SPON2, COL1A1, and NQO1 ($P<0.005$; Figure 3.3).

Network analysis using Genemania was performed to evaluate the connectivity between the twenty-three “in common” set of genes between CDDO-Im and CDDO-Me (Figure 3.8) and the “differences” between the two compounds by network analysis of the 382 CDDO-Im only expressed genes (Figure 3.9).

3.3.4 RT-PCR and Western Blotting confirms expression differences

To validate the microarray results, quantitative RT- PCR was performed on several key genes at 6 h. The results confirmed that the HMOX1 gene was up-regulated about 29-fold for CDDO-Im and 20-fold for CDDO-Me (Figure 3.5) while the protein product (6h time point) for Heme Oxygenase-1 was shown to have a 4-fold increase for CDDO-Im compared to a 2.4-fold increase for CDDO-Me compared to DMSO control (Figure 3.6). mRNA induction of heat shock protein 70 (HSPA1A) similarly confirmed the microarray results such that CDDO-Im had a 5.5-fold increase compared to CDDO-Me (2.8-fold) (Figure 3.5). BCL2 binding component 3 (BBC3) mRNA expression, through RT-PCR, showed cogent down-regulation for CDDO-Im and CDDO-Me (0.71-fold and 0.76-fold respectively; Figure 3.5). Additionally, gene expression differences between the compounds seen in the microarray studies were confirmed by RT-PCR including increased induction of expression by CDDO-Im treatment of SPON2, COL1A1, and NQO1 (Figure 3.5). Furthermore, CDDO-Im treatment resulted in significantly greater protein induction of NQO1 compared to DMSO control ($P<0.05$) while CDDO-Me was unchanged compared to the same control (Figure 3.6).

3.3.5 Heme oxygenase-1 inhibitor (SnPPIX) abrogates CDDO-Im cytoprotection

To test whether the cytoprotective component responsible for the protection shown by CDDO was dependent on HMOX1 activity, HMOX1 activity was blocked by its competitive inhibitor SnPPIX [2, 215, 216]. By coincubation with varying concentrations of SnPPIX and 200 nM CDDO-Im a reduction in cytoprotective activity was seen against a 70 μM induced menadione oxidative stress injury in HUVEC (Figure 3.7).

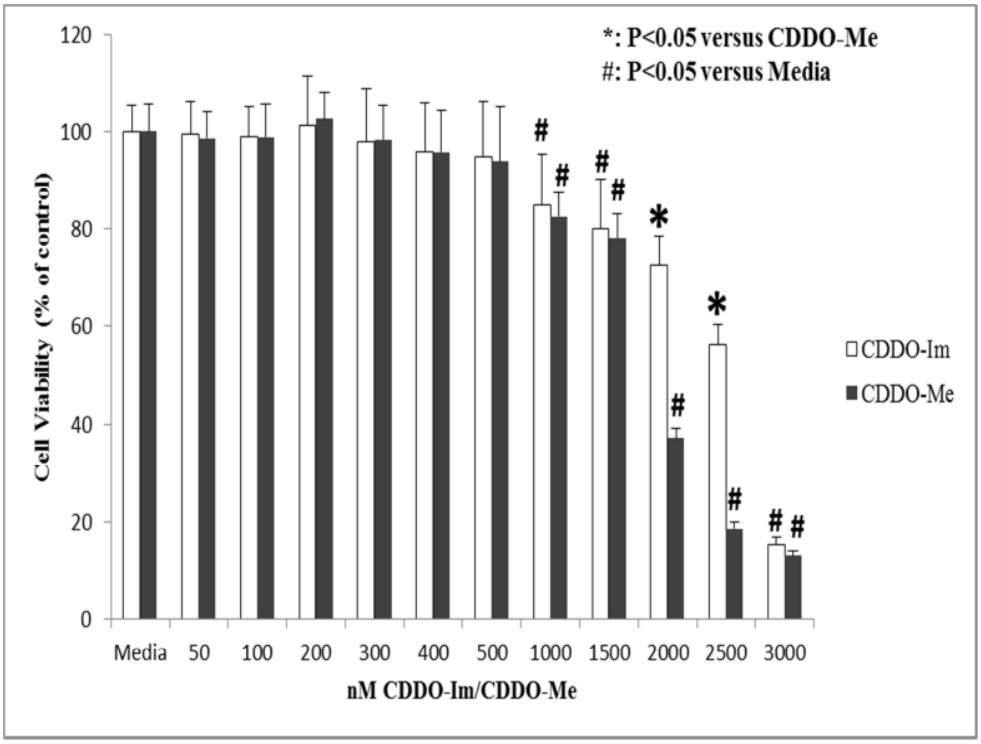

Figure 3.1: Cytotoxicity of CDDO-Im and CDDO-Me to HUVEC. Values are presented as means with standard deviations (n=3). Cell viability is shown as percent of control, and less than 90% was considered toxic. CDDO-Me was significantly more toxic in HUVEC at 2000 and 2500 nM.

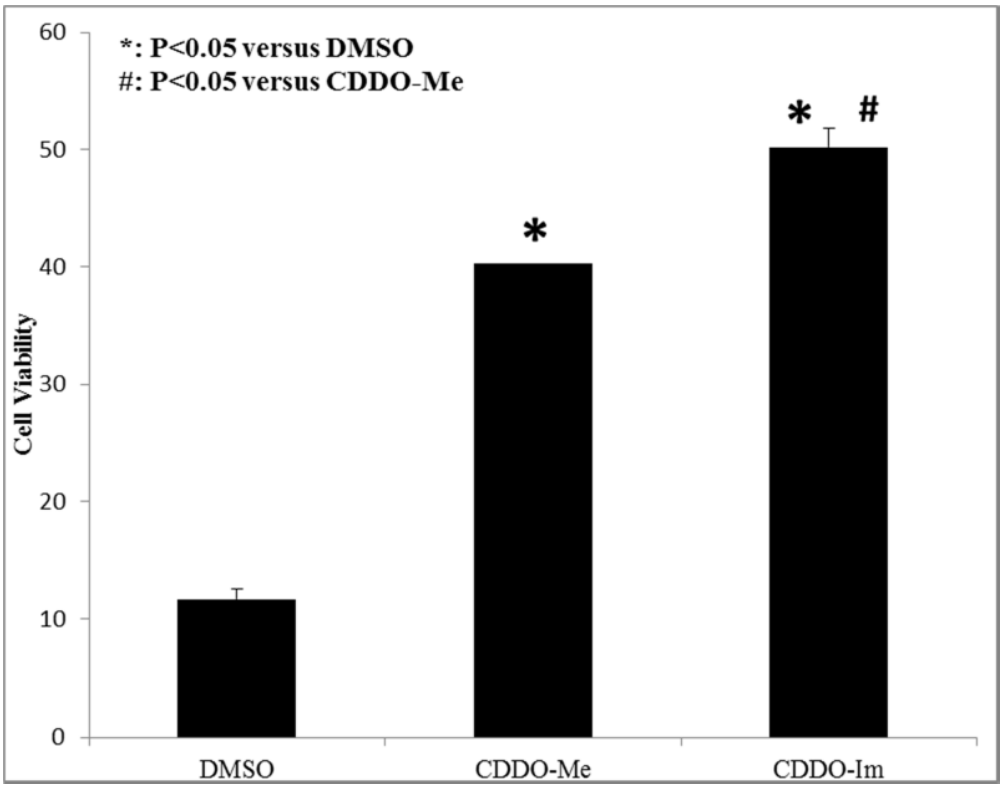

Figure 3.2: Cytoprotection against a 70 µM dose of menadione-induced injury in HUVEC by CDDO-Im and CDDO-Me (200 nM). Values are presented as means with standard deviations (n=4). Treatment with CDDO-Im resulted in a significant difference in cell viability compared to CDDO-Me. DMSO treated HUVEC were used as control at a final concentration of 0.1%.

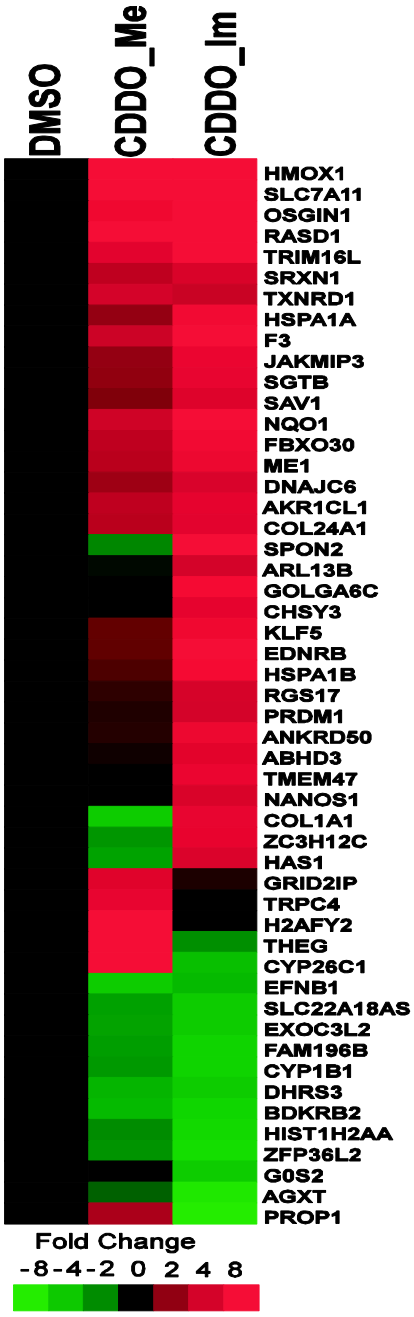

Figure 3.3: Cluster image showing most up and down regulated genes compared to vehicle control. Hierarchical agglomerative clustering of genes exhibiting more than an 8-fold statistical alteration in expression (FDR<10%) based on Pearson's correlation coefficient.

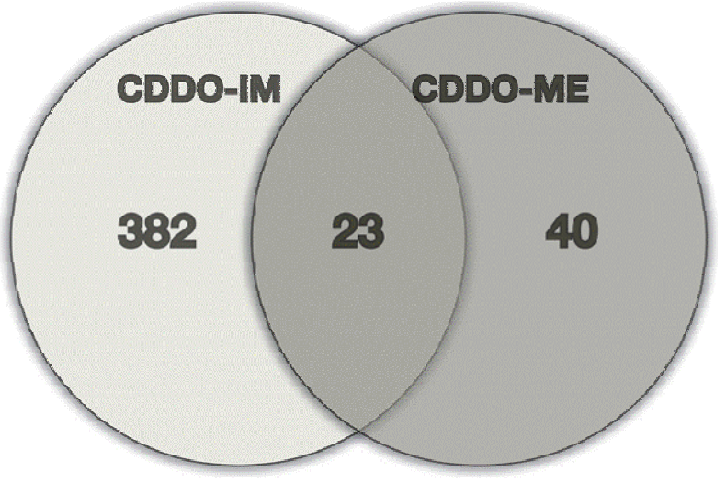

Figure 3.4: Venn diagram showing similarities and differences between CDDO-Im and-Me gene expression.

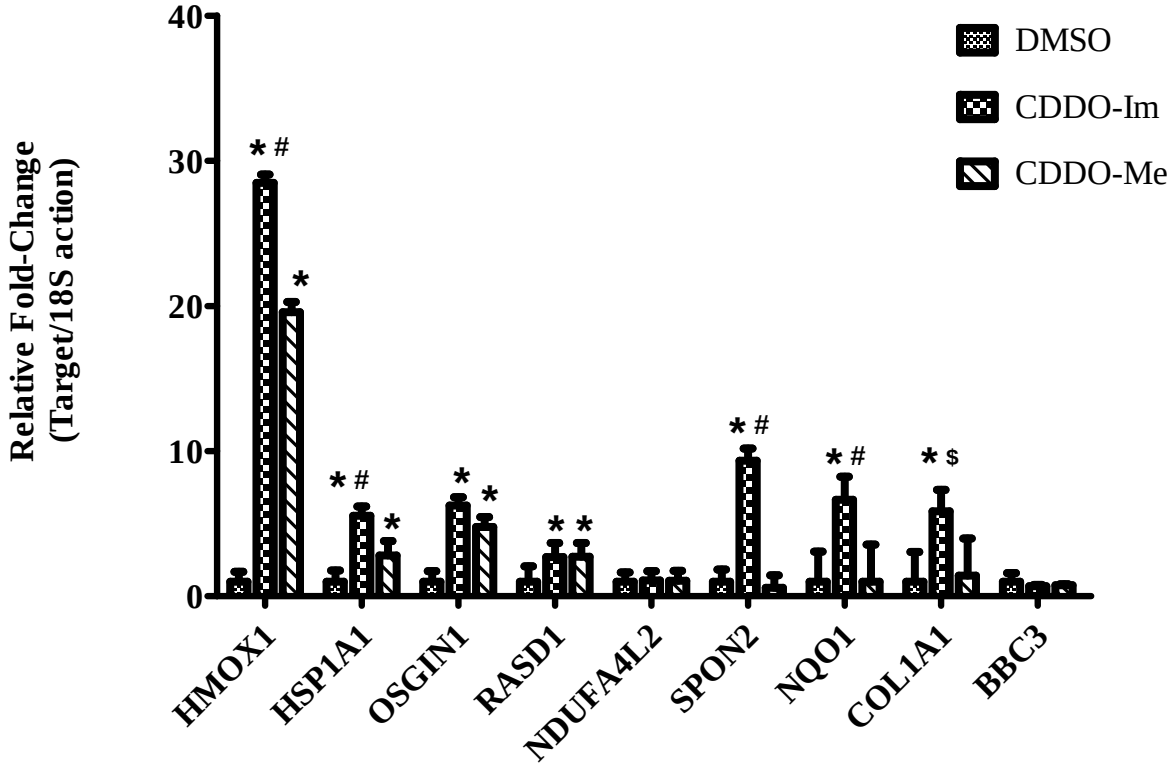

Figure 3.5: Gene expression levels induced by CDDO-Im and CDDO-Me in HUVEC measured with quantitative real-time PCR (RT-PCR). HMOX1 expression was highly increased (29-fold) in CDDO-Im group compared to DMSO control. CDDO-Me group induced HMOX1 to a lesser extent (20-fold) compared to the control group. HSPA1A, SPON2, NQO1, and COL1A1 genes similarly demonstrated significantly higher expression levels in CDDO-Im treated samples when compared to CDDO-Me. Values are presented as means with standard deviations (n=4). *P<0.005 versus DMSO; #P<0.005 versus CDDO-Me; $P<0.05 versus CDDO-Me.

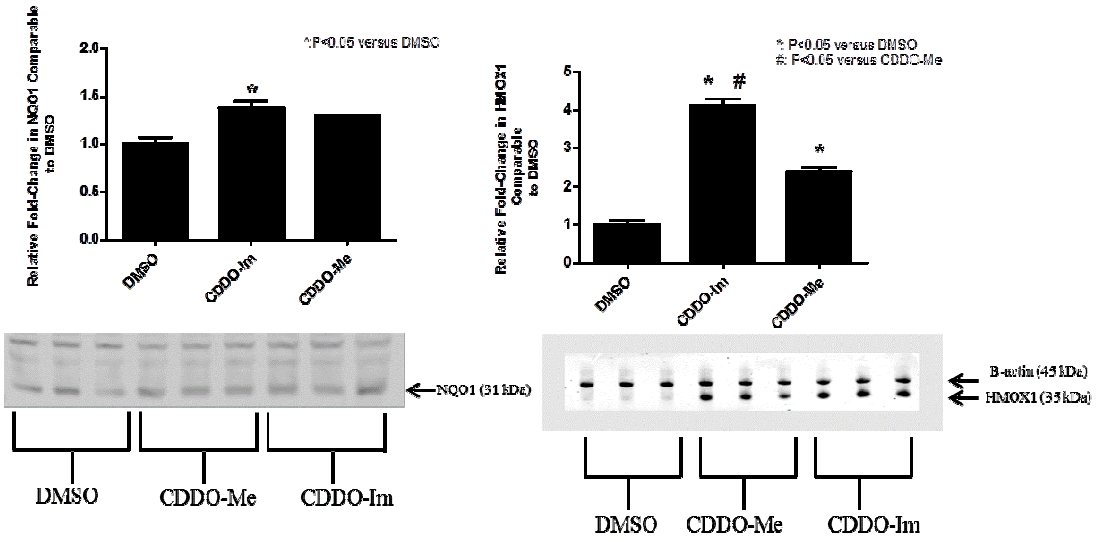

Figure 3.6: Heme oxygenase-1 and NQO1 protein induction by CDDO-Im and CDDO-Me in HUVEC by relative Western blot analysis. Heme oxygenase-1 protein expression was increased (4-fold) in CDDO-Im group compared to DMSO control (final concentration of 0.1%). CDDO-Me group induced HMOX1 protein expression to a lesser extent (2.4-fold) compared to the control group (n=3). NQO1 protein induction by CDDO-Im was significantly greater than DMSO control ($P < 0.05$), but not statistically different than CDDO-Me treated samples which showed similar protein induction as the controls (n=3). Values are presented as means with standard deviations.

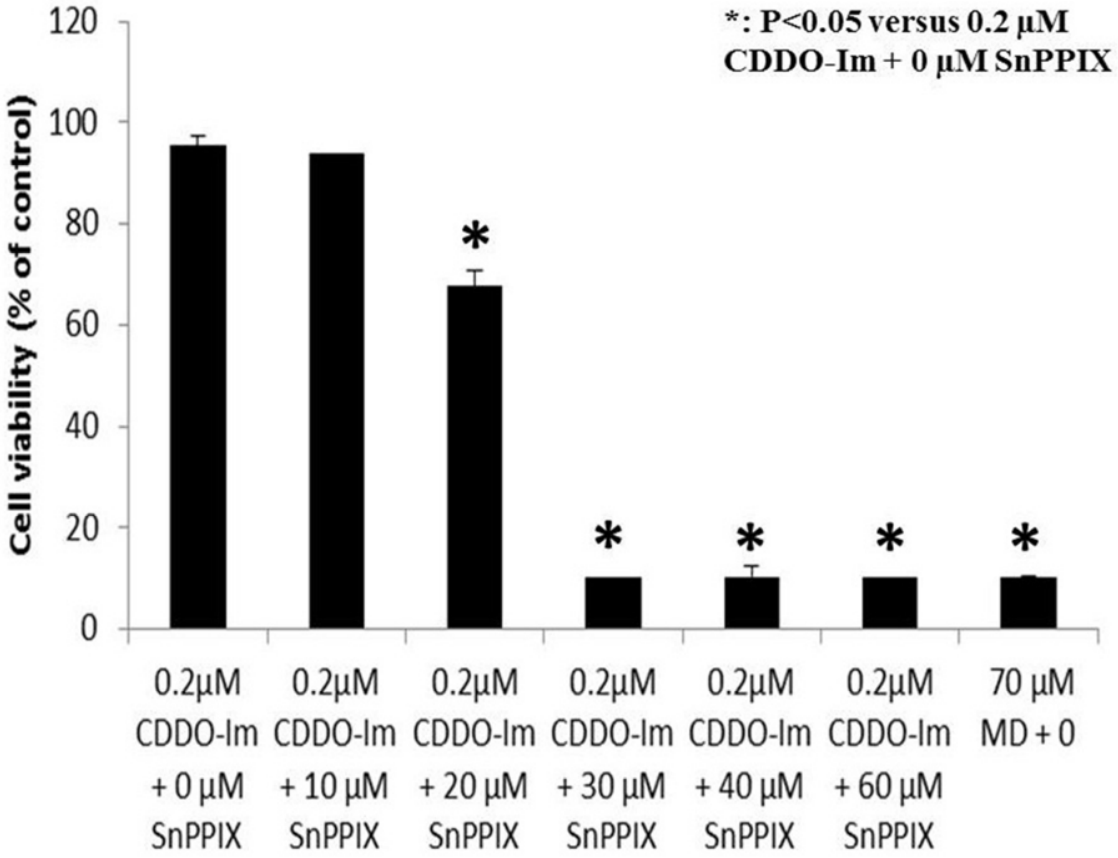

Figure 3.7: The effect of HMOX1 inhibitor SnPPIX on 200 nM CDDO-Im cytoprotection against menadione (MD)-mediated oxidative injury in HUVEC. Values are presented as means with standard deviations (n=3). SnPPIX exerted dose-dependent suppression on 200 nM CDDO-Im and CDDO-Me (data not shown) protection against 70 µM MD-induced oxidative injury (70 µM menadione dose used at all doses of SnPPIX). Control was 70 µM menadione without addition of SnPPIX resulting in ≈90% toxicity.

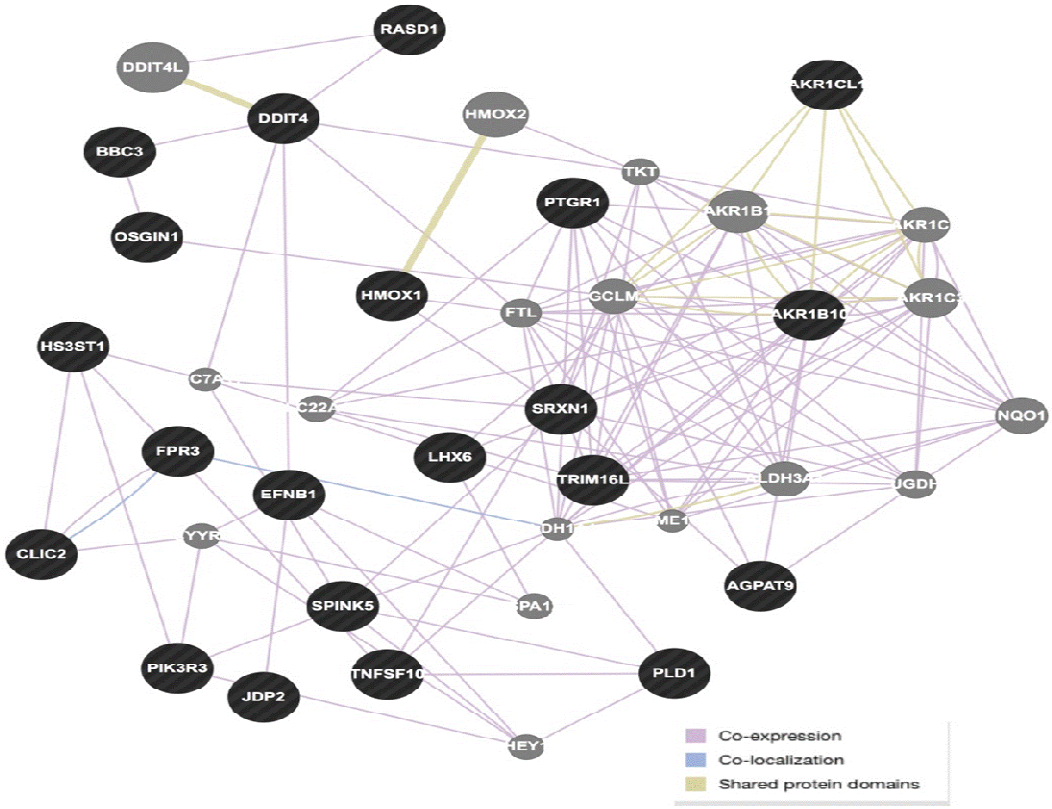

Figure 3.8: Network of genes constructed on the basis of the functional and biological connectivity of genes. This network highlights the genes induced in common by CDDO-Im and CDDO-Me. The network is graphically represented as nodes (genes) and edges (the biological relationship between genes).

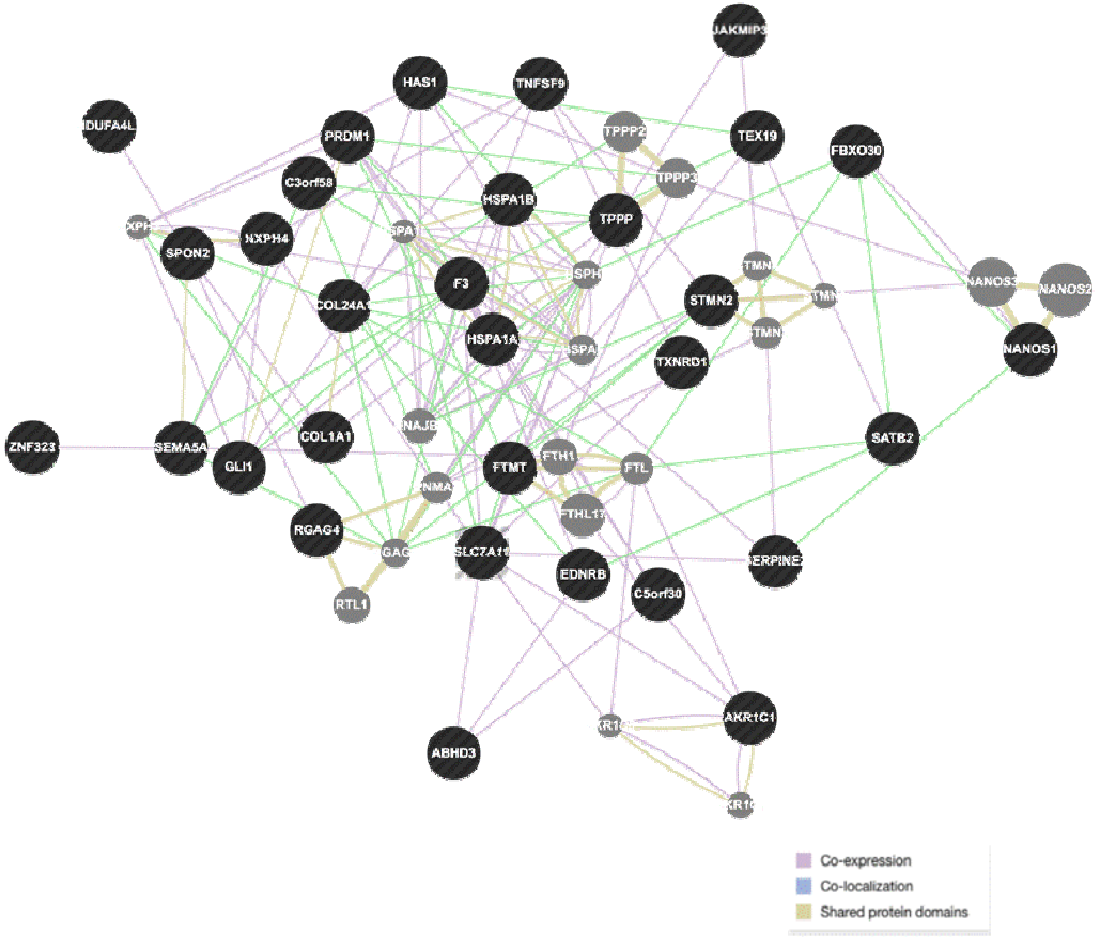

Figure 3.9: Network analysis using Genemania to highlight genes highly expressed by CDDO-Im. This network was constructed by reference to molecular functional and biological connectivity of genes. The network is graphically represented as nodes (genes) and edges (the biological relationship between genes). This response related to topologically incorrect proteins and the response to unfolded proteins.

3.4 DISCUSSION AND CONCLUSIONS

Oxidative stress is a well-known pathology of ischemia/reperfusion injury [217, 218]. Compounds that are capable of influencing pathways involved in oxidative stress-related injuries may be attractive drug targets. CDDO and derivatives were developed as anti-inflammatory [219-221] and anti-tumor agents [222] and has recently been shown to possess a variety of mechanisms [107]. At high doses, CDDO-Im and CDDO-Me along with CDDO have been shown to induce apoptosis and inhibit proliferation of malignant as well as premalignant cells [223]; while non-apoptotic low doses such as those studied here have recently been demonstrated to provide potent activation of the protective Nuclear factor-erythroid 2 p45-related factor 2 (Nrf2) pathway including genes such as GCLC, NQO1, and HMOX1 [131]. Nrf2 plays a pivotal role in regulating the cell's antioxidant response through the antioxidant response element and has been shown to be involved in repair and recovery from acute kidney injury in mice primarily through the upregulation of Nrf2 and activation of its downstream genes. Further highlighting the importance of this class of genes Lie, M et al. showed that Nrf2-deficient mice resulted in significant worsening of ischemic and nephrotoxic acute kidney injury compared to wild-type mice in the same ischemic model [224].

In this study, it was determined that there are differences in cytotoxicity and cytoprotection between these two derivatives of CDDO. Potent cytoprotection by each compound was obtained when administered at the initiation of injury indicating that these compounds provide rapid induction of the cytoprotective response that is long lasting. This result revealed that this class of compounds can stimulate the cytoprotective response more rapidly than has been reported for other inducers of cytoprotection, although greater cytoprotection was provided with a preincubation of 6 hrs [188].Gene

expression differences of these two structurally similar CDDO derivatives in human umbilical vein endothelial cells suggests that small changes in structure can potentially have significant transcriptional effects including potency, cytoprotection, and induction of gene expression as highlighted in this study [2]. Gene expression differences highlighted in the heat map and network analysis could explain the observed differences between the two compounds, but the mechanisms are still unclear. Network analysis of biological systems provided a means to represent complex interactions between genes and their products with a systems perspective. Network representation considers molecular components as nodes and their direct or indirect interactions as links or edges and enables integrations of data from many sources into a single framework [225].

Previous work using caffeic acid phenethyl ester (CAPE) provided cytoprotection in a dose-dependent fashion and was determined to be a good inducer of HMOX1. However, this and similar compounds used for cytoprotection had to be utilized as a pre-treatment against oxidative stress injury, mainly attributed to the need for development of a transcriptional response. The more rapidly this cytoprotective response can be induced the greater the improvement in survivability of oxidant stressed cells [2, 49, 50].

This is the first study to compare the association of cytoprotective activity of CDDO-Im and CDDO-Me in HUVEC in an immediate post-treatment setting and to describe the transcriptional differences between the two derivatives of CDDO in this cell type. While it is known that differences in potency between derivatives of CDDO exist [195, 226], a transcriptional basis for this difference had not been established. In the comparison between the different derivatives it was determined that both are potent inducers of HMOX1 which was confirmed by RT-PCR and western blot, but results showed that CDDO-Im was a better inducer of the cytoprotective gene than CDDO-Me. Under oxidative stress conditions, HMOX1 expression is rapidly induced in most cell

types, including HUVEC [227, 228] [191, 229, 230]. HMOX1 becomes the rate-limiting enzyme responsible for the initial step in the oxidative degradation of heme into biliverdin, iron, and carbon monoxide (CO)[231]. Several studies report that the induction of HMOX1 or its catalyzed heme products protect various organs from ischemia/reperfusion injury in vivo including a recent study using rats to study the tissue damage caused by an ischemia/ reperfusion injury [232].

In the present study, HMOX1 was determined to be largely responsible for the observed cytoprotection by use of a known HMOX1 inhibitor. Studies using SnPPIX, a well-known inhibitor of HMOX1 [233, 234] revealed that cytoprotection was decreased in a dose-dependent manner as the concentration of the inhibitor was increased, indicating HMOX1 was key for protection. However, other genes as demonstrated by gene expression profiling may modulate cytoprotection as well.

Gene expression studies using CDDO-Im and CDDO-Me with different cell types have shown similar up-regulation of HMOX1 and NQO1 and were similarly shown to be controlled by Nrf2 activation [131, 191, 235]. Unique to the transcriptional response of HUVEC were potentially protective genes such as heat shock protein 70 (HSPA1A) and down-regulation of pro-apoptotic gene BCL2 binding component (BBC3). It was determined that HSPA1A was induced significantly more by treatment with CDDO-Im than CDDO-Me. HSPA1A has been shown in many disease models to be highly protective and induction of this gene has been related to ischemia/reperfusion injuries and activation of the Nrf2 pathway [236, 237]. The difference in the expression levels between the CDDO-Im and CDDO-Me could partially explain the apparent difference in cytoprotection. Induction of BCL2 binding component (BBC3) gene functions by triggering mitochondrial associated events that lead to apoptosis by involvement with a conserved cell death pathway [191, 238, 239]. Our results show that BBC3 is down-

regulated in HUVEC by treatment with both CDDO-Im and CDDO-Me, suggesting an additional potential means for the observed cytoprotection. While not the main source of protection against oxidative stress injury; protection from down-regulation of pro-apoptotic genes like BBC3 and induction of genes such as HSPA1A combined with the potent HMOX1 response could be provide a synergistic effect allowing for increased protection against injury. Furthermore, the value of incorporating gene expression analysis into the early stages of drug evaluation for specific disease processes is demonstrated.

Understanding the actions and potential adverse effects of drugs by considering the targets in context of biological networks allows integration of the systems-level understanding of drug action [240] [153, 241]. While this study highlights cytoprotection and gene expression differences in two structurally similar compounds; some limitations of the study do exist. First, the studies presented here only test cytoprotection and gene expression in a single cell type. HUVEC have thoroughly been studied in similar models and are an appropriate cell type to use in evaluating drug effects in an *in vitro* oxidative stress injury model; testing the response of CDDO derivatives in other tissue specific cell types could provide further understanding to overall mechanisms. Moreover, while gene expression differences was identified as a compelling cause for observed differences between CDDO-Im and CDDO-Me; no pharmacokinetic or metabolism data was presented here to elucidate actual reasons for seen differences. Future studies in these areas could shed light on differences in mechanisms of action between the two compounds. Finally, future studies examining gene expression over a time course could provide valuable information on upstream initiators of observed gene expression at later time points such as presented here.

In conclusion, the results here confirm our previous findings that induction of cytoprotective genes, such as HMOX1, provide significant cytoprotection against oxidative stress injury and when used in this *in vitro* model of oxidative stress injury provide insight into the eventual use of these types of compounds for therapeutic use. This study compared the gene expression profiles between CDDO-Im and CDDO-Me in HUVEC and revealed that significant differences exist between the structurally similar compounds. Cytoprotective effect was attributed to novel findings such as the expression of genes like BBC3 and differences in induction of HSPA1A as well as HMOX1.

CHAPTER 4

Transcriptome Kinetics of 1[2-cyano-3,12-dioxooleana-1,9(11)-dien-28-oyl] imidazole (CDDO-Im) in Human Umbilical Vein Endothelial Cells (HUVEC): Mechanism of Action of Cytoprotection

4.1 INTRODUCTION

The synthetic oleanane triterpenoids 2-cyano-3,12 dioxooleana-1,9 dien-28-imidazolide (CDDO-Im) and 2-cyano-3,12-dioxooleana-1,9-dien-28-oic acid (CDDO-Me) have been shown to protect against oxidative stress in various cell and animal models [127, 181, 189-191] and exhibit anti-inflammatory properties [107]. In addition, these two compounds have been shown to provide a chemopreventative effect against certain tumors, largely by reducing the viability of these cells [192-194]. Comparing these two structurally different forms of CDDO, I previously determined that there is a similar degree of cytoprotection between the two compounds; however, significant differences in gene expression were seen between the two following a 6 hour treatment on human umbilical vein endothelial cells (HUVEC). CDDO-Im was shown to induce more gene expression changes than CDDO-Me and resulted in significantly higher expression levels of key cytoprotective genes including heme oxygenase-1 (HMOX1) [242].

CDDO-Im and its analogs have been shown to elicit protective effects largely through activation of the transcription factor nuclear factor erythroid 2-related factor 2 (Nrf2) [122, 125, 131]. Previous work in our lab with CDDO-Im and CDDO-Me

supported the central role of Nrf2 in homeostasis [188, 243] and its role in HMOX1 induction; additionally, it identified potentially new genes that provide additional cytoprotection. A recent study evaluated the kinetics of HMOX1 induction by four different transcription factors (HSF-1, AP-1, NRF2, and NF-κB) and showed that they differ in their mechanism of action and kinetics of inducing HMOX1 [244]. That study highlighted the need for a better understanding of protective mechanisms of action that accurately takes into account the temporal nature of gene response over time; through the use of mathematical modeling the study revealed multiple pathways for HMOX1 induction. The study presented here expands on that approach by studying transcriptional kinetics of a relevant system that not only allows for modeling with experimentally-derived data, but also extends the study of mechanism of action by employing further analysis to identify upstream initiators of observed gene expression.

CDDO-Im cytoprotection of HUVEC was investigated by studying gene expression over a time course (0.5, 1, 3, 6, and 24 h). The purpose of the present study was to utilize the changes in gene expression caused by CDDO-Im over time as a model for identifying key genes, particularly at early time points, that are responsible for our previously reported cytoprotective effect [188, 243]. Additionally, analysis with Expression2Kinases (X2K) was used to further identify relevant transcription factors, kinases, and complexes that drive observed changes in global gene expression [245].

Observing and measuring temporal changes in an experimental model such as the one presented here will allow for better understanding of this dynamic response and may provide insight into the actual regulatory mechanisms responsible for cytoprotection;

critical processes required for downstream initiation of cytoprotective genes will be investigated by focusing on early time points. This study also seeks to provide methods that allow for the discovery of mechanisms of action involved in cytoprotection from CDDO-Im by describing observed regulatory effects through detection of cellular processes over time, using regulatory networks and clustering methods, and assigning function to the genes throughout the time course in an approach that can be applied to additional model systems.

4.2 MATERIALS AND METHODS

4.2.1 Materials

CDDO-Im (96% purity) was purchased from Toronto Research Chemicals Inc. (Toronto, Ontario, Canada). DMSO was from Sigma-Aldrich (Saint Louis, MO, USA).

4.2.2 Cell Culture

Stock cultures of gender-mixed HUVEC (Lifeline Cell Technology, Walkersville, MD) pooled from 10 different donors were cultivated on T75 flasks (Corning in MCDB 131 medium at 37 °C in a humidified atmosphere of 92% nitrogen and 3% oxygen 5% CO2 with medium changes every 2 days until confluent [203, 204]. MCDB 131 Medium, Trypsin/EDTA, antibiotic/antimycotic were obtained from Life Technologies (Carlsbad,

CA). Endothelial supplements were obtained from ATCC. Prior to an experiment, HUVEC were subcultivated with Trypsin/EDTA onto Costar® 96-well multiplates (Corning Incorporated, Corning, NY, USA) at 5000 cells/cm2, grown to confluence and kept for 72 h to produce a quiescent cell layer. Only the second through fifth population doublings of cells were used as described in [2].

4.2.3 Total RNA Isolation

Total RNA was extracted from cultured HUVEC grown in 12-well multiplates with TRI™ reagent according to the manufacturer's instructions (Molecular Research Center, Cincinnati, OH, USA). RNA yield was quantified using NanoDrop® ND-1000 Spectrophotometer (NanoDrop Technologies, Wilmington, DE, USA), and its quality was assessed by electrophoresis on 1% agarose gels containing 1:1000 SYBR Gold in the loading buffer (Invitrogen, Carlsbad, CA, USA).

4.2.4 Polyacrylamide gel electrophoresis and western blotting

Protein was extracted from the HUVEC after incubation with CDDO-Im (0.2 μM) for each of the time points represented in the microarray experiment (0.5,1, 3, 6, 24 hr), by addition of 50 μl of lysis buffer (Life Technologies, Grand Island, NY) containing 10 mM tris (carboxyethyl) phosphine hydrochloride (Sigma, St Louis, MO, USA). Fifteen microliters, containing approximately 5 μg of protein, from each treatment were run on E-PAGE 96-well 6% gels (Life Technologies) and then transferred to a nitrocellulose membranes (Life Technologies). After blocking in blocking buffer

(LICOR, Lincoln, Nebraska USA), the blots were then incubated with rabbit HMOX1, HSP105, PHD, DYRK3, or HSP70 primary antibodies (Assay Designs Inc., Ann Arbor, MI, USA; 1:5000) for 1 h. The blots were washed three times with 0.1% Tween 20 in PBS and incubated with donkey anti-rabbit secondary antibody (LICOR) for 30 minutes before three more washes and then allowed to dry for visualization. Visualization was performed using the Odyssey imaging system (LI-COR Biosciences) that allowed for dual labeling of two different proteins.

4.2.5 Gene expression analysis

RNA (500 ng) from four replicates for each time point (0.5, 1, 3, 6, and 24 hrs) were labeled following Agilent's Low RNA Input Linear Amplification Kit (Agilent, Santa Clara, CA). All sample-labeling, hybridization, washing, and scanning steps were conducted according to the manufacturer's specifications. For each group, 200ng of cRNA from each labeling reaction was hybridized to the Agilent Whole Human Genome Oligo Microarray (Agilent). The Whole Human Genome Oligo Microarray is in an 8 X 60k slide format and microarray interrogates all known genes. After hybridization, the slides were washed and then scanned with the Agilent G2505C Microarray Scanner System (Agilent). The fluorescence intensities on scanned images were extracted and preprocessed by Agilent Feature Extraction Software.

4.2.6 Statistical analysis

Microarray data analysis and statistical analysis were performed with BRB Array Tools [209]. Heat maps were generated in the BRB Array Tools utilizing the time course module that incorporates the Cluster and TreeView programs [210]. Genes were considered statistically significant with P value <0.001 and false discovery rate (FDR) value of <5%. Filtered data analyzed by BRB Array Tools was submitted to GeneMANIA for network analysis. This program represents the complexity of biological regulatory systems as networks whose topology provides a manageable technique for analyzing the principal components of a complex system. Principal components (genes or proteins) are nodes and interactions are depicted as edges [213].

4.2.7 Expression 2 Kinases (X2K) analysis

The early-immediate time-course gene expression data (30 min & 1 h) were submitted to Expression2Kinases (X2K) used to identify upstream regulators likely responsible for observed patterns of genome wide gene expression [245]. This bioinformatic package works by integrating ChIP seq/chip and position weight matrices (PWMs) data, protein-protein interactions, and kinase substrate phosphorylation reactions into gene expression studies to further investigate upstream regulators of expression. The most likely transcription factors that regulate the differences in gene expression are inferred, then known protein-protein interactions are connected to the identified transcription factors using additional proteins for building transcriptional regulatory subnetworks centered on these factors, and finally use kinase substrate protein

phosphorylation reactions, to identify and rank candidate protein kinases that most likely regulate the formation of the identified transcriptional complexes.

4.2.8 Transcriptokinetic analysis

Gene expression-time profiles of HMOX1, JUNB, and FOS were modeled using WinNonLin version 2.1 by Pharsight (Sunnyvale, CA) to determine half-life (t1/2) for gene expression as a function of time. Observed and model-predicted fits of the data were graphed.

The gene expression-time profile data was analyzed for purposes of calculating t1/2 using the following model:

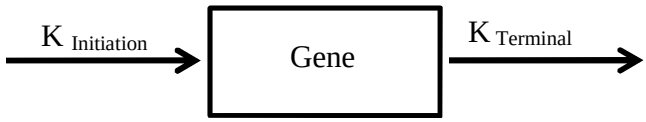

The $K_{Initiation}$ phase represents the initiation of the gene expression response caused by treatment of the compound; $K_{Terminal}$ represents the terminal phase of gene expression response as expression decreases towards baseline levels. Half-life was calculated for $K_{Initiation}$ and $K_{Terminal}$ phases.

4.3 RESULTS

4.3.1 Time course gene expression profiling of CDDO-Im reveals different response phases

Gene Expression profiling of CDDO-Im treated for 0.5, 1, 3, 6, and 24 hours was performed using Agilent Whole Human Genome microarrays. Clustering of the time course yielded good correlation between the replicates and expresses the similarity/differences between time points as shown in (Figure 4.1). A heat map of genes statistically altered in their expression up- or down-regulated more than 8-fold across the time following clustering is shown in (Figure 4.2). CDDO-Im induced genes as quickly as 0.5 h including genes involved in early growth response (ERG1, EGR2, and EGR3) as well as genes such as FOS (regulators of cell proliferation, differentiation, and transformation in the early phases (0.5-1 h) of gene expression response induced by CDDO-Im (Table 4.2). Additionally, protein coding genes (CXCL2 and CXCR4) and genes induced by cytokines such as SOCS3 were present by 0.5 h. These genes were up-regulated by 0.5 h and quickly returned by 3 h to basal levels.

Genes identified in the intermediate phase (3 and 6 h expression levels) of the global gene expression analysis included known protective-related genes such as: HMOX1, NQO1, HSP1A1, HSP1AB, TAGLN, SRXN1, PTPRU, and UNC5B (Table 4.3). Several of these genes, as illustrated in (Table 4.1), are directly related to the NRF2 or ARE pathways and are known to be downstream protective genes induced through signaling and phosphorylating events.

Expression of genes in the late phase (24 h) of the expression profile (24 h) included PGD, MYCN, SPRY1, and EPHX1 and largely resembled the control (DMSO-treated) gene expression profile (Table 4.4).

Symbol	Gene Name	Function	0.5/DMSO	1h/DMSO	3h/DMSO	6h/DMSO	24h/DMSO
HMOX1	heme oxygenase (decycling) 1	IL-10 Anti-inflammatory Signaling Pathway, Oxidative Stress Induced Gene Expression Via Nrf2, Porphyrin and chlorophyll metabolism	1.72	5.17	7.96	7.69	6.21
NQO1	NAD(P)H dehydrogenase, quinone 1	Hypoxia and p53 in the Cardiovascular system	0.79	0.66	1.50	2.57	4.52
JUNB	jun B proto-oncogene	Osteoclast differentiation	7.81	4.58	1.85	1.17	1.30
FOS	FBJ murine osteosarcoma viral oncogene homolog	B Cell Survival Pathway, BCR Signaling Pathway, Oxidative Stress Induced Gene Expression Via Nrf2	45.26	7.03	4.15	1.53	1.20
DNAJA4	DnaJ (Hsp40) homolog, subfamily A, member 4		0.94	1.19	1.82	1.94	0.87
DNAJB11	DnaJ (Hsp40) homolog, subfamily B, member 11	Protein processing in endoplasmic reticulum	0.67	0.83	1.06	1.00	0.77
GCLC	glutamate-cysteine ligase, catalytic subunit	Glutathione metabolism, Metabolic pathways	1.08	0.77	0.67	1.43	1.29
GCLM	glutamate-cysteine ligase, modifier subunit	Glutathione metabolism, Metabolic pathways	1.00	0.83	1.11	1.36	1.25

Table 4.1: Altered NRF2-mediated gene set. This table shows gene expression values in response to CDDO-Im treatment throughout the time-course that are known to be mediated through the NRF2 oxidative stress response pathway.

Symbol	Name	0.5h/ DMSO	1h/ DMSO	3h/ DMSO	6h/ DMSO	24h/ DMSO
EGR3	early growth response 3	80.6	42.4	1.6	0.3	0.3
NR4A1	nuclear receptor subfamily 4, group A, member 1	63.9	22.9	0.6	0.4	0.4
FOS	FBJ murine osteosarcoma viral oncogene homolog	45.3	7.0	4.2	1.5	1.2
EGR2	early growth response 2	26.1	10.8	0.8	0.9	0.2
FOSB	FBJ murine osteosarcoma viral oncogene homolog B	23.5	24.3	3.7	1.0	2.8
EGR4	early growth response 4	15.6	16.9	3.1	1.0	1.0
EGR1	early growth response 1	8.5	2.1	1.8	1.3	0.4
DUSP1	dual specificity phosphatase 1	8.4	1.2	0.6	0.9	0.7
KLF4	Kruppel-like factor 4 (gut)	8.1	8.4	1.8	1.0	0.6
JUNB	jun B proto-oncogene	7.8	4.6	1.9	1.2	1.3

Table 4.2 Top 10 most highly expressed genes in the “early” phase (0.5-1 h) of induction resulting from treatment with a 200 nM dose of CDDO-Im in HUVEC.

Symbol	Name	0.5h/ DMSO	1h/ DMSO	3h/ DMSO	6h/ DMSO	24h/ DMSO
NOG	noggin	12.2	31.5	24.6	0.7	0.7
F3	coagulation factor III (thromboplastin, tissue factor)	2.9	5.7	9.2	5.6	1.3
DACT1	dapper, antagonist of beta-catenin, homolog 1 (Xenopus laevis)	2.3	8.5	8.2	1.4	0.9
HMOX1	heme oxygenase (decycling) 1	1.7	5.2	8.0	7.7	6.2
ATOH8	atonal homolog 8 (Drosophila)	1.9	7.9	7.2	1.4	1.4
CLDN23	claudin 23	6.1	13.0	5.6	1.4	2.2
HEY1	hairy/enhancer-of-split related with YRPW motif 1	43.6	55.7	5.4	0.9	1.2
ALPK2	alpha-kinase 2	1.8	1.0	5.4	1.0	2.1
FZD7	frizzled family receptor 7	6.8	20.8	5.3	4.1	0.9
RASL11B	RAS-like, family 11, member B	8.4	16.9	5.1	0.9	0.4

Table 4.3 Top 10 most highly expressed genes in the “intermediate” phase (3-6 h) of induction resulting from treatment with a 200 nM dose of CDDO-Im in HUVEC.

Symbol	Name	0.5h/ DMSO	1h/ DMSO	3h/ DMSO	6h/ DMSO	24h/ DMSO
GPIHBP1	glycosylphosphatidylinositol anchored high density lipoprotein binding protein 1	1.6	2.1	1.8	1.5	12.6
CXCR4	chemokine (C-X-C motif) receptor 4	1.8	1.1	0.5	0.9	12.0
MAN1C1	mannosidase, alpha, class 1C, member 1	4.9	5.4	4.0	1.1	9.8
TFEC	transcription factor EC	1.7	0.8	1.7	3.4	7.1
FLJ34503	uncharacterized FLJ34503	3.5	2.6	1.7	1.0	6.7
AFAP1L2	actin filament associated protein 1-like 2	5.1	4.9	2.6	1.6	6.6
TIMP3	TIMP metallopeptidase inhibitor 3	4.8	5.0	3.7	1.1	6.2
SEMA6A	sema domain, transmembrane domain (TM), and cytoplasmic domain, (semaphorin) 6A	5.3	1.6	0.7	0.7	5.9
INHBB	inhibin, beta B	7.7	9.0	2.0	0.7	5.9
APCDD1	adenomatosis polyposis coli down-regulated 1	1.6	1.9	0.8	0.6	5.4

Table 4.4 Top 10 most highly expressed genes in the “late” phase (24 h) of induction resulting from treatment with a 200 nM dose of CDDO-Im in HUVEC.

4.3.2 Profiling reveals time points for maximal expression of NRF2 mediated genes

Gene expression levels of known NRF2 mediated genes are shown in (Table 4.1). Examining the results over time shows the time point at which maximal expression is achieved. Early genes such as JUNB and FOS exhibit rapid increases in gene expression (7.81 and 45.26, respectively) at the 0.5 h time-point. Other NRF2 mediated genes such as HMOX1 and NQO1 obtain peak expression later in the time-course (7.96 at 3 h for HMOX1 and 4.52 at 24 h for NQO1).

4.3.3 Western blotting across time course

To validate the microarray results, as well as investigate translation of protein products over the time course; western blotting was performed on several of the significantly expressed genes. (Figure 4.3) shows protein expression for HSP105, DYRK3, PHD, HSP70 and HMOX1 at 1, 3, and 6 h. HMOX1 showed 2, 3, and 12-fold increases in protein expression compared to DMSO at 1, 3, and 6h respectively, $P<0.05$ for all time points. HSP105 showed 1.2, 1.4, and 4.7-fold increases compared to DMSO, $P<0.05$. PHD exhibited protein expression levels that were all close to 1-fold increase compared to DMSO which were consistent with mRNA levels from the microarray. DYRK3 had small, but significant increases in mRNA levels in the gene expression profiles; this finding was confirmed by protein expression levels (1.0, 1.3, 1.8-fold) compared to DMSO, $P<0.05$. HSPA1A showed similar trend such that the protein expression levels exhibited small increases over the time course (1.2, 1.4, and 1.6),

$P<0.05$. The mRNA expression obtained from the microarray analysis for HSPA1A at the same time points (1, 3, and 6 h) were 0.74, 2.1, and 4.8-fold increased respectively.

4.3.4 Correlation of functional and biological connectivity using network analysis

To focus on early initiators of the gene expression profile, network analysis was performed using Genemania on the 0.5 h samples after dosing with 200 nM CDDO-Im. The network graphically represents nodes (genes) and edges (the biological relationship between genes). This network included genes such as NR4A2, FOS, JUNB, several EGR variations and identified DUSP1 as a key immediate-early gene. This class of genes includes functions such as early growth stimulation, cell differentiation and growth, and signal transduction (Figure 4.4). (Figure 4.5) demonstrates a network that highlights intermediate gene expression 3 h after treatment with CDDO-Im.

4.3.5 Expression2Kinases reveals key protein kinase events including role of MAP2K1

To identify key early regulators of protection provided by CDDO-Im, the time-course gene expression study was submitted to Expression2 Kinases (X2K) for analysis of transcription factors, intermediate proteins, and protein kinases that regulate downstream induction of cytoprotective genes. Once the expression data was submitted to the software for analysis a list of predicted transcription factors were generated.

Using the top predicted transcription factors as seeds for building protein complexes a subnetwork of intermediate proteins were identified; these proteins connect

through known protein-protein associations to the transcription factors as well as the known protein kinases involved that phosphorylate the protein complexes. Among these predicted kinases dual specificity mitogen-activated protein kinase kinase (MAP2K1) was identified as playing a compelling early role in the regulation of subsequent gene expression (Figure 4.6).

4.3.6 Gene expression-time profiling

The gene expression-time profiling data was analyzed for HMOX1, JUNB, and FOS genes. The fit and half-lives of the HMOX1 gene expression-time profile can be seen in (Figure 4.7). Modeling of HMOX1 gene expression revealed a t1/2 $K_{Initiation}$ = 0.9 h and t1/2 $K_{Terminal}$ = 44.9 h. JUNB fit and half-lives are shown in (Figure 4.8) and resulted in $K_{Initiation}$ = 0.02 h and t1/2 $K_{Terminal}$ = 1.2 h. Modeling of FOS gene expression revealed a t1/2 $K_{Initiation}$ = 0.3 h and t1/2 $K_{Terminal}$ = 0.2 h and are shown in (Figure 4.9).

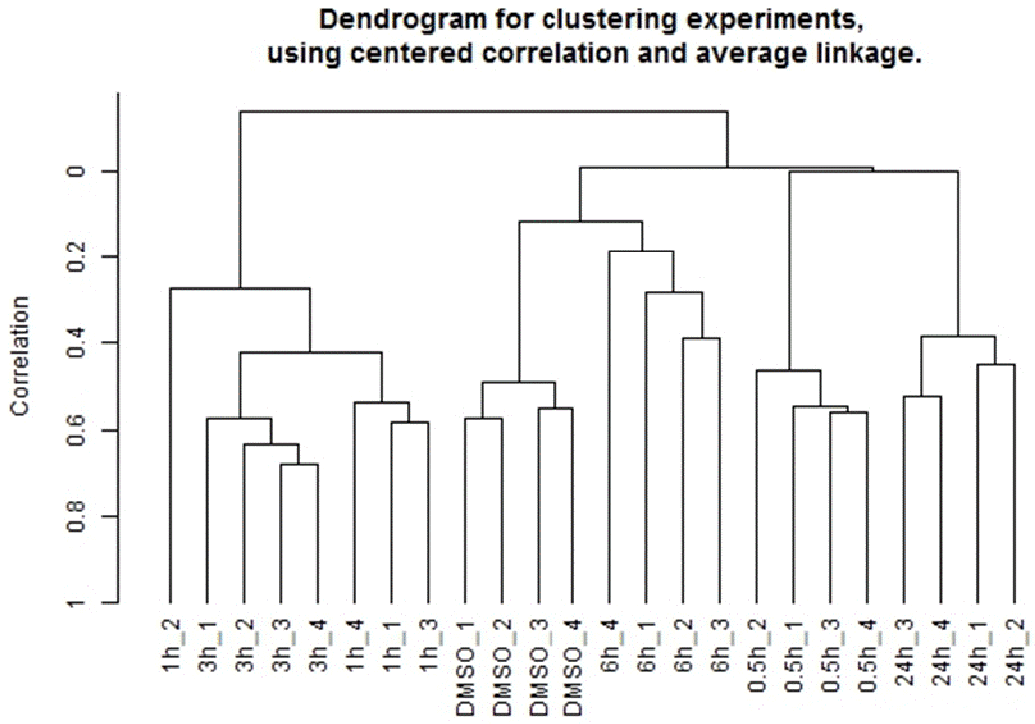

Figure 4.1: Dendrogram used for clustering time-course gene expression data. Clustered analyzed using centered correlation and average linkage. Dendrogram generation was done with Treeview [211] and analysis performed with Cluster 3. This dendrogram demonstrates the connectedness of each sample used in the microarray studies and illustrates tight grouping of the biological replicates.

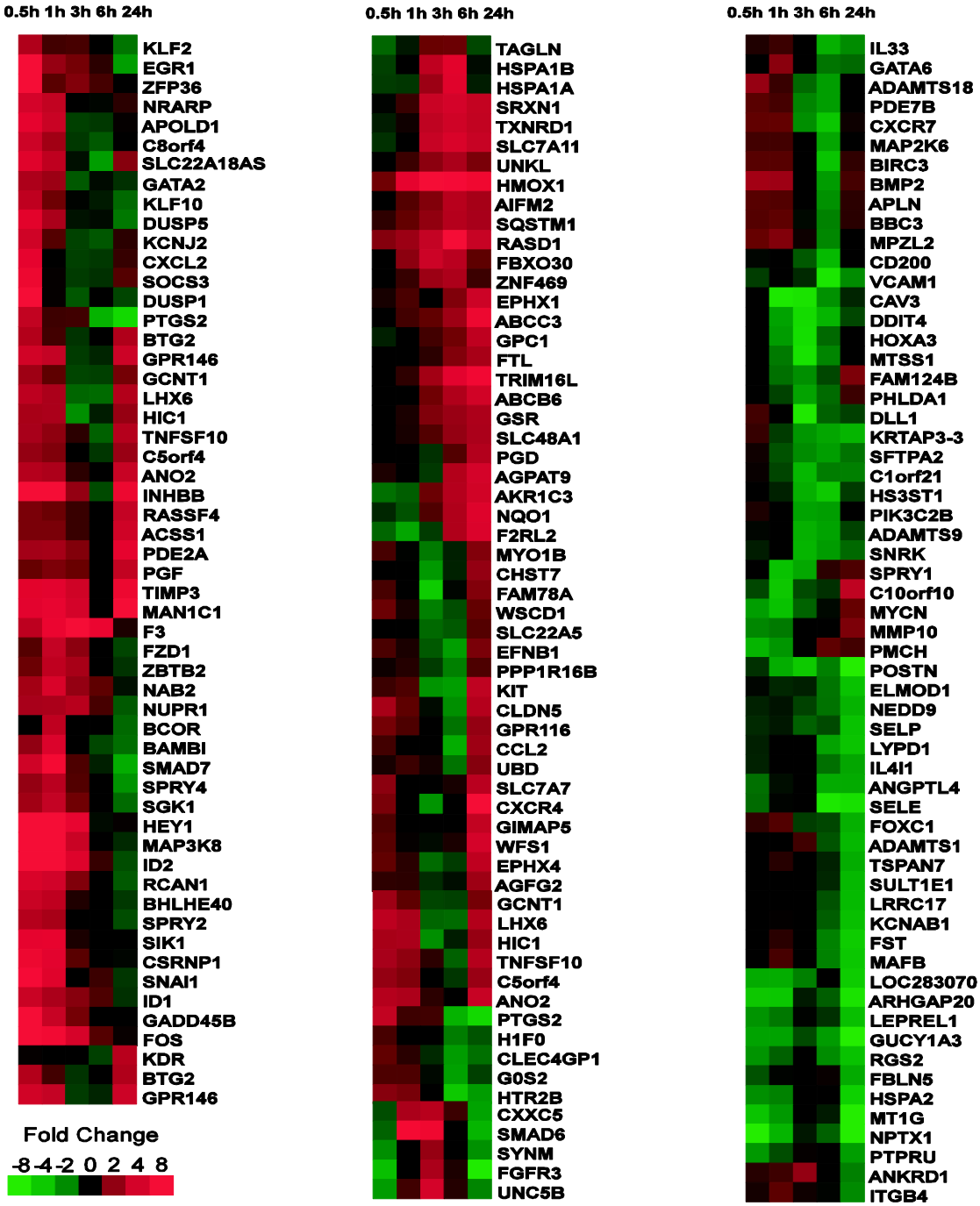

Figure 4.2: Hierarchical agglomerative clustering of genes exhibiting more than an 8-fold statistical alteration in expression (FDR<10%) based on Pearson's correlation coefficient.

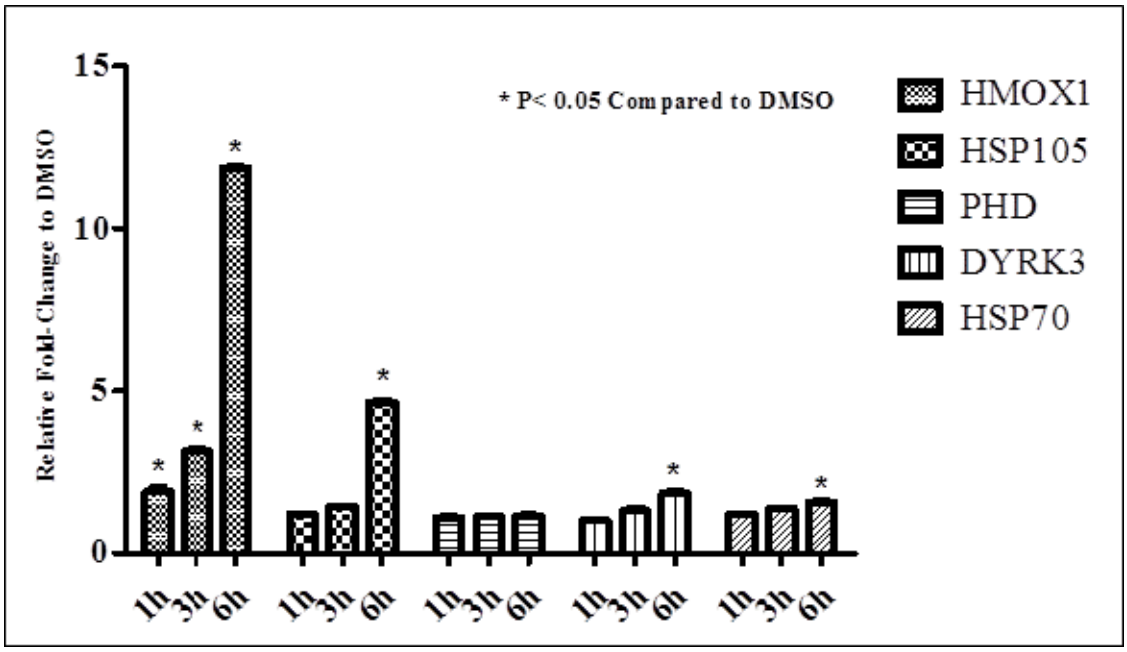

Figure 4.3: Protein induction by CDDO-Im in HUVEC by relative Western blot analysis for time-points 1, 3, and 6 h. HMOX1, HSP105, PHD, DYRK3, and HSP70 were all compared to DMSO control (0.1% final concentration). Values are presented as means with standard deviations (n=4). *P<0.05

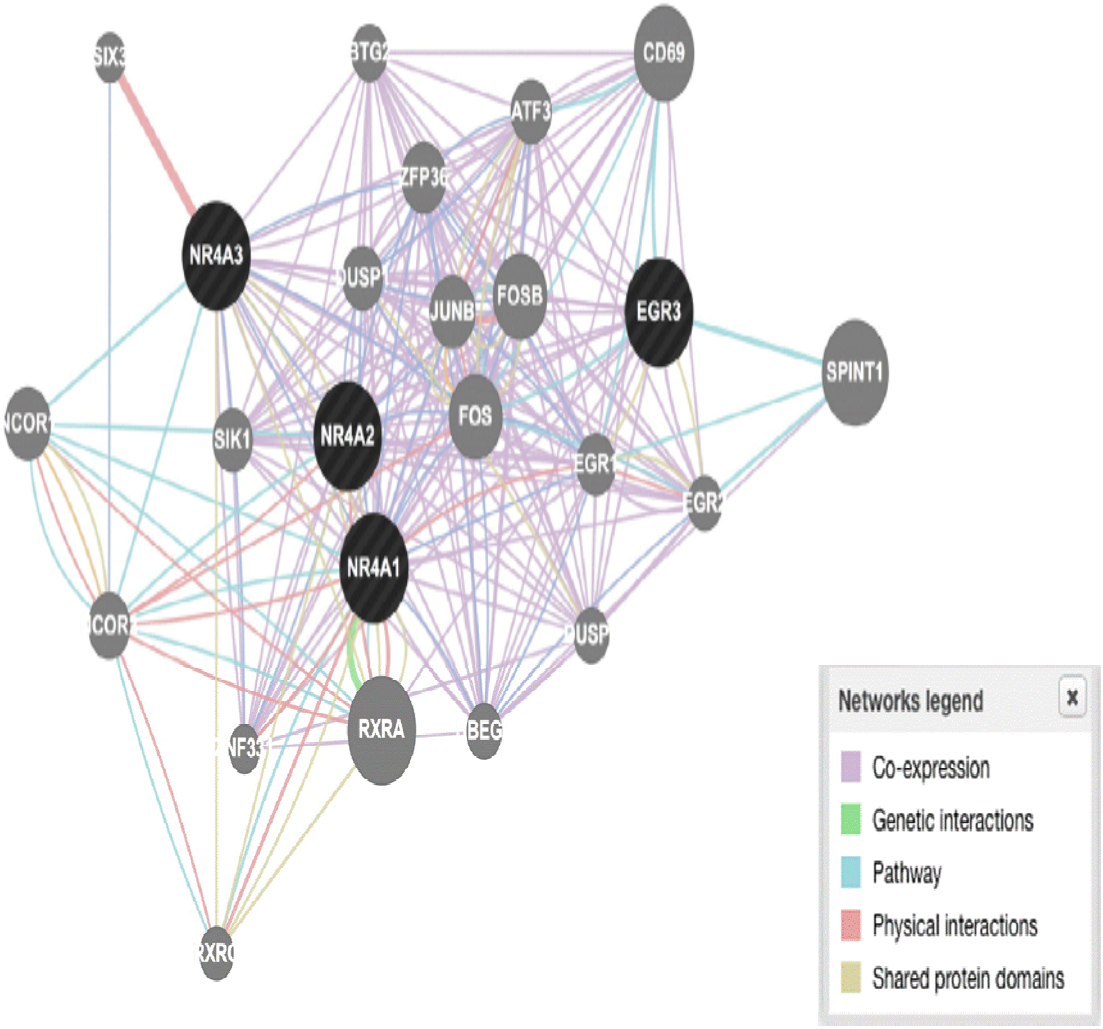

Figure 4.4: Network of genes constructed by GeneMania Software on the basis of the functional and biological connectivity of genes. This network highlights the genes induced by CDDO-Im after treatment for 0.5 h and represents the immediate early gene response. The network is graphically represented as nodes (genes) and edges (the biological relationship between genes). Black nodes represent significantly expressed genes present in the input data submitted to Genemania. Grey nodes represent genes returned by Genemania. The size of each node is proportional to the degree of connectivity within the network while the edge width is proportional to the confidence of the connection.

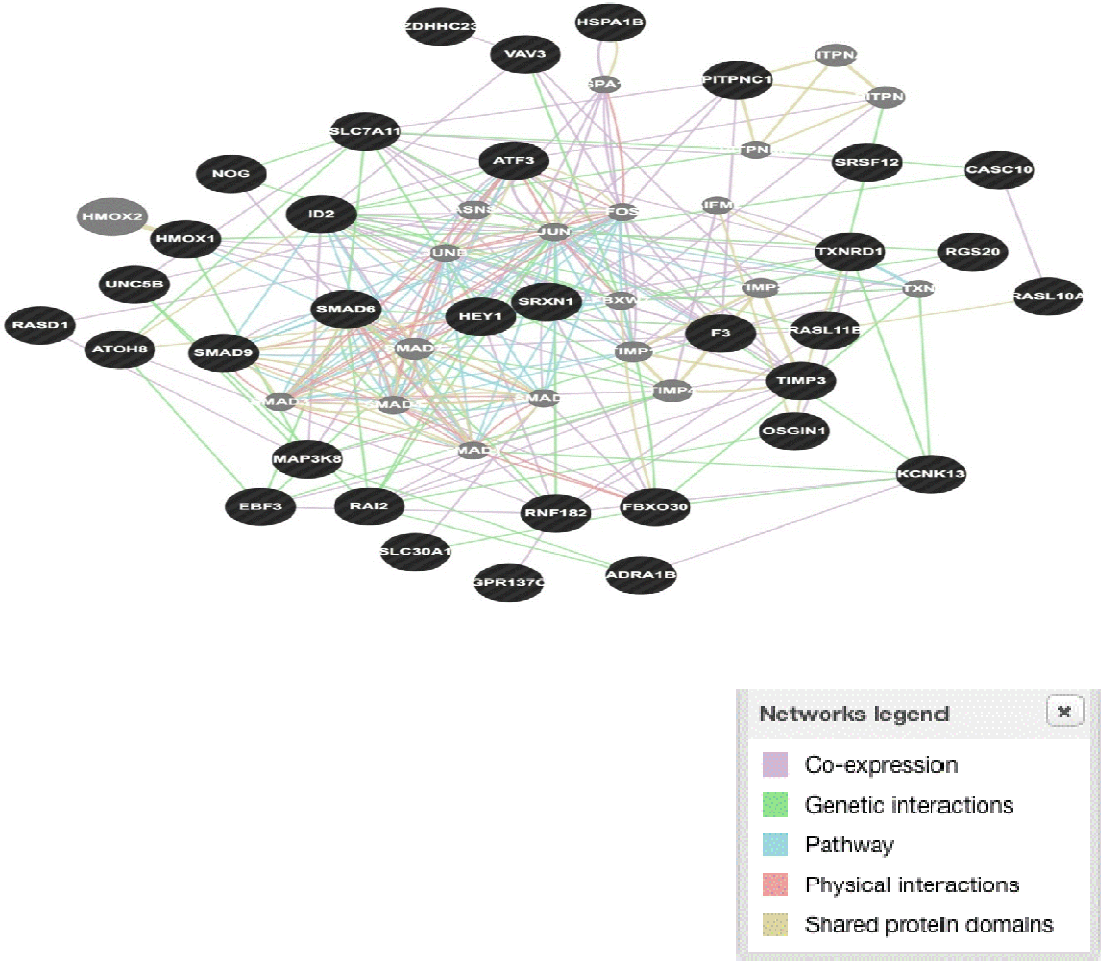

Figure 4.5: Network of genes constructed by GeneMania Software on the basis of the functional and biological connectivity of genes. This network highlights the genes induced by CDDO-Im after treatment for 3 h and represents intermediate gene expression response to CDDO-Im. The network is graphically represented as nodes (genes) and edges (the biological relationship between genes). Black nodes represent significantly expressed genes present in the input data submitted to Genemania. Grey nodes represent genes returned by Genemania. The size of each node is proportional to the degree of connectivity within the network while the edge width is proportional to the confidence of the connection.

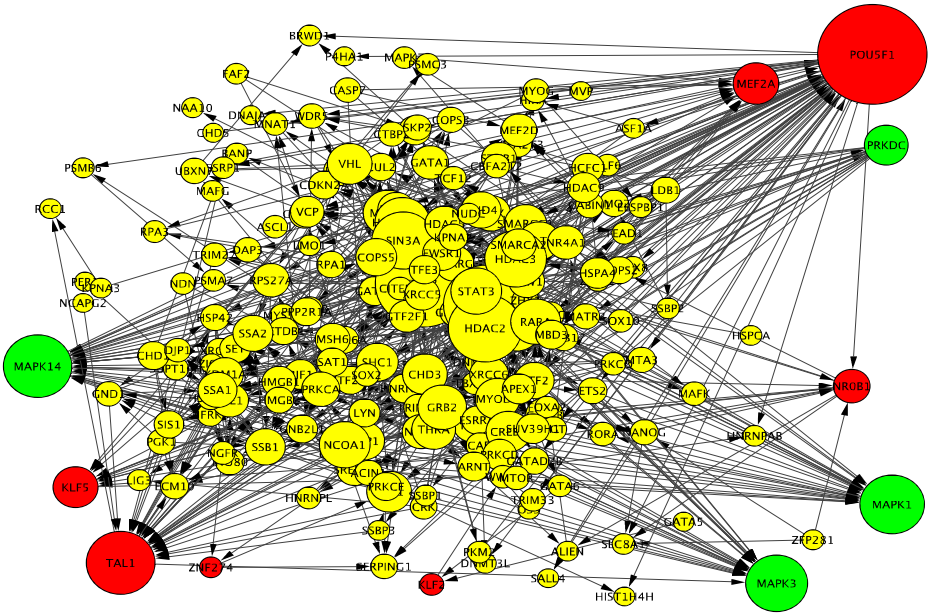

Figure 4.6: Expression2Kinases network constructed on the basis of the transcription factors, protein protein interactions and protein kinases acting within 30 min of treatment with CDDO-Im. Transcription factor nodes (red) Protein-Protein Interactions nodes (yellow) and kinase (green). Network generated with Cytoscape 3.1.1.

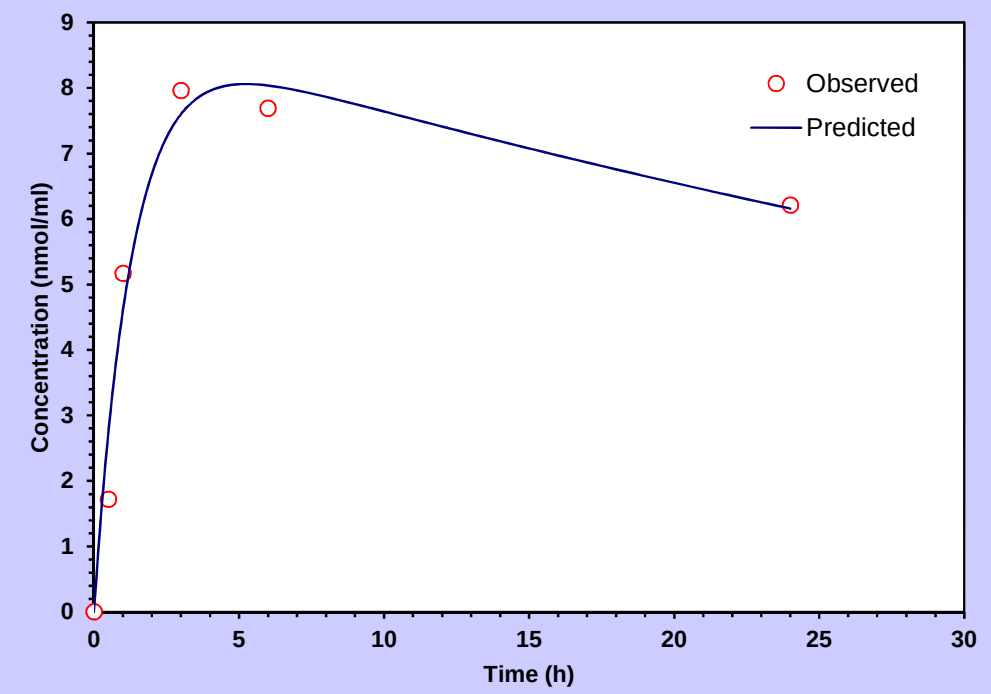

Parameter	Unit	Value
$t1/2k_{Initiation}$	h	0.913545616
$t1/2k_{Terminal}$	h	44.90462934

Figure 4.7: Gene expression-time profile of HMOX1 after treatment with a 200 nM dose of CDDO-Im. Observed concentrations are shown along with the fitted line.

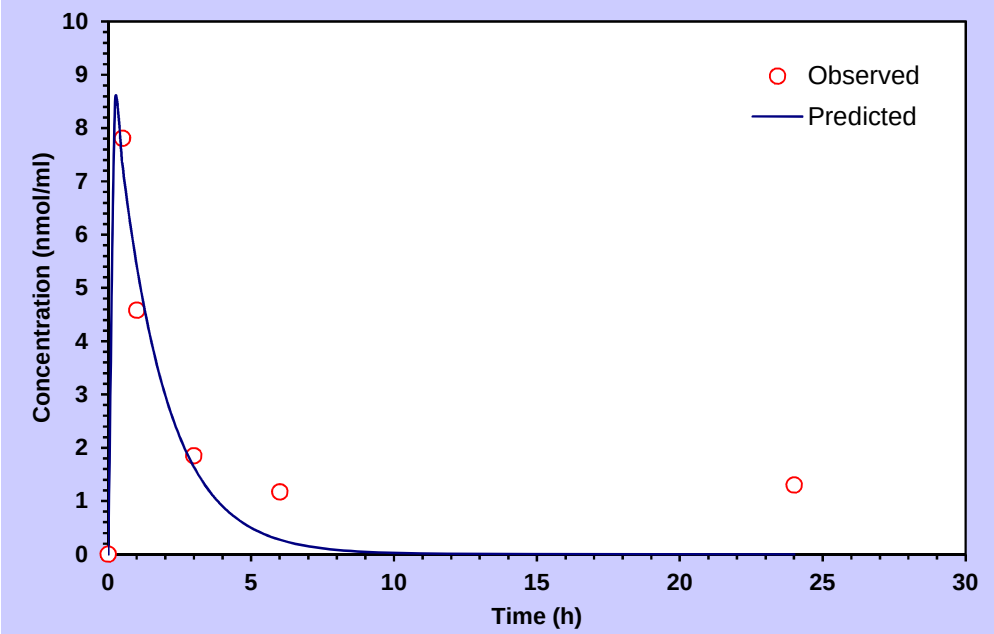

Parameter	Unit	Value
$t1/2k_{Initiation}$	h	0.017340815
$t1/2k_{Terminal}$	h	1.160720757

Figure 4.8: Gene expression-time profile of JUNB after treatment with a 200 nM dose of CDDO-Im. Observed concentrations are shown along with the fitted line.

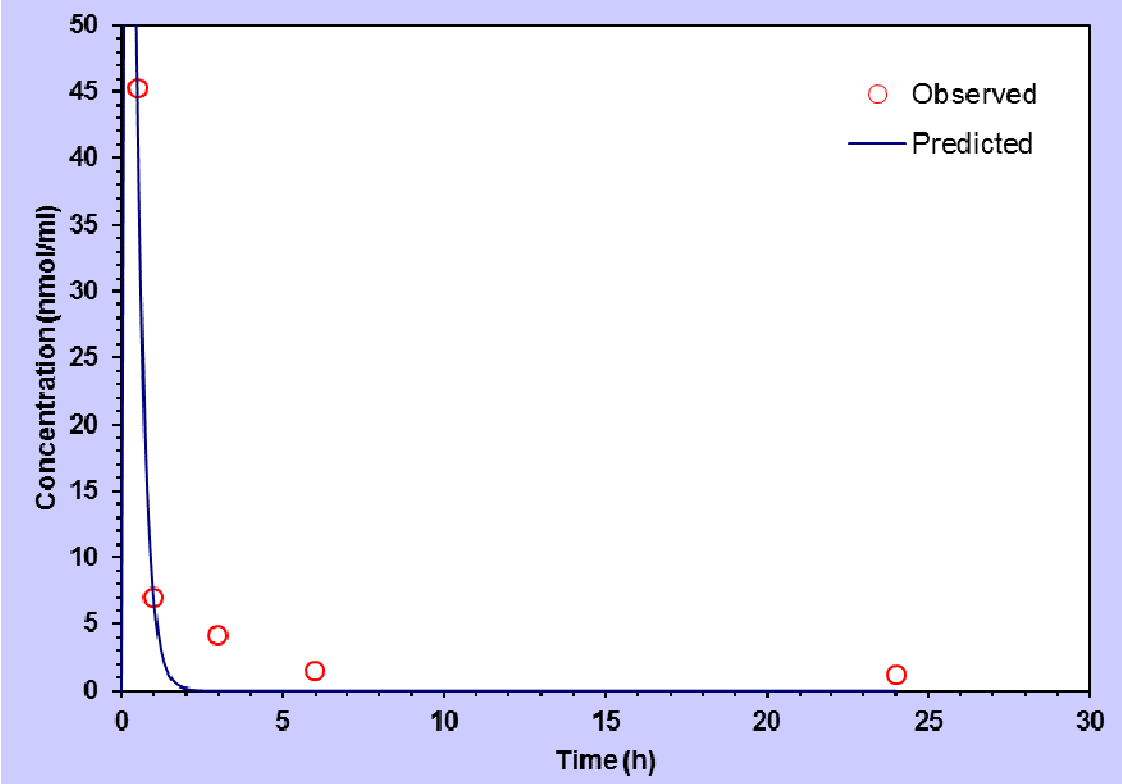

Parameter	Unit	Value
$t1/2k_{Initiation}$	h	0.029374985
$t1/2k_{Terminal}$	h	0.186283131

Figure 4.9: Gene expression-time profile of FOS after treatment with a 200 nM dose of CDDO-Im. Observed concentrations are shown along with the fitted line..

4.4 DISCUSSION

Time-course gene expression through transcriptomic and proteomic data analysis has increasingly become a well-recognized approach in the study of cellular responses to stimuli such as potential drug discovery, development, and drug therapeutics [164, 246]. The technology is well-suited for the dynamic nature of gene expression over time and allows for detailed examination of underlying mechanisms. This study highlights a multileveled use of bioinformatics tools that incorporates human time-course gene expression data in a systems pharmacology approach to illustrate a method for detailing mechanisms for observed genome-wide gene expression patterns.

The model as presented in this study addresses several limitations that often exist in much of current gene expression research to date. First, researchers too often focus on a single or final time point alone and fail to take full advantage of the temporal nature of genes over time [247, 248]. Understanding the transcriptional kinetics offered by time course studies allows for more accurate profiling of not just a single gene, but sets of related genes that potentially offer greater significance when studied from a series of time points. Secondly, utilizing a multileveled approach such as the one presented here offers superior understanding into the underlying mechanisms responsible for observed responses [249]. The integration of programs such as expression to kinases (X2K) takes expression data one-step further and allows for identification of regulatory mechanisms upstream of gene expression.

Time course gene expression analysis of HUVEC treated with 200 nM CDDO-Im revealed distinct phases of gene expression as a function of time; the dynamic nature of

the most significantly expressed genes are illustrated in the clustering analysis and heat map presented in this work. Of particular interest is the early response (0.5 h), which is key for understanding mechanisms that drive downstream gene expression responses and regulate critical cellular signaling events. This work is the first of its kind to examine CDDO-Im in HUVEC from a systems pharmacology approach by utilizing time course gene expression and applying further novel analysis to truly elucidate initiators of upstream gene expression.

Furthermore, a novel approach to analyzing time course gene expression data using transcriptome modeling was demonstrated in this work by using HMOX1, JUNB and FOS genes as examples of data that could be obtained by evaluating gene expression levels as a function of time. Transcriptome modeling of gene expression levels through the time course revealed key parameters, such as half-lives of expression in key genes. This approach combined with other processes highlighted in this work has the potential of revolutionizing the way pharmaceutical industry focuses on drug development and discovery. For example, the ability to monitor potential biomarkers in a controlled system over time through the use of modeling and genomics could allow a researcher access to data never before seen such as actual half-life data on a target biomarker gene. This use of systems pharmacology could potentially maximize the design of a drug that relies on such biomarkers and avoid the all too common unintended adverse effects.

Analysis of this gene expression data set with integration of data obtained from protein-protein interactions and kinase-substrate phosphorylation reactions showed that CDDO-Im initiates rapid responses as early as 0.5 h and causes early key phosphorylation events that lead to activation of several initiators of downstream expression. This analysis identified a key role provided by the protein kinase kinase MAP2K1, also commonly known as MEK1. MAP2K1 lies upstream of MAP kinases and

regulates this class of kinases through a wide variety of extra- and intracellular signals [250]. MAP kinases, also known as extracellular signal-regulated kinases or (ERK), are well known to act as initiation points for further signaling events [251]. MAP2K1 has been shown to obtain activation through events such as the binding of extracellular ligands to cell-surface receptors which in turn activates RAS and RAF1 [252]. RAF1, through phosphorylation of threonine and tyrosine residues of MAP2K1, leads to further activation and transduction of signaling pathways such as MAPK/ERK. The MAPK/ERK pathway has widely been reported to mediate biological functions such as survival, cell growth, and metabolism largely through downstream gene transcription [253-255].

The identification of the DUSP1 gene through gene expression analysis (Genemania) of the 0.5 h time-point revealed a crucial link in the understanding of the mechanism related to CDDO-Im. DUSP1, also known as (MKP-1), is a key phosphatase that has recently been shown to be rapidly induced in response to several anti-inflammatory drugs including glucocorticoids [256]. DUSP1 preferentially dephosphorylates both threonine and tyrosine residues on MAPK thereby modulating inflammation [256, 257]. Consistent with other studies; here we show that activation of DUSP1 is mediated by upstream activation of MAP2K1 [258, 259]. Several studies have shown the dependence on DUSP1 induction including two anti-inflammatory cytokines drugs (IL-10 and TGF-β), corticosteroids and rapamycin [260-262]. The data in this present study identifies the potential role of DUSP1 and the required upstream mediator MAP2K1 and further suggests that CDDO-Im may initiate its cytoprotective effects through similar signaling precursors as other anti-inflammatory compounds.

CHAPTER 5

Summary and Conclusions

CDDO has been shown to be an effective cytoprotectant against oxidative stress *in vitro* and against I/R injury *in vivo* and was shown to be 200,000 times more potent than its parent compound, oleanolic acid. In an effort to maximize the pharmacodynamic effect and further increase CDDO potency additional derivatives were synthesized by Michael Sporn and colleagues that eventually led to the formation of CDDO-Im and later CDDO-Me.

In vitro cytoprotection assays were developed and utilized to initially compare whether CDDO-Im was more cytoprotective than CAPE, a known cytoprotectant and inducer of phase II enzymes including heme oxygenase-1 (HMOX1). This work revealed that not only was CDDO-Im and CDDO-Me significantly more cytoprotective than CAPE; but surprisingly CDDO-Im and CDDO-Me additionally provided cytoprotection when given at the initiation of oxidant stress. These findings led me to investigate the mechanism of action and further revealed that CDDO-Im and CDDO-Me possess the unique ability of inducing cytoprotective genes as early as 0.5 h after administration. Cytoprotection profiles of CDDO-Im and CDDO-Me were compared and gene expression studies were completed to measure transcriptional responses of each compound in HUVEC. Finally transcriptional kinetic studies were performed with CDDO-Im treated HUVEC samples over a time course to investigate the temporal effects

of genes in response to CDDO-Im and to study the mechanism of action including key initiators of observed gene expression.

CYTOPROTECTION COMPARISON OF CDDO-IM TO CAPE IN HUVEC

We previously reported that CAPE protected HUVEC from menadione-induced oxidative stress and that this cytoprotective effect was correlated with the capacity to induce heme-oxygenase-1 (HMOX1). In an effort to further improve this cytoprotective effect, we studied CDDO-Im and compared its cytoprotective activity to CAPE. CDDO-Im at a dose of 200 nM provided more protection to HUVEC against oxidative stress than 20 μM CAPE. The mechanism of CDDO-Im was further explored with gene expression profiling and pathway analysis and again compared to that of CAPE. In addition to potent up-regulation of HMOX1, heat shock proteins (HSPs) were also found to be highly induced by CDDO-Im in HUVEC. Pathway analysis showed that transcription factor Nrf2-mediated oxidative stress response was among the top canonical pathways commonly activated by both CDDO-Im and CAPE. Compared to CAPE, CDDO-Im up-regulated more HSPs and to a much higher extent. In addition, CDDO-Im treatment affected Nrf2 pathway to greater extent. These findings may explain why CDDO-Im is a more potent cytoprotectant than CAPE against oxidative stress in HUVEC.

CYTOPROTECTION OF HUVEC FROM OXIDANT STRESS WITH CDDO DERIVATIVES

The cytoprotective responses of HUVEC was compared between CDDO-Im and CDDO-Me and gene expression profiles of each were explored to identify key genes and

pathways involved in the cytoprotective response. While most *in vitro* studies in the literature utilized CDDO-Im and CDDO-Me as a pretreatment, this study was unique in the fact that the compounds were administered at the initiation of oxidant stress and showed that both provided good cytoprotection (51.25% ±2.6 and 40.12% ±1.7 respectively), CDDO-Im provided more cytoprotection than CDDO-Me and was less cytotoxic (73% ±5.8 and 37% ±2 respectively). In contrast, HUVEC pretreated with CDDO-Im and CDDO-Me for 6 h resulted in 100% ±2 cytoprotection against the same 70 μM dose of menadione. These studies revealed that these particular triterpenoids, unlike most other antioxidants, are rapid inducers of the cytoprotective response and possess great therapeutic potential in the treatment of oxidative stress-induced injuries. While the compounds do not exhibit direct antioxidant activity, we compared them in HUVEC for transcriptional activity with whole genome microarrays and found that a gene set centered around heme oxygenase-1 was expressed in common. However, 319 more genes were statistically altered in their expression by CDDO-Im than CDDO-Me. In addition to up-regulating heme oxygenase-1 (HMOX1), both compounds also induced members of the heat shock protein family and down-regulated pro-apoptotic genes. Gene expression profiling, revealed networks of genes known to be related to cellular development, growth, proliferation and cell signaling. Additionally, canonical pathways including NRF2-mediated oxidative stress response and peroxisome proliferator-activated receptor (PPAR) signaling indicated that cytoprotection involves multiple pathways. While the cytoprotective responses of human endothelial cells to equivalent doses of the two compounds were similar; there were considerable differences observed in their gene expression patterns that might explain differences in cytotoxicity and cytoprotection.

TRANSCRIPTOME KINETICS OF CDDO-IM IN HUVEC: MECHANISM OF ACTION

While this previous work showed heme oxygenase-1 to be a major effector of cytoprotection in HUVEC, the mechanism by which the overall effect was mediated was largely unknown. This work evaluated temporal gene expression profiles to better characterize the early transcriptional events and their relationship to the dynamics of the cytoprotective response in human umbilical vein endothelial cells (HUVEC) to CDDO-Im. Time-course gene expression profiling was performed on HUVEC treated with CDDO-Im for 0.5, 1, 3, 6, and 24 hours. The approach described here combined time-dependent gene expression microarray profiling, hierarchal clustering and network analysis from a systems pharmacology focus. Confirmation of gene data was obtained by western blotting of selected genes. 10,747 genes were statistically altered in their expression in at least one time point across the time course with a low parametric p-value ($p<0.001$) and false discovery rate (<1e-07). Integration of gene expression data with protein-protein interactions and kinase-substrate phosphorylation interactions showed that CDDO-Im initiated intense gene expression responses as early as 0.5 h and that early key phosphorylation events resulted in activation of several initiators of downstream expression. Large alterations in immediate early gene (IEG) expression were readily detectable within 0.5 h after administration of CDDO-Im including the DUSP1 gene, a known modulator of inflammation in several other classes of drugs. Expression2Kinases software identified a key role provided by the protein kinase kinase, MAP2K1. Utilizing global gene expression screening as a function of time was shown to be a useful tool for investigating mechanism of action.

SUMMARY

In conclusion, CDDO-Im was shown to be 100X more potent than CAPE and provided better cytoprotection against oxidant stress in HUVEC. Additionally, gene expression studies showed that CDDO-Im was a better inducer of the HMOX1 as well as other potentially protective genes such as the HSPs. The comparison between the cytoprotective activities of CDDO-Im and CDDO-Me given at the initiation of an oxidant stress-induced injury in HUVEC revealed that CDDO-Im was a better cytoprotectant and induced more genes; potentially explaining the differences seen in cytoprotection and cytotoxicity. Transcriptional kinetics of CDDO-Im in HUVEC through integration of systems pharmacology uncovered a previously unreported mechanism of action which centered around early initiators of downstream gene expression such as the interactions of DUSP1 and MAP2K1. Future studies should investigate the effect of inhibiting early key initiators of observed gene expression and measuring cytoprotection response. Additionally, administration of CDDO-Im *in vivo* would greatly advance the understanding of mechanism of action and provide valuable information regarding actual pharmacokinetic data, survivability, and gene expression profiling in an actual I/R injury model.

Appendix A- Top up-regulated genes in early response (0.5 h) to CDDO-Im treatment

Parametric p-value	FDR	DMSO	0.5 h	1 h	3 h	6 h	24 h	Symbol	Name	0.5h/DMSO	1h/DMSO	3h/DMSO	6h/DMSO	24h/DMSO
< 1e-07	< 1e-07	42	4590	7261	111	35	19	NR4A3	nuclear receptor subfamily 4, group A, member 3	110.4	174.6	2.7	0.9	0.5
< 1e-07	< 1e-07	39	3107	1637	63	12	10	EGR3	early growth response 3	80.6	42.4	1.6	0.3	0.3
< 1e-07	< 1e-07	27	1732	620	17	11	10	NR4A1	nuclear receptor subfamily 4, group A, member 1	63.9	22.9	0.6	0.4	0.4
< 1e-07	< 1e-07	68	4262	2865	140	51	48	NR4A2	nuclear receptor subfamily 4, group A, member 2	62.4	41.9	2.0	0.8	0.7
< 1e-07	< 1e-07	202	9162	1424	841	309	242	FOS	FBJ murine osteosarcoma viral oncogene homolog	45.3	7.0	4.2	1.5	1.2
< 1e-07	< 1e-07	378	16451	21043	2038	323	447	HEY1	hairy/enhancer-of-split related with YRPW motif 1	43.6	55.7	5.4	0.9	1.2
< 1e-07	< 1e-07	310	8092	3342	263	281	49	EGR2	early growth response 2	26.1	10.8	0.8	0.9	0.2
< 1e-07	< 1e-07	130	3052	3156	483	126	365	FOSB	FBJ murine osteosarcoma viral oncogene homolog B	23.5	24.3	3.7	1.0	2.8
< 1e-07	< 1e-07	360	8394	8187	1624	485	242	ID2	inhibitor of DNA binding 2, dominant negative helix-loop-helix protein	23.3	22.8	4.5	1.3	0.7

Parametric p-value	FDR	DMSO	0.5 h	1 h	3 h	6 h	24 h	Symbol	Name	0.5h/DMSO	1h/DMSO	3h/DMSO	6h/DMSO	24h/DMSO
< 1e-07	< 1e-07	11	167	181	33	10	10	EGR4	early growth response 4	15.6	16.9	3.1	1.0	1.0
< 1e-07	< 1e-07	3008	42628	4732	5591	4349	3338	ZFP36	ZFP36 ring finger protein	14.2	1.6	1.9	1.4	1.1
< 1e-07	< 1e-07	41	497	1288	1003	30	28	NOG	noggin	12.2	31.5	24.6	0.7	0.7
< 1e-07	< 1e-07	312	3275	3730	1080	286	245	MAP3K8	mitogen-activated protein kinase kinase kinase 8	10.5	11.9	3.5	0.9	0.8
< 1e-07	< 1e-07	30	303	122	14	28	16	DUSP2	dual specificity phosphatase 2	10.0	4.0	0.5	0.9	0.5
< 1e-07	< 1e-07	62	552	392	70	83	47	ARC	activity-regulated cytoskeleton-associated protein	8.9	6.3	1.1	1.3	0.8
< 1e-07	< 1e-07	4235	36056	8787	7417	5570	1885	EGR1	early growth response 1	8.5	2.1	1.8	1.3	0.4
< 1e-07	< 1e-07	200	1686	158	28	129	118	HES1	hairy and enhancer of split 1, (Drosophila)	8.4	0.8	0.1	0.6	0.6
< 1e-07	< 1e-07	2907	24368	3459	1861	2739	2024	DUSP1	dual specificity phosphatase 1	8.4	1.2	0.6	0.9	0.7
< 1e-07	< 1e-07	46	382	772	234	43	18	RASL11B	RAS-like, family 11, member B	8.4	16.9	5.1	0.9	0.4
< 1e-07	< 1e-07	9842	80288	32442	17234	9588	9073	GADD45B	growth arrest and DNA-damage-inducible, beta	8.2	3.3	1.8	1.0	0.9

Parametric p-value	FDR	DMSO	0.5 h	1 h	3 h	6 h	24 h	Symbol	Name	0.5h/DMSO	1h/DMSO	3h/DMSO	6h/DMSO	24h/DMSO
< 1e-07	< 1e-07	152	1224	1268	268	145	96	KLF4	Kruppel-like factor 4 (gut)	8.1	8.4	1.8	1.0	0.6
< 1e-07	< 1e-07	43	345	359	154	39	151	KIF19	kinesin family member 19	7.9	8.2	3.5	0.9	3.5
< 1e-07	< 1e-07	187	1459	856	346	218	243	JUNB	jun B proto-oncogene	7.8	4.6	1.9	1.2	1.3
< 1e-07	< 1e-07	142	1097	457	242	107	14	LOC100128054	uncharacterized LOC100128054	7.7	3.2	1.7	0.8	0.1
< 1e-07	< 1e-07	530	4098	4751	1077	360	3128	INHBB	inhibin, beta B	7.7	9.0	2.0	0.7	5.9
< 1e-07	< 1e-07	4197	32204	20105	4438	5819	3138	SNAI1	snail homolog 1 (Drosophila)	7.7	4.8	1.1	1.4	0.7
< 1e-07	< 1e-07	86	618	927	51	113	54	RIMBP3	RIMS binding protein 3	7.2	10.8	0.6	1.3	0.6
< 1e-07	< 1e-07	14	95	289	74	57	13	FZD7	frizzled family receptor 7	6.8	20.8	5.3	4.1	0.9
< 1e-07	< 1e-07	41	253	535	231	59	90	CLDN23	claudin 23	6.1	13.0	5.6	1.4	2.2
< 1e-07	< 1e-07	127	767	399	28	131	104	NFKBID	nuclear factor of kappa light polypeptide gene enhancer in B-cells inhibitor, delta	6.0	3.1	0.2	1.0	0.8
< 1e-07	< 1e-07	417	2478	2062	653	440	363	CSRNP1	cysteine-serine-rich nuclear protein 1	5.9	4.9	1.6	1.1	0.9

Parametric p-value	FDR	DMSO	0.5 h	1 h	3 h	6 h	24 h	Symbol	Name	0.5h/DMSO	1h/DMSO	3h/DMSO	6h/DMSO	24h/DMSO
< 1e-07	< 1e-07	2385	13947	2838	1740	1806	3671	SOCS3	suppressor of cytokine signaling 3	5.8	1.2	0.7	0.8	1.5
0	0	50	275	151	32	38	23	LOC283484	uncharacterized LOC283484	5.5	3.0	0.6	0.8	0.5
0	0	16	84	25	10	11	94	SEMA6A	sema domain, transmembrane domain (TM), and cytoplasmic domain, (semaphorin) 6A	5.3	1.6	0.7	0.7	5.9
< 1e-07	< 1e-07	670	3463	2297	480	494	794	APOLD1	apolipoprotein L domain containing 1	5.2	3.4	0.7	0.7	1.2
< 1e-07	< 1e-07	520	2650	2744	648	589	512	SIK1	salt-inducible kinase 1	5.1	5.3	1.2	1.1	1.0
< 1e-07	< 1e-07	13	68	236	64	12	17	BHLHE41	basic helix-loop-helix family, member e41	5.1	17.5	4.7	0.9	1.3
0	0	29	146	141	76	45	191	AFAP1L2	actin filament associated protein 1-like 2	5.1	4.9	2.6	1.6	6.6
< 1e-07	< 1e-07	2298	11531	2397	1628	1702	3106	CXCL2	chemokine (C-X-C motif) ligand 2	5.0	1.0	0.7	0.7	1.4
< 1e-07	< 1e-07	58	292	220	164	58	50	NUDT9P1	nudix (nucleoside diphosphate linked moiety X)-type motif 9 pseudogene 1	5.0	3.8	2.8	1.0	0.8
< 1e-07	< 1e-07	18	87	362	61	22	18	DLX2	distal-less homeobox 2	4.9	20.4	3.4	1.2	1.0
< 1e-07	< 1e-07	515	2506	2780	2049	555	5043	MAN1C1	mannosidase, alpha, class 1C, member 1	4.9	5.4	4.0	1.1	9.8

Parametric p-value	FDR	DMSO	0.5 h	1 h	3 h	6 h	24 h	Symbol	Name	0.5h/DMSO	1h/DMSO	3h/DMSO	6h/DMSO	24h/DMSO
< 1e-07	< 1e-07	983	4747	2395	822	839	550	DUSP5	dual specificity phosphatase 5	4.8	2.4	0.8	0.9	0.6
< 1e-07	< 1e-07	295	1419	1467	1083	329	1813	TIMP3	TIMP metallopeptidase inhibitor 3	4.8	5.0	3.7	1.1	6.2
< 1e-07	< 1e-07	382	1819	1144	321	168	727	SLC22A18AS	solute carrier family 22 (organic cation transporter), member 18 antisense	4.8	3.0	0.8	0.4	1.9
< 1e-07	< 1e-07	15	70	185	48	16	11	FOXD1	forkhead box D1	4.7	12.6	3.2	1.1	0.8
< 1e-07	< 1e-07	197	875	996	559	336	96	LRRC4	leucine rich repeat containing 4	4.5	5.1	2.8	1.7	0.5
< 1e-07	< 1e-07	289	1263	973	972	742	772	ATF3	activating transcription factor 3	4.4	3.4	3.4	2.6	2.7
< 1e-07	< 1e-07	81	346	650	175	65	49	GEM	GTP binding protein overexpressed in skeletal muscle	4.3	8.1	2.2	0.8	0.6
< 1e-07	< 1e-07	3455	14555	13444	6286	3853	2193	RCAN1	regulator of calcineurin 1	4.2	3.9	1.8	1.1	0.6
< 1e-07	< 1e-07	2886	12042	13100	6792	3188	3973	C11orf96	chromosome 11 open reading frame 96	4.2	4.5	2.4	1.1	1.4
< 1e-07	< 1e-07	32	129	180	26	29	25	HES5	hairy and enhancer of split 5 (Drosophila)	4.1	5.7	0.8	0.9	0.8
< 1e-07	< 1e-07	171	693	241	153	148	170	PIPOX	pipecolic acid oxidase	4.1	1.4	0.9	0.9	1.0

Parametric p-value	FDR	DMSO	0.5 h	1 h	3 h	6 h	24 h	Symbol	Name	0.5h/DMSO	1h/DMSO	3h/DMSO	6h/DMSO	24h/DMSO
< 1e-07	< 1e-07	483	1926	2151	922	613	990	IRS2	insulin receptor substrate 2	4.0	4.5	1.9	1.3	
< 1e-07	< 1e-07	4419	17345	13933	4463	3841	5782	NRARP	NOTCH-regulated ankyrin repeat protein	3.9	3.2	1.0	0.9	
< 1e-07	< 1e-07	660	2485	2158	485	527	2351	GPR146	G protein-coupled receptor 146	3.8	3.3	0.7	0.8	1.3
< 1e-07	< 1e-07	1700	6353	12815	2528	1372	624	SMAD7	SMAD family member 7	3.7	7.5	1.5	0.8	0.9
< 1e-07	< 1e-07	2391	8906	3669	1688	1536	3126	KCNJ2	potassium inwardly-rectifying channel, subfamily J, member 2	3.7	1.5	0.7	0.6	3.6
0	0	559	2013	1234	414	353	617	C8orf4	chromosome 8 open reading frame 4	3.6	2.2	0.7	0.6	1.2
< 1e-07	< 1e-07	64	231	282	150	61	152	TTC39A	tetratricopeptide repeat domain 39A	3.6	4.4	2.3	1.0	0.8
< 1e-07	< 1e-07	52	185	178	91	22	248	SESN3	sestrin 3	3.6	3.4	1.8	0.4	1.1
0	0	39	137	62	51	43	29	RPS16P5	ribosomal protein S16 pseudogene 5	3.5	1.6	1.3	1.1	4.8
0	0	20	70	22	11	20	57	RSPH10B	radial spoke head 10 homolog B (Chlamydomonas)	3.5	1.1	0.6	1.0	0.5
< 1e-07	< 1e-07	70	244	180	120	69	465	FLJ34503	uncharacterized FLJ34503	3.5	2.6	1.7	1.0	0.8

Parametric p-value	FDR	DMSO	0.5 h	1 h	3 h	6 h	24 h	Symbol	Name	0.5h/DMSO	1h/DMSO	3h/DMSO	6h/DMSO	24h/DMSO
< 1e-07	< 1e-07	28225	98091	69023	53361	41826	21578	ID1	inhibitor of DNA binding 1, dominant negative helix-loop-helix protein	3.5	2.4	1.9	1.5	2.9
< 1e-07	< 1e-07	426	1476	1236	1230	413	578	HSD17B2	hydroxysteroid (17-beta) dehydrogenase 2	3.5	2.9	2.9	1.0	6.7
< 1e-07	< 1e-07	134	462	329	248	132	148	NFKBIZ	nuclear factor of kappa light polypeptide gene enhancer in B-cells inhibitor, zeta	3.5	2.5	1.9	1.0	0.8
< 1e-07	< 1e-07	1101	3807	3315	1393	1075	811	BHLHE40	basic helix-loop-helix family, member e40	3.5	3.0	1.3	1.0	1.4
0	0	111	363	281	261	485	259	TNFSF9	tumor necrosis factor (ligand) superfamily, member 9	3.3	2.5	2.4	4.4	1.1
< 1e-07	< 1e-07	490	1603	1393	777	667	840	CHAC1	ChaC, cation transport regulator homolog 1 (E. coli)	3.3	2.8	1.6	1.4	0.7
0	0	46	151	146	48	25	69	GAS1	growth arrest-specific 1	3.3	3.1	1.0	0.5	2.3
< 1e-07	< 1e-07	22	71	32	22	20	22	RGS16	regulator of G-protein signaling 16	3.2	1.5	1.0	0.9	1.7
< 1e-07	< 1e-07	214	676	659	539	290	200	SLC6A9	solute carrier family 6 (neurotransmitter transporter, glycine), member 9	3.2	3.1	2.5	1.4	1.6
< 1e-07	< 1e-07	7151	22549	14739	13155	8172	18431	AQP1	aquaporin 1 (Colton blood group)	3.2	2.1	1.8	1.1	1.2
< 1e-07	< 1e-07	838	2636	1170	1183	295	174	PTGS2	prostaglandin-endoperoxide synthase 2 (prostaglandin G/H synthase and cyclooxygenase)	3.1	1.4	1.4	0.4	0.9

Parametric p-value	FDR	DMSO	0.5 h	1 h	3 h	6 h	24 h	Symbol	Name	0.5h/DMSO	1h/DMSO	3h/DMSO	6h/DMSO	24h/DMSO
< 1e-07	< 1e-07	144	452	324	212	148	593	TRIL	TLR4 interactor with leucine-rich repeats	3.1	2.2	1.5	1.0	2.6
0	0	13	40	64	23	14	13	HOXA13	homeobox A13	3.1	4.9	1.8	1.1	0.2
< 1e-07	< 1e-07	2333	6964	6353	2463	3112	4336	CDKN1C	cyclin-dependent kinase inhibitor 1C (p57, Kip2)	3.0	2.7	1.1	1.3	4.1
< 1e-07	< 1e-07	417	1237	1663	512	283	295	FOXF1	forkhead box F1	3.0	4.0	1.2	0.7	1.0
< 1e-07	< 1e-07	4085	12021	6946	3597	3350	2429	KLF10	Kruppel-like factor 10	2.9	1.7	0.9	0.8	1.9
< 1e-07	< 1e-07	192	562	704	165	199	408	RHOU	ras homolog family member U	2.9	3.7	0.9	1.0	0.7
< 1e-07	< 1e-07	322	943	1401	762	571	480	FOSL2	FOS-like antigen 2	2.9	4.4	2.4	1.8	0.6
< 1e-07	< 1e-07	258	755	1467	2387	1445	326	F3	coagulation factor III (thromboplastin, tissue factor)	2.9	5.7	9.2	5.6	2.1
0	0	21	61	108	42	24	18	CEBPA	CCAAT/enhancer binding protein (C/EBP), alpha	2.9	5.2	2.0	1.2	1.5
< 1e-07	< 1e-07	64	187	66	99	64	48	FLJ46875	uncharacterized LOC440918	2.9	1.0	1.5	1.0	1.3
< 1e-07	< 1e-07	238	691	657	504	255	258	DDIT3	DNA-damage-inducible transcript 3	2.9	2.8	2.1	1.1	0.7

Parametric p-value	FDR	DMSO	0.5 h	1 h	3 h	6 h	24 h	Symbol	Name	0.5h/DMSO	1h/DMSO	3h/DMSO	6h/DMSO	24h/DMSO
< 1e-07	< 1e-07	143	414	456	334	146	417	HERC5	HECT and RLD domain containing E3 ubiquitin protein ligase 5	2.9	3.2	2.3	1.0	1.1
< 1e-07	< 1e-07	2154	6237	5262	1293	1264	5620	LHX6	LIM homeobox 6	2.9	2.4	0.6	0.6	1.1
< 1e-07	< 1e-07	8925	25760	26461	12039	9819	8392	ID3	inhibitor of DNA binding 3, dominant negative helix-loop-helix protein	2.9	3.0	1.3	1.1	2.9
< 1e-07	< 1e-07	1411	4044	5620	3502	1981	1400	JDP2	Jun dimerization protein 2	2.9	4.0	2.5	1.4	2.6
< 1e-07	< 1e-07	922	2625	2870	609	1069	1296	GATA3	GATA binding protein 3	2.8	3.1	0.7	1.2	0.9
< 1e-07	< 1e-07	1324	3767	3791	1397	1423	1382	KLF11	Kruppel-like factor 11	2.8	2.9	1.1	1.1	1.0
< 1e-07	< 1e-07	69	191	180	61	18	35	NPR3	natriuretic peptide receptor C/guanylate cyclase C (atrionatriuretic peptide receptor C)	2.8	2.6	0.9	0.3	1.4
< 1e-07	< 1e-07	30	83	72	34	18	144	SKAP1	src kinase associated phosphoprotein 1	2.8	2.4	1.1	0.6	0.5
0	0	16	44	81	22	19	18	IRX5	iroquois homeobox 5	2.7	5.0	1.3	1.1	0.6
< 1e-07	< 1e-07	27	73	99	50	23	110	CREG2	cellular repressor of E1A-stimulated genes 2	2.7	3.7	1.9	0.9	4.8
< 1e-07	< 1e-07	69	188	214	128	15	111	CCL20	chemokine (C-C motif) ligand 20	2.7	3.1	1.8	0.2	1.1

Parametric p-value	FDR	DMSO	0.5 h	1 h	3 h	6 h	24 h	Symbol	Name	0.5h/DMSO	1h/DMSO	3h/DMSO	6h/DMSO	24h/DMSO
< 1e-07	< 1e-07	3123	8498	7235	3296	2825	2116	SPRY2	sprouty homolog 2 (Drosophila)	2.7	2.3	1.1	0.9	4.1
< 1e-07	< 1e-07	835	2265	2897	1264	1078	947	MOAP1	modulator of apoptosis 1	2.7	3.5	1.5	1.3	1.6
< 1e-07	< 1e-07	410	1109	694	377	359	531	FGF2	fibroblast growth factor 2 (basic)	2.7	1.7	0.9	0.9	0.7
< 1e-07	< 1e-07	10	27	72	10	10	10	OVOL1	ovo-like 1(Drosophila)	2.7	7.1	1.0	1.0	0.9
< 1e-07	< 1e-07	654	1737	1617	866	622	2176	ANO2	anoctamin 2	2.7	2.5	1.3	1.0	2.9
< 1e-07	< 1e-07	16	43	118	70	21	24	LOC389332	uncharacterized LOC389332	2.7	7.4	4.4	1.3	1.0
< 1e-07	< 1e-07	326	851	962	664	387	526	HSBP1L1	heat shock factor binding protein 1-like 1	2.6	3.0	2.0	1.2	3.3
< 1e-07	< 1e-07	78	203	196	140	82	123	PLEKHA7	pleckstrin homology domain containing, family A member 7	2.6	2.5	1.8	1.1	1.5
< 1e-07	< 1e-07	5984	15533	8489	4510	6567	15290	BTG2	BTG family, member 2	2.6	1.4	0.8	1.1	1.6
< 1e-07	< 1e-07	1004	2573	3569	3361	1021	1399	C10orf114	chromosome 10 open reading frame 114	2.6	3.6	3.3	1.0	2.6
< 1e-07	< 1e-07	9194	23280	13190	13453	9136	5194	KLF2	Kruppel-like factor 2 (lung)	2.5	1.4	1.5	1.0	0.9

Parametric p-value	FDR	DMSO	0.5 h	1 h	3 h	6 h	24 h	Symbol	Name	0.5h/DMSO	1h/DMSO	3h/DMSO	6h/DMSO	24h/DMSO
< 1e-07	< 1e-07	78	196	80	10	43	116	DLL4	delta-like 4 (Drosophila)	2.5	1.0	0.1	0.6	1.4
< 1e-07	< 1e-07	3417	8533	8139	3649	4073	3444	MAFF	v-maf musculoaponeurotic fibrosarcoma oncogene homolog F (avian)	2.5	2.4	1.1	1.2	0.6
< 1e-07	< 1e-07	572	1422	1212	366	489	434	GATA2	GATA binding protein 2	2.5	2.1	0.6	0.9	1.5
< 1e-07	< 1e-07	357	885	908	742	391	657	HIF3A	hypoxia inducible factor 3, alpha subunit	2.5	2.5	2.1	1.1	1.0
< 1e-07	< 1e-07	90	224	262	151	103	196	RAB11FIP1	RAB11 family interacting protein 1 (class I)	2.5	2.9	1.7	1.1	0.8
< 1e-07	< 1e-07	399	986	936	884	366	1335	FILIP1	filamin A interacting protein 1	2.5	2.3	2.2	0.9	1.8
< 1e-07	< 1e-07	481	1189	1240	812	548	744	DHRS13	dehydrogenase/reductase (SDR family) member 13	2.5	2.6	1.7	1.1	2.2
< 1e-07	< 1e-07	271	668	695	540	384	747	NOXA1	NADPH oxidase activator 1	2.5	2.6	2.0	1.4	3.3
< 1e-07	< 1e-07	229	561	570	331	254	222	GZF1	GDNF-inducible zinc finger protein 1	2.5	2.5	1.4	1.1	1.5
< 1e-07	< 1e-07	311	744	726	676	356	924	KALRN	kalirin, RhoGEF kinase	2.4	2.3	2.2	1.1	1.1
< 1e-07	< 1e-07	5716	13589	13910	15627	8337	3620	NUPR1	nuclear protein, transcriptional regulator, 1	2.4	2.4	2.7	1.5	0.4

Parametric p-value	FDR	DMSO	0.5 h	1 h	3 h	6 h	24 h	Symbol	Name	0.5h/DMSO	1h/DMSO	3h/DMSO	6h/DMSO	24h/DMSO
< 1e-07	< 1e-07	2657	6315	5247	3519	1643	7223	TNFSF10	tumor necrosis factor (ligand) superfamily, member 10	2.4	2.0	1.3	0.6	3.0
< 1e-07	< 1e-07	8502	20056	18947	9585	8676	8243	MIDN	midnolin	2.4	2.2	1.1	1.0	0.6
< 1e-07	< 1e-07	367	865	1254	415	299	342	ZNF503	zinc finger protein 503	2.4	3.4	1.1	0.8	2.7
0	0	73	173	178	156	93	153	C1orf51	chromosome 1 open reading frame 51	2.4	2.4	2.1	1.3	1.0
< 1e-07	< 1e-07	27	64	60	28	22	13	PKNOX2	PBX/knotted 1 homeobox 2	2.4	2.2	1.0	0.8	0.9
< 1e-07	< 1e-07	17268	40580	27426	14798	8544	45977	CLDN5	claudin 5	2.4	1.6	0.9	0.5	0.5
< 1e-07	< 1e-07	887	2076	2155	439	722	1824	HIC1	hypermethylated in cancer 1	2.3	2.4	0.5	0.8	2.7
< 1e-07	< 1e-07	2584	6030	5271	3154	2649	3463	FAM117A	family with sequence similarity 117, member A	2.3	2.0	1.2	1.0	0.8
0	0	1065	2484	1760	1786	888	834	HBEGF	heparin-binding EGF-like growth factor	2.3	1.7	1.7	0.8	2.1
< 1e-07	< 1e-07	127	295	381	143	105	95	HLX	H2.0-like homeobox	2.3	3.0	1.1	0.8	1.3
< 1e-07	< 1e-07	6188	14297	5935	6436	5428	5287	TRIB1	tribbles homolog 1 (Drosophila)	2.3	1.0	1.0	0.9	0.8

Parametric p-value	FDR	DMSO	0.5 h	1 h	3 h	6 h	24 h	Symbol	Name	0.5h/DMSO	1h/DMSO	3h/DMSO	6h/DMSO	24h/DMSO
< 1e-07	< 1e-07	40	92	101	49	29	65	LRMP	lymphoid-restricted membrane protein	2.3	2.5	1.2	0.7	0.7
0	0	439	1011	763	784	420	447	FILIP1L	filamin A interacting protein 1-like	2.3	1.7	1.8	1.0	0.9
< 1e-07	< 1e-07	112	256	290	469	123	217	EBF3	early B-cell factor 3	2.3	2.6	4.2	1.1	1.6
< 1e-07	< 1e-07	49976	#####	34686	43386	37891	31645	IER2	immediate early response 2	2.3	0.7	0.9	0.8	1.0
0	0	22	50	100	22	24	23	ID4	inhibitor of DNA binding 4, dominant negative helix-loop-helix protein	2.3	4.6	1.0	1.1	0.6
< 1e-07	< 1e-07	4024	9150	9180	7460	3718	21084	PDE2A	phosphodiesterase 2A, cGMP-stimulated	2.3	2.3	1.9	0.9	0.3
0	0	17	39	36	34	12	12	TMEM200B	transmembrane protein 200B	2.3	2.1	2.0	0.7	1.0
0	0	140	317	246	115	133	167	DBP	D site of albumin promoter (albumin D-box) binding protein	2.3	1.8	0.8	1.0	5.2
< 1e-07	< 1e-07	9276	21028	19010	12252	7784	14248	SPNS2	spinster homolog 2 (Drosophila)	2.3	2.0	1.3	0.8	0.7
< 1e-07	< 1e-07	608	1379	1658	1367	991	1383	UAP1L1	UDP-N-acteylglucosamine pyrophosphorylase 1-like 1	2.3	2.7	2.2	1.6	1.2
< 1e-07	< 1e-07	107	242	329	317	151	136	PNMA6C	paraneoplastic Ma antigen family member 6C	2.3	3.1	3.0	1.4	1.5

Parametric p-value	FDR	DMSO	0.5 h	1 h	3 h	6 h	24 h	Symbol	Name	0.5h/DMSO	1h/DMSO	3h/DMSO	6h/DMSO	24h/DMSO
< 1e-07	< 1e-07	70	158	206	89	65	110	JPH3	junctophilin 3	2.3	2.9	1.3	0.9	2.3
< 1e-07	< 1e-07	37	84	316	307	54	34	DACT1	dapper, antagonist of beta-catenin, homolog 1 (Xenopus laevis)	2.3	8.5	8.2	1.4	1.3
< 1e-07	< 1e-07	530	1196	1099	627	410	517	C1orf226	chromosome 1 open reading frame 226	2.3	2.1	1.2	0.8	1.6
0	0	140	315	202	194	141	163	FAM162B	family with sequence similarity 162, member B	2.3	1.4	1.4	1.0	0.9
< 1e-07	< 1e-07	2324	5216	6538	2822	2924	2797	NFIL3	nuclear factor, interleukin 3 regulated	2.2	2.8	1.2	1.3	1.2
< 1e-07	< 1e-07	6895	15476	29431	14104	11110	5784	NAB2	NGFI-A binding protein 2 (EGR1 binding protein 2)	2.2	4.3	2.0	1.6	0.7
< 1e-07	< 1e-07	1145	2564	2446	1169	514	1656	BMP2	bone morphogenetic protein 2	2.2	2.1	1.0	0.4	0.8
0	0	15	34	32	26	16	17	PLCE1	phospholipase C, epsilon 1	2.2	2.0	1.7	1.0	1.2
< 1e-07	< 1e-07	539	1201	1327	1229	617	1120	EPB41L1	erythrocyte membrane protein band 4.1-like 1	2.2	2.5	2.3	1.1	1.4
< 1e-07	< 1e-07	80	175	211	156	62	314	ABCG2	ATP-binding cassette, sub-family G (WHITE), member 2	2.2	2.6	2.0	0.8	1.6
< 1e-07	< 1e-07	517	1136	1327	757	579	610	SERTAD4	SERTA domain containing 4	2.2	2.6	1.5	1.1	1.6

Parametric p-value	FDR	DMSO	0.5 h	1 h	3 h	6 h	24 h	Symbol	Name	0.5h/DMSO	1h/DMSO	3h/DMSO	6h/DMSO	24h/DMSO
< 1e-07	< 1e-07	24052	52691	78045	41329	24170	14149	SGK1	serum/glucocorticoid regulated kinase 1	2.2	3.2	1.7	1.0	3.9
< 1e-07	< 1e-07	21	46	49	43	22	23	TCHH	trichohyalin	2.2	2.3	2.1	1.1	1.1
< 1e-07	< 1e-07	1931	4216	4028	3163	1688	3108	FAM167B	family with sequence similarity 167, member B	2.2	2.1	1.6	0.9	1.5
0	0	98	214	273	196	113	128	PLIN5	perilipin 5	2.2	2.8	2.0	1.2	1.1
0	0	1463	3194	2632	1212	2031	2255	ABHD6	abhydrolase domain containing 6	2.2	1.8	0.8	1.4	1.6
< 1e-07	< 1e-07	929	2027	2674	1155	1109	875	PER1	period circadian clock 1	2.2	2.9	1.2	1.2	1.3
0	0	45	97	92	62	39	94	PNMT	phenylethanolamine N-methyltransferase	2.2	2.1	1.4	0.9	1.5
0	0	64	139	149	93	70	129	RAB6B	RAB6B, member RAS oncogene family	2.2	2.3	1.4	1.1	0.9
0	0	583	1256	938	407	416	1021	GCNT1	glucosaminyl (N-acetyl) transferase 1, core 2	2.2	1.6	0.7	0.7	2.1
< 1e-07	< 1e-07	1666	3583	3608	2331	2584	5922	FAM89A	family with sequence similarity 89, member A	2.2	2.2	1.4	1.6	2.0
< 1e-07	< 1e-07	3427	7360	6910	5924	4026	4063	CAMK2N1	calcium/calmodulin-dependent protein kinase II inhibitor 1	2.1	2.0	1.7	1.2	1.8

Parametric p-value	FDR	DMSO	0.5 h	1 h	3 h	6 h	24 h	Symbol	Name	0.5h/DMSO	1h/DMSO	3h/DMSO	6h/DMSO	24h/DMSO
< 1e-07	< 1e-07	439	942	1201	547	553	952	TGFBR3	transforming growth factor, beta receptor III	2.1	2.7	1.2	1.3	3.6
0	0	217	464	683	239	315	244	KBTBD11	kelch repeat and BTB (POZ) domain containing 11	2.1	3.2	1.1	1.5	2.2
0	0	15	33	23	10	10	12	NEURL3	neuralized homolog 3 (Drosophila) pseudogene	2.1	1.5	0.7	0.7	0.7
< 1e-07	< 1e-07	87	185	290	199	188	180	RAB3IL1	RAB3A interacting protein (rabin3)-like 1	2.1	3.3	2.3	2.2	1.0
< 1e-07	< 1e-07	418	881	820	379	634	706	PLD6	phospholipase D family, member 6	2.1	2.0	0.9	1.5	1.9
< 1e-07	< 1e-07	668	1405	1661	1205	585	1651	BCL2L11	BCL2-like 11 (apoptosis facilitator)	2.1	2.5	1.8	0.9	2.1
< 1e-07	< 1e-07	173	363	337	288	214	497	BCL2L10	BCL2-like 10 (apoptosis facilitator)	2.1	1.9	1.7	1.2	1.7
< 1e-07	< 1e-07	2931	6130	5395	2721	2058	4567	KLHL3	kelch-like family member 3	2.1	1.8	0.9	0.7	2.9
< 1e-07	< 1e-07	451	938	905	879	251	800	RTP4	receptor (chemosensory) transporter protein 4	2.1	2.0	2.0	0.6	1.0
< 1e-07	< 1e-07	8348	17339	20232	10055	12367	6657	SERTAD1	SERTA domain containing 1	2.1	2.4	1.2	1.5	1.8
< 1e-07	< 1e-07	725	1505	2347	1157	701	713	ARL4C	ADP-ribosylation factor-like 4C	2.1	3.2	1.6	1.0	1.0

Parametric p-value	FDR	DMSO	0.5 h	1 h	3 h	6 h	24 h	Symbol	Name	0.5h/DMSO	1h/DMSO	3h/DMSO	6h/DMSO	24h/DMSO
0	0	4616	9579	6298	2728	2039	4958	ADAMTS18	ADAM metallopeptidase with thrombospondin type 1 motif, 18	2.1	1.4	0.6	0.4	0.8
0	0	27	55	33	106	32	41	C19orf26	chromosome 19 open reading frame 26	2.1	1.3	4.0	1.2	1.0
< 1e-07	< 1e-07	207	429	490	326	158	296	CEACAM1	carcinoembryonic antigen-related cell adhesion molecule 1 (biliary glycoprotein)	2.1	2.4	1.6	0.8	1.1
0	0	25	53	55	50	37	72	PLCB4	phospholipase C, beta 4	2.1	2.2	2.0	1.5	1.5
0	0	18	38	51	30	20	21	LOC100127951	ISPF6484	2.1	2.8	1.6	1.1	1.4
< 1e-07	< 1e-07	829	1704	1578	992	556	1173	SMCR6	Smith-Magenis syndrome chromosome region, candidate 6	2.1	1.9	1.2	0.7	1.2
< 1e-07	< 1e-07	132	271	373	294	111	275	C10orf128	chromosome 10 open reading frame 128	2.0	2.8	2.2	0.8	1.4
< 1e-07	< 1e-07	225	460	649	395	218	734	ABCG1	ATP-binding cassette, sub-family G (WHITE), member 1	2.0	2.9	1.8	1.0	1.6
< 1e-07	< 1e-07	253	517	561	444	225	445	ABCA1	ATP-binding cassette, sub-family A (ABC1), member 1	2.0	2.2	1.8	0.9	1.2
< 1e-07	< 1e-07	280	572	583	330	330	653	CLMN	calmin (calponin-like, transmembrane)	2.0	2.1	1.2	1.2	1.5
< 1e-07	< 1e-07	4606	9395	11012	6066	4223	4046	FJX1	four jointed box 1 (Drosophila)	2.0	2.4	1.3	0.9	1.8

Parametric p-value	FDR	DMSO	0.5 h	1 h	3 h	6 h	24 h	Symbol	Name	0.5h/DMSO	1h/DMSO	3h/DMSO	6h/DMSO	24h/DMSO
< 1e-07	< 1e-07	116	236	267	108	95	190	SLC16A6	solute carrier family 16, member 6 (monocarboxylic acid transporter 7)	2.0	2.3	0.9	0.8	2.3
< 1e-07	< 1e-07	445	905	1263	675	404	210	SPRY4	sprouty homolog 4 (Drosophila)	2.0	2.8	1.5	0.9	0.9
< 1e-07	< 1e-07	1321	2687	2404	1337	981	2794	C5orf4	chromosome 5 open reading frame 4	2.0	1.8	1.0	0.7	1.6
< 1e-07	< 1e-07	5970	12091	12255	8654	5229	10682	TMEM88	transmembrane protein 88	2.0	2.1	1.4	0.9	0.5
0	0	476	961	769	613	485	698	DNASE1L3	deoxyribonuclease I-like 3	2.0	1.6	1.3	1.0	2.1
< 1e-07	< 1e-07	3347	6728	8533	6491	6232	4667	CEBPB	CCAAT/enhancer binding protein (C/EBP), beta	2.0	2.5	1.9	1.9	1.5
< 1e-07	< 1e-07	10517	21136	19398	11960	7673	22209	JUP	junction plakoglobin	2.0	1.8	1.1	0.7	1.1
< 1e-07	< 1e-07	1974	3963	4376	3504	1357	4219	GPRC5B	G protein-coupled receptor, family C, group 5, member B	2.0	2.2	1.8	0.7	1.4
< 1e-07	< 1e-07	1861	3733	3347	1885	2492	4484	GPR162	G protein-coupled receptor 162	2.0	1.8	1.0	1.3	2.1
< 1e-07	< 1e-07	4368	8737	19141	5098	2990	2539	BAMBI	BMP and activin membrane-bound inhibitor homolog (Xenopus laevis)	2.0	4.4	1.2	0.7	2.4
< 1e-07	< 1e-07	46	92	61	14	11	155	NAT8	N-acetyltransferase 8 (GCN5-related, putative)	2.0	1.3	0.3	0.2	0.6

Parametric p-value	FDR	DMSO	0.5 h	1 h	3 h	6 h	24 h	Symbol	Name	0.5h/DMSO	1h/DMSO	3h/DMSO	6h/DMSO	24h/DMSO
< 1e-07	< 1e-07	4206	8345	5722	4366	3503	7020	MTMR9LP	myotubularin related protein 9-like, pseudogene	2.0	1.4	1.0	0.8	3.4
< 1e-07	< 1e-07	150	297	353	278	181	361	HMHA1	histocompatibility (minor) HA-1	2.0	2.4	1.9	1.2	0.9
0	0	131	260	275	207	126	228	NXN	nucleoredoxin	2.0	2.1	1.6	1.0	1.7
< 1e-07	< 1e-07	3141	6206	5949	3922	2589	4509	TBX1	T-box 1	2.0	1.9	1.2	0.8	2.4
< 1e-07	< 1e-07	5358	10547	12220	8494	6038	8478	ZNF395	zinc finger protein 395	2.0	2.3	1.6	1.1	1.7
< 1e-07	< 1e-07	2842	5584	5766	4024	2410	7168	AFAP1L1	actin filament associated protein 1-like 1	2.0	2.0	1.4	0.8	1.4
0	0	36	70	57	44	32	37	RASL11A	RAS-like, family 11, member A	2.0	1.6	1.2	0.9	2.5
< 1e-07	< 1e-07	113	221	241	156	82	158	PPFIBP2	PTPRF interacting protein, binding protein 2 (liprin beta 2)	2.0	2.1	1.4	0.7	2.2
0	0	933	1822	852	887	1153	2651	SLC7A7	solute carrier family 7 (amino acid transporter light chain, y+L system), member 7	2.0	0.9	1.0	1.2	1.0
< 1e-07	< 1e-07	268	522	644	517	339	686	PRR5	proline rich 5 (renal)	1.9	2.4	1.9	1.3	2.1
< 1e-07	< 1e-07	202	394	463	328	252	132	STAB2	stabilin 2	1.9	2.3	1.6	1.2	0.8

Parametric p-value	FDR	DMSO	0.5 h	1 h	3 h	6 h	24 h	Symbol	Name	0.5h/DMSO	1h/DMSO	3h/DMSO	6h/DMSO	24h/DMSO
< 1e-07	< 1e-07	1314	2552	3354	2217	1233	1133	BCL6	B-cell CLL/lymphoma 6	1.9	2.6	1.7	0.9	2.6
0	0	51	98	130	84	72	57	RHCG	Rh family, C glycoprotein	1.9	2.6	1.7	1.4	0.7
0	0	156	302	384	243	189	275	WNT3	wingless-type MMTV integration site family, member 3	1.9	2.5	1.6	1.2	1.1
< 1e-07	< 1e-07	75	146	178	162	79	84	RENBP	renin binding protein	1.9	2.4	2.2	1.0	1.5
0	0	22	42	43	39	31	44	DUSP10	dual specificity phosphatase 10	1.9	2.0	1.8	1.4	1.8
0	0	36	70	67	20	21	42	MTL5	metallothionein-like 5, testis-specific (tesmin)	1.9	1.8	0.5	0.6	1.1
0	0	42	81	56	30	58	91	OCLN	occludin	1.9	1.3	0.7	1.4	2.0
0	0	1057	2033	2035	1682	975	1869	SEMA6B	sema domain, transmembrane domain (TM), and cytoplasmic domain, (semaphorin) 6B	1.9	1.9	1.6	0.9	2.2
0	0	27	51	14	18	10	99	FAM74A3	family with sequence similarity 74, member A3	1.9	0.5	0.7	0.4	0.8
0	0	10	20	31	39	10	10	TMEM229A	transmembrane protein 229A	1.9	3.0	3.8	1.0	3.8
< 1e-07	< 1e-07	496	951	1119	945	704	757	RNF208	ring finger protein 208	1.9	2.3	1.9	1.4	1.0

Parametric p-value	FDR	DMSO	0.5 h	1 h	3 h	6 h	24 h	Symbol	Name	0.5h/DMSO	1h/DMSO	3h/DMSO	6h/DMSO	24h/DMSO
0	0	245	470	573	529	334	569	TPD52	tumor protein D52	1.9	2.3	2.2	1.4	1.5
0	0	279	534	398	290	243	419	HRASLS	HRAS-like suppressor	1.9	1.4	1.0	0.9	2.3
0	0	14	26	18	18	12	52	SCN9A	sodium channel, voltage-gated, type IX, alpha subunit	1.9	1.3	1.3	0.9	1.1
< 1e-07	< 1e-07	83	159	185	89	114	79	N4BP2L1	NEDD4 binding protein 2-like 1	1.9	2.2	1.1	1.4	3.8
< 1e-07	< 1e-07	912	1730	1603	1031	228	413	HTR2B	5-hydroxytryptamine (serotonin) receptor 2B, G protein-coupled	1.9	1.8	1.1	0.3	1.1
< 1e-07	< 1e-07	983	1860	2714	1575	1228	940	MAFK	v-maf musculoaponeurotic fibrosarcoma oncogene homolog K (avian)	1.9	2.8	1.6	1.2	1.2
< 1e-07	< 1e-07	1495	2828	2889	2276	1458	3616	NR1H3	nuclear receptor subfamily 1, group H, member 3	1.9	1.9	1.5	1.0	0.5
0	0	29	55	62	46	32	40	TTBK1	tau tubulin kinase 1	1.9	2.1	1.6	1.1	2.4
< 1e-07	< 1e-07	8074	15178	14361	8840	7141	7088	ITPRIP	inositol 1,4,5-trisphosphate receptor interacting protein	1.9	1.8	1.1	0.9	3.4
0	0	33	62	70	47	41	43	C8orf46	chromosome 8 open reading frame 46	1.9	2.1	1.4	1.2	0.9
< 1e-07	< 1e-07	578	1085	965	847	464	555	SNAP25	synaptosomal-associated protein, 25kDa	1.9	1.7	1.5	0.8	0.8

Parametric p-value	FDR	DMSO	0.5 h	1 h	3 h	6 h	24 h	Symbol	Name	0.5h/DMSO	1h/DMSO	3h/DMSO	6h/DMSO	24h/DMSO
< 1e-07	< 1e-07	93	174	190	98	59	97	NRG2	neuregulin 2	1.9	2.1	1.1	0.6	1.3
< 1e-07	< 1e-07	1536	2877	3249	5002	13742	5235	RASD1	RAS, dexamethasone-induced 1	1.9	2.1	3.3	8.9	1.0
< 1e-07	< 1e-07	70	130	130	85	42	149	SPINK5	serine peptidase inhibitor, Kazal type 5	1.9	1.9	1.2	0.6	1.0
< 1e-07	< 1e-07	609	1135	872	317	610	1221	SOCS2	suppressor of cytokine signaling 2	1.9	1.4	0.5	1.0	3.4
0	0	2455	4578	4358	4559	3887	5452	CLIP3	CAP-GLY domain containing linker protein 3	1.9	1.8	1.9	1.6	2.1
< 1e-07	< 1e-07	271	504	2153	1950	384	367	ATOH8	atonal homolog 8 (Drosophila)	1.9	7.9	7.2	1.4	2.2
< 1e-07	< 1e-07	710	1317	1561	1546	895	988	C9orf91	chromosome 9 open reading frame 91	1.9	2.2	2.2	1.3	1.4
0	0	23	43	70	35	22	36	ESR2	estrogen receptor 2 (ER beta)	1.9	3.0	1.5	0.9	1.4
0	0	353	652	737	541	460	617	MTSS1L	metastasis suppressor 1-like	1.8	2.1	1.5	1.3	1.2
0	0	674	1242	355	212	555	665	SHISA8	shisa homolog 8 (Xenopus laevis)	1.8	0.5	0.3	0.8	1.5
< 1e-07	< 1e-07	1927	3551	3710	3154	1902	4111	THRA	thyroid hormone receptor, alpha	1.8	1.9	1.6	1.0	1.7

Parametric p-value	FDR	DMSO	0.5 h	1 h	3 h	6 h	24 h	Symbol	Name	0.5h/DMSO	1h/DMSO	3h/DMSO	6h/DMSO	24h/DMSO
< 1e-07	< 1e-07	507	933	1156	795	532	520	ZC3H12A	zinc finger CCCH-type containing 12A	1.8	2.3	1.6	1.0	1.0
0	0	10	19	10	55	10	22	ALPK2	alpha-kinase 2	1.8	1.0	5.4	1.0	2.1
0	0	51	94	97	98	40	60	PDE1A	phosphodiesterase 1A, calmodulin-dependent	1.8	1.9	1.9	0.8	1.0
0	0	40	72	88	71	51	87	NTN5	netrin 5	1.8	2.2	1.8	1.3	2.1
0	0	388	708	119	88	280	1741	IL8	interleukin 8	1.8	0.3	0.2	0.7	1.2
0	0	932	1704	1424	949	890	1070	HERC2	HECT and RLD domain containing E3 ubiquitin protein ligase 2	1.8	1.5	1.0	1.0	2.2
0	0	194	353	387	314	231	228	JUND	jun D proto-oncogene	1.8	2.0	1.6	1.2	1.4
< 1e-07	< 1e-07	7192	13088	17262	13855	5255	8600	CABLES1	Cdk5 and Abl enzyme substrate 1	1.8	2.4	1.9	0.7	1.4
< 1e-07	< 1e-07	743	1351	1332	1028	768	1527	MYO5C	myosin VC	1.8	1.8	1.4	1.0	1.2
< 1e-07	< 1e-07	423	768	870	861	579	576	PNMA5	paraneoplastic Ma antigen family member 5	1.8	2.1	2.0	1.4	2.1
0	0	880	1592	1617	1165	956	1411	SAMD10	sterile alpha motif domain containing 10	1.8	1.8	1.3	1.1	0.9

Parametric p-value	FDR	DMSO	0.5 h	1 h	3 h	6 h	24 h	Symbol	Name	0.5h/DMSO	1h/DMSO	3h/DMSO	6h/DMSO	24h/DMSO
< 1e-07	< 1e-07	392	710	702	639	456	694	SECTM1	secreted and transmembrane 1	1.8	1.8	1.6	1.2	1.4
< 1e-07	< 1e-07	289	522	497	294	195	183	PIK3R3	phosphoinositide-3-kinase, regulatory subunit 3 (gamma)	1.8	1.7	1.0	0.7	1.8
0	0	49	89	78	71	28	124	RNASE6	ribonuclease, RNase A family, k6	1.8	1.6	1.5	0.6	1.7
0	0	16987	30690	19002	20111	16947	20768	NFKBIA	nuclear factor of kappa light polypeptide gene enhancer in B-cells inhibitor, alpha	1.8	1.1	1.2	1.0	0.6
< 1e-07	< 1e-07	276	498	578	495	258	581	IQCA1	IQ motif containing with AAA domain 1	1.8	2.1	1.8	0.9	2.5
< 1e-07	< 1e-07	4306	7769	11764	4949	4161	5657	KLF3	Kruppel-like factor 3 (basic)	1.8	2.7	1.1	1.0	2.1
0	0	54	98	153	102	48	48	CD38	CD38 molecule	1.8	2.8	1.9	0.9	1.4
< 1e-07	< 1e-07	133	239	294	149	111	310	ACACB	acetyl-CoA carboxylase beta	1.8	2.2	1.1	0.8	1.3
0	0	81	146	155	119	157	177	C20orf195	chromosome 20 open reading frame 195	1.8	1.9	1.5	1.9	0.9
< 1e-07	< 1e-07	34	61	64	108	56	84	NR6A1	nuclear receptor subfamily 6, group A, member 1	1.8	1.9	3.2	1.6	2.3
0	0	947	1697	1496	2099	1604	1590	PMAIP1	phorbol-12-myristate-13-acetate-induced protein 1	1.8	1.6	2.2	1.7	2.2

Parametric p-value	FDR	DMSO	0.5 h	1 h	3 h	6 h	24 h	Symbol	Name	0.5h/DMSO	1h/DMSO	3h/DMSO	6h/DMSO	24h/DMSO
< 1e-07	< 1e-07	775	1388	864	367	720	9271	CXCR4	chemokine (C-X-C motif) receptor 4	1.8	1.1	0.5	0.9	2.5
0	0	22	40	27	28	22	15	FBP2	fructose-1,6-bisphosphatase 2	1.8	1.2	1.3	1.0	1.7
0	0	49	88	88	49	45	52	GPR31	G protein-coupled receptor 31	1.8	1.8	1.0	0.9	12.0
0	0	21	37	32	20	21	37	NXPH3	neurexophilin 3	1.8	1.5	1.0	1.0	0.7
< 1e-07	< 1e-07	207	369	501	302	256	270	FZD5	frizzled family receptor 5	1.8	2.4	1.5	1.2	1.0
< 1e-07	< 1e-07	231	412	496	390	242	462	CORO2B	coronin, actin binding protein, 2B	1.8	2.1	1.7	1.0	2.3
< 1e-07	< 1e-07	650	1157	1158	888	680	2408	ACSS1	acyl-CoA synthetase short-chain family member 1	1.8	1.8	1.4	1.0	2.0
< 1e-07	< 1e-07	1819	3234	4693	3577	2492	2467	TMEM121	transmembrane protein 121	1.8	2.6	2.0	1.4	3.7
< 1e-07	< 1e-07	187	333	524	308	214	342	TMEM170B	transmembrane protein 170B	1.8	2.8	1.6	1.1	1.4
< 1e-07	< 1e-07	7146	12664	16433	11668	9894	11762	KLHL21	kelch-like family member 21	1.8	2.3	1.6	1.4	1.8
< 1e-07	< 1e-07	412	729	693	563	454	1345	RASSF4	Ras association (RalGDS/AF-6) domain family member 4	1.8	1.7	1.4	1.1	1.6

Parametric p-value	FDR	DMSO	0.5 h	1 h	3 h	6 h	24 h	Symbol	Name	0.5h/DMSO	1h/DMSO	3h/DMSO	6h/DMSO	24h/DMSO
0	0	1386	2450	2443	1662	1364	937	BEX2	brain expressed X-linked 2	1.8	1.8	1.2	1.0	3.3
< 1e-07	< 1e-07	154	272	353	391	283	235	CLDN3	claudin 3	1.8	2.3	2.5	1.8	0.7
< 1e-07	< 1e-07	4584	8092	8378	6687	4129	9222	LHFPL2	lipoma HMGIC fusion partner-like 2	1.8	1.8	1.5	0.9	1.3
< 1e-07	< 1e-07	191	337	590	673	311	196	ZDHHC23	zinc finger, DHHC-type containing 23	1.8	3.1	3.5	1.6	1.5
0	0	763	1345	1003	743	671	1317	LOC100130876	uncharacterized LOC100130876	1.8	1.3	1.0	0.9	2.0
< 1e-07	< 1e-07	931	1642	1748	1516	983	981	SLC22A18	solute carrier family 22, member 18	1.8	1.9	1.6	1.1	1.0
0	0	72	128	62	36	95	101	SLC5A12	solute carrier family 5 (sodium/glucose cotransporter), member 12	1.8	0.9	0.5	1.3	1.7
< 1e-07	< 1e-07	2734	4810	5516	3178	2294	3407	HOXA6	homeobox A6	1.8	2.0	1.2	0.8	1.1
< 1e-07	< 1e-07	1096	1927	1795	1362	1264	2060	ZNF219	zinc finger protein 219	1.8	1.6	1.2	1.2	1.4
< 1e-07	< 1e-07	1372	2411	2195	1810	977	1697	WDFY4	WDFY family member 4	1.8	1.6	1.3	0.7	1.2
0	0	7322	12854	12298	9047	6920	14037	SGK223	homolog of rat pragma of Rnd2	1.8	1.7	1.2	0.9	1.9

Parametric p-value	FDR	DMSO	0.5 h	1 h	3 h	6 h	24 h	Symbol	Name	0.5h/DMSO	1h/DMSO	3h/DMSO	6h/DMSO	24h/DMSO
< 1e-07	< 1e-07	614	1077	1129	1087	728	1736	TSPAN15	tetraspanin 15	1.8	1.8	1.8	1.2	1.2
0	0	30	52	29	13	28	51	STON1-GTF2A1L	STON1-GTF2A1L readthrough	1.8	1.0	0.4	0.9	1.9
0	0	304	530	244	87	155	166	ITGB8	integrin, beta 8	1.7	0.8	0.3	0.5	2.8
0	0	1373	2394	2047	1438	782	2809	GPR116	G protein-coupled receptor 116	1.7	1.5	1.0	0.6	1.7
< 1e-07	< 1e-07	132	231	347	320	203	171	ULBP1	UL16 binding protein 1	1.7	2.6	2.4	1.5	0.5
0	0	27	47	49	34	34	123	C11orf45	chromosome 11 open reading frame 45	1.7	1.8	1.2	1.3	0.6
0	0	74778	#####	#####	#####	75112	69768	CYR61	cysteine-rich, angiogenic inducer, 61	1.7	1.5	1.5	1.0	4.6
< 1e-07	< 1e-07	135	235	290	225	126	303	VLDLR	very low density lipoprotein receptor	1.7	2.1	1.7	0.9	0.9
< 1e-07	< 1e-07	105	181	239	159	95	134	CHN2	chimerin 2	1.7	2.3	1.5	0.9	1.3
0	0	44	76	62	45	44	40	C6orf132	chromosome 6 open reading frame 132	1.7	1.4	1.0	1.0	2.2
0	0	7576	13105	12852	10937	6687	12923	ARHGEF17	Rho guanine nucleotide exchange factor (GEF) 17	1.7	1.7	1.4	0.9	1.3

Parametric p-value	FDR	DMSO	0.5 h	1 h	3 h	6 h	24 h	Symbol	Name	0.5h/DMSO	1h/DMSO	3h/DMSO	6h/DMSO	24h/DMSO
0	0	72	124	148	108	73	81	GDF1	growth differentiation factor 1	1.7	2.1	1.5	1.0	0.9
< 1e-07	< 1e-07	6934	11975	13696	13000	9182	10332	PPP1R3B	protein phosphatase 1, regulatory subunit 3B	1.7	2.0	1.9	1.3	0.9
< 1e-07	< 1e-07	122	211	256	242	139	178	PARD6A	par-6 partitioning defective 6 homolog alpha (C. elegans)	1.7	2.1	2.0	1.1	1.0
0	0	127	220	241	96	122	127	KDM6B	lysine (K)-specific demethylase 6B	1.7	1.9	0.8	1.0	1.5
0	0	1538	2648	2300	1787	1467	3945	ABCA6	ATP-binding cassette, sub-family A (ABC1), member 6	1.7	1.5	1.2	1.0	1.0
0	0	107	184	219	198	106	157	EDA	ectodysplasin A	1.7	2.0	1.8	1.0	1.7
< 1e-07	< 1e-07	3369	5789	3870	2585	2573	5982	MGC16121	uncharacterized protein MGC16121	1.7	1.1	0.8	0.8	1.5
< 1e-07	< 1e-07	277	475	505	429	287	370	ADHFE1	alcohol dehydrogenase, iron containing, 1	1.7	1.8	1.6	1.0	1.1
< 1e-07	< 1e-07	18742	32155	96831	#####	#####	#####	HMOX1	heme oxygenase (decycling) 1	1.7	5.2	8.0	7.7	1.3
0	0	91	156	150	126	126	63	SNAP91	synaptosomal-associated protein, 91kDa	1.7	1.7	1.4	1.4	6.2
< 1e-07	< 1e-07	202	346	327	286	279	382	MXI1	MAX interactor 1, dimerization protein	1.7	1.6	1.4	1.4	1.2

Parametric p-value	FDR	DMSO	0.5 h	1 h	3 h	6 h	24 h	Symbol	Name	0.5h/DMSO	1h/DMSO	3h/DMSO	6h/DMSO	24h/DMSO
< 1e-07	< 1e-07	3287	5625	3860	1937	3423	3327	IER5L	immediate early response 5-like	1.7	1.2	0.6	1.0	0.7
0	0	17	29	59	12	10	17	CSF2	colony stimulating factor 2 (granulocyte-macrophage)	1.7	3.5	0.7	0.6	1.9
0	0	52	89	47	41	44	42	ZNF204P	zinc finger protein 204, pseudogene	1.7	0.9	0.8	0.8	1.0
0	0	3169	5409	4580	3388	2030	3577	ZBTB8A	zinc finger and BTB domain containing 8A	1.7	1.4	1.1	0.6	1.0
< 1e-07	< 1e-07	33	55	40	54	63	88	TNFSF18	tumor necrosis factor (ligand) superfamily, member 18	1.7	1.2	1.7	1.9	0.8
< 1e-07	< 1e-07	126	215	225	216	109	212	TMEM163	transmembrane protein 163	1.7	1.8	1.7	0.9	1.1
< 1e-07	< 1e-07	27	46	14	10	19	25	GALNT3	UDP-N-acetyl-alpha-D-galactosamine:polypeptide N-acetylgalactosaminyltransferase 3 (GalNAc-T3)	1.7	0.5	0.4	0.7	2.7
< 1e-07	< 1e-07	7567	12858	12855	9543	6385	8414	PLSCR4	phospholipid scramblase 4	1.7	1.7	1.3	0.8	0.9
< 1e-07	< 1e-07	222	378	511	372	259	381	CLEC10A	C-type lectin domain family 10, member A	1.7	2.3	1.7	1.2	1.2
< 1e-07	< 1e-07	191	324	403	347	256	235	RASGRP2	RAS guanyl releasing protein 2 (calcium and DAG-regulated)	1.7	2.1	1.8	1.3	1.1
0	0	1736	2944	3074	1952	1676	3449	AIM1	absent in melanoma 1	1.7	1.8	1.1	1.0	1.2

Parametric p-value	FDR	DMSO	0.5 h	1 h	3 h	6 h	24 h	Symbol	Name	0.5h/DMSO	1h/DMSO	3h/DMSO	6h/DMSO	24h/DMSO
0	0	54	92	46	95	187	384	TFEC	transcription factor EC	1.7	0.8	1.7	3.4	0.8
0	0	21	36	24	13	22	22	ARHGAP9	Rho GTPase activating protein 9	1.7	1.1	0.6	1.0	2.0
0	0	345	584	521	231	206	268	SSTR1	somatostatin receptor 1	1.7	1.5	0.7	0.6	7.1
< 1e-07	< 1e-07	423	715	579	585	723	1208	SLC22A23	solute carrier family 22, member 23	1.7	1.4	1.4	1.7	1.3
< 1e-07	< 1e-07	198	335	330	239	135	415	C6orf141	chromosome 6 open reading frame 141	1.7	1.7	1.2	0.7	2.5
< 1e-07	< 1e-07	10698	18074	19619	17364	10785	13728	CMTM7	CKLF-like MARVEL transmembrane domain containing 7	1.7	1.8	1.6	1.0	2.9
0	0	636	1073	787	342	431	1038	WSCD1	WSC domain containing 1	1.7	1.2	0.5	0.7	2.1
< 1e-07	< 1e-07	766	1291	1514	1131	948	1398	IL15	interleukin 15	1.7	2.0	1.5	1.2	1.3
< 1e-07	< 1e-07	93	156	320	204	97	120	SIX1	SIX homeobox 1	1.7	3.5	2.2	1.0	1.8
< 1e-07	< 1e-07	10221	17214	18631	13151	9958	17981	TOX2	TOX high mobility group box family member 2	1.7	1.8	1.3	1.0	1.0
0	0	20	34	15	14	16	27	STK31	serine/threonine kinase 31	1.7	0.7	0.7	0.8	1.3

Parametric p-value	FDR	DMSO	0.5 h	1 h	3 h	6 h	24 h	Symbol	Name	0.5h/DMSO	1h/DMSO	3h/DMSO	6h/DMSO	24h/DMSO
< 1e-07	< 1e-07	1116	1878	1873	1866	1360	2659	CPT1C	carnitine palmitoyltransferase 1C	1.7	1.7	1.7	1.2	1.3
0	0	11	19	14	30	13	18	S100A12	S100 calcium binding protein A12	1.7	1.3	2.7	1.2	1.3
0	0	5337	8964	9226	6264	4393	10768	TPST2	tyrosylprotein sulfotransferase 2	1.7	1.7	1.2	0.8	1.3
< 1e-07	< 1e-07	40	66	77	13	41	126	KIAA1257	KIAA1257	1.7	1.9	0.3	1.0	1.1
< 1e-07	< 1e-07	521	873	970	437	594	781	NFATC4	nuclear factor of activated T-cells, cytoplasmic, calcineurin-dependent 4	1.7	1.9	0.8	1.1	2.0
0	0	32	53	27	29	32	43			1.7	0.8	0.9	1.0	3.2
0	0	97	163	73	16	57	183	FLVCR2	feline leukemia virus subgroup C cellular receptor family, member 2	1.7	0.8	0.2	0.6	1.5
< 1e-07	< 1e-07	2330	3896	3775	3830	3165	5800	TNFRSF10C	tumor necrosis factor receptor superfamily, member 10c, decoy without an intracellular domain	1.7	1.6	1.6	1.4	1.9
< 1e-07	< 1e-07	173	289	375	271	133	235	PION	pigeon homolog (Drosophila)	1.7	2.2	1.6	0.8	1.0
< 1e-07	< 1e-07	279	467	558	718	264	365	RNF152	ring finger protein 152	1.7	2.0	2.6	0.9	2.5

Parametric p-value	FDR	DMSO	0.5 h	1 h	3 h	6 h	24 h	Symbol	Name	0.5h/DMSO	1h/DMSO	3h/DMSO	6h/DMSO	24h/DMSO
0	0	33	55	33	13	40	34	LOC100130057	uncharacterized LOC100130057	1.7	1.0	0.4	1.2	1.3
0	0	10	17	12	43	10	19	C3orf30	chromosome 3 open reading frame 30	1.7	1.2	4.2	1.0	0.9
< 1e-07	< 1e-07	905	1510	2669	2106	1010	680	ZBTB2	zinc finger and BTB domain containing 2	1.7	2.9	2.3	1.1	1.0
0	0	15	24	21	18	18	12	HS3ST2	heparan sulfate (glucosamine) 3-O-sulfotransferase 2	1.7	1.4	1.2	1.2	1.7
0	0	146	243	273	188	111	117	NOS1AP	nitric oxide synthase 1 (neuronal) adaptor protein	1.7	1.9	1.3	0.8	0.7
0	0	219	365	503	406	311	232	CDKN1A	cyclin-dependent kinase inhibitor 1A (p21, Cip1)	1.7	2.3	1.8	1.4	0.8
< 1e-07	< 1e-07	410	680	705	456	458	1052	ARHGAP28	Rho GTPase activating protein 28	1.7	1.7	1.1	1.1	0.8
< 1e-07	< 1e-07	1555	2580	2480	2069	1666	1540	CCNL1	cyclin L1	1.7	1.6	1.3	1.1	1.1
0	0	677	1122	1136	884	787	957	MERTK	c-mer proto-oncogene tyrosine kinase	1.7	1.7	1.3	1.2	2.2
0	0	12	20	13	57	11	26	GNG2	guanine nucleotide binding protein (G protein), gamma 2	1.7	1.1	4.7	0.9	1.4
< 1e-07	< 1e-07	6108	10084	14065	13849	9467	6949	METRNL	meteorin, glial cell differentiation regulator-like	1.7	2.3	2.3	1.5	0.9

Parametric p-value	FDR	DMSO	0.5 h	1 h	3 h	6 h	24 h	Symbol	Name	0.5h/DMSO	1h/DMSO	3h/DMSO	6h/DMSO	24h/DMSO
< 1e-07	< 1e-07	6095	10047	11387	7377	3138	5675	MPZL2	myelin protein zero-like 2	1.6	1.9	1.2	0.5	1.1
0	0	476	784	376	187	386	311	LOC153546	uncharacterized LOC153546	1.6	0.8	0.4	0.8	1.8
< 1e-07	< 1e-07	9236	15206	16610	15304	9338	29566	PGF	placental growth factor	1.6	1.8	1.7	1.0	0.9
0	0	547	899	655	478	474	930	ARVCF	armadillo repeat gene deleted in velocardiofacial syndrome	1.6	1.2	0.9	0.9	3.2
< 1e-07	< 1e-07	2376	3905	5320	5082	3185	3935	CHKA	choline kinase alpha	1.6	2.2	2.1	1.3	1.3
< 1e-07	< 1e-07	338	554	540	349	281	1033	ACOX2	acyl-CoA oxidase 2, branched chain	1.6	1.6	1.0	0.8	1.7
< 1e-07	< 1e-07	1087	1784	2163	1313	1380	1043	FUT4	fucosyltransferase 4 (alpha (1,3) fucosyltransferase, myeloid-specific)	1.6	2.0	1.2	1.3	1.7
0	0	593	974	957	1094	737	1236	YPEL3	yippee-like 3 (Drosophila)	1.6	1.6	1.8	1.2	3.1
0	0	294	482	516	309	390	390	GLIS2	GLIS family zinc finger 2	1.6	1.8	1.1	1.3	1.0
< 1e-07	< 1e-07	2160	3544	3848	3393	2124	3229	VWCE	von Willebrand factor C and EGF domains	1.6	1.8	1.6	1.0	2.1
0	0	106	174	195	84	95	156	TRERF1	transcriptional regulating factor 1	1.6	1.8	0.8	0.9	1.3

Parametric p-value	FDR	DMSO	0.5 h	1 h	3 h	6 h	24 h	Symbol	Name	0.5h/DMSO	1h/DMSO	3h/DMSO	6h/DMSO	24h/DMSO
0	0	30	49	40	33	17	24	CNIH3	cornichon homolog 3 (Drosophila)	1.6	1.3	1.1	0.6	1.5
0	0	40	65	49	31	22	74	LOC440028	uncharacterized LOC440028	1.6	1.2	0.8	0.5	0.8
< 1e-07	< 1e-07	356	582	625	796	608	523	PPARG	peroxisome proliferator-activated receptor gamma	1.6	1.8	2.2	1.7	1.5
< 1e-07	< 1e-07	717	1171	1386	770	681	1266	C2CD2	C2 calcium-dependent domain containing 2	1.6	1.9	1.1	0.9	1.5
0	0	3737	6102	3701	5571	6358	6044	C2CD4B	C2 calcium-dependent domain containing 4B	1.6	1.0	1.5	1.7	1.4
0	0	609	995	895	469	759	1092	ZCCHC24	zinc finger, CCHC domain containing 24	1.6	1.5	0.8	1.2	1.8
0	0	22	36	36	43	27	27	KAZN	kazrin, periplakin interacting protein	1.6	1.6	2.0	1.3	1.6
0	0	878	1431	1145	801	899	1113	SALL2	sal-like 2 (Drosophila)	1.6	1.3	0.9	1.0	1.8
< 1e-07	< 1e-07	129	210	243	107	72	702	APCDD1	adenomatosis polyposis coli down-regulated 1	1.6	1.9	0.8	0.6	1.2
< 1e-07	< 1e-07	319	520	485	132	502	740	ARID3A	AT rich interactive domain 3A (BRIGHT-like)	1.6	1.5	0.4	1.6	1.3
0	0	638	1037	1211	1206	720	1161	SLC15A3	solute carrier family 15, member 3	1.6	1.9	1.9	1.1	5.4

Parametric p-value	FDR	DMSO	0.5 h	1 h	3 h	6 h	24 h	Symbol	Name	0.5h/DMSO	1h/DMSO	3h/DMSO	6h/DMSO	24h/DMSO
< 1e-07	< 1e-07	6049	9835	9423	10238	6274	9706	ABLIM1	actin binding LIM protein 1	1.6	1.6	1.7	1.0	2.3
0	0	182	296	289	126	73	185	CXCL6	chemokine (C-X-C motif) ligand 6	1.6	1.6	0.7	0.4	1.8
< 1e-07	< 1e-07	2349	3809	3061	1832	1056	1361	CLEC4GP1	C-type lectin domain family 4, member G pseudogene 1	1.6	1.3	0.8	0.4	1.6
< 1e-07	< 1e-07	1385	2244	2448	1267	1288	2013	NFATC1	nuclear factor of activated T-cells, cytoplasmic, calcineurin-dependent 1	1.6	1.8	0.9	0.9	1.0
0	0	68	109	101	152	77	108	ENTPD8	ectonucleoside triphosphate diphosphohydrolase 8	1.6	1.5	2.2	1.1	1.5
< 1e-07	< 1e-07	4229	6846	6887	2095	1133	5089	CXCR7	chemokine (C-X-C motif) receptor 7	1.6	1.6	0.5	0.3	0.9
< 1e-07	< 1e-07	663	1072	864	390	484	1952	EPHX4	epoxide hydrolase 4	1.6	1.3	0.6	0.7	1.6
< 1e-07	< 1e-07	109	177	151	204	106	108	MIR17HG	miR-17-92 cluster host gene (non-protein coding)	1.6	1.4	1.9	1.0	1.2
< 1e-07	< 1e-07	172	279	354	303	252	2181	GPIHBP1	glycosylphosphatidylinositol anchored high density lipoprotein binding protein 1	1.6	2.1	1.8	1.5	2.9
< 1e-07	< 1e-07	467	754	811	846	447	1029	CD36	CD36 molecule (thrombospondin receptor)	1.6	1.7	1.8	1.0	1.0
< 1e-07	< 1e-07	261	421	557	519	342	339	MSX1	msh homeobox 1	1.6	2.1	2.0	1.3	12.6

Parametric p-value	FDR	DMSO	0.5 h	1 h	3 h	6 h	24 h	Symbol	Name	0.5h/DMSO	1h/DMSO	3h/DMSO	6h/DMSO	24h/DMSO
0	0	548	885	866	765	493	814	PLXNB3	plexin B3	1.6	1.6	1.4	0.9	1.3
0	0	49	79	87	54	47	93	CTTNBP2	cortactin binding protein 2	1.6	1.8	1.1	1.0	1.3
< 1e-07	< 1e-07	6668	10716	8795	3654	6156	11745	CHST15	carbohydrate (N-acetylgalactosamine 4-sulfate 6-O) sulfotransferase 15	1.6	1.3	0.5	0.9	1.5
0	0	67	108	92	65	54	51	ZNF620	zinc finger protein 620	1.6	1.4	1.0	0.8	1.8

Bibliography

1. Wang, X., et al., *Cytoprotective effect of caffeic acid phenethyl ester (CAPE) and catechol ring-fluorinated CAPE derivatives against menadione-induced oxidative stress in human endothelial cells.* Bioorg Med Chem, 2006. **14**(14): p. 4879-87.
2. Wang, X., et al., *Cytoprotection of human endothelial cells from menadione cytotoxicity by caffeic acid phenethyl ester: the role of heme oxygenase-1.* Eur J Pharmacol, 2008. **591**(1-3): p. 28-35.
3. *Heart attack and stroke: men vs. women. For both men and women, cardiovascular disease is the leading cause of death. But their risks and symptoms can differ.* Harv Heart Lett, 2014. **24**(9): p. 1, 7.
4. Di Filippo, C., et al., *Oxidative stress as the leading cause of acute myocardial infarction in diabetics.* Cardiovasc Drug Rev, 2006. **24**(2): p. 77-87.
5. Hoyert, D.L. and J. Xu, *Deaths: preliminary data for 2011.* Natl Vital Stat Rep, 2012. **61**(6): p. 1-51.
6. Granger, D.N., *Ischemia-reperfusion: mechanisms of microvascular dysfunction and the influence of risk factors for cardiovascular disease.* Microcirculation, 1999. **6**(3): p. 167-78.
7. Finkel, T., *Signal transduction by mitochondrial oxidants.* J Biol Chem, 2012. **287**(7): p. 4434-4440.
8. Ma, Q., *Transcriptional responses to oxidative stress: pathological and toxicological implications.* Pharmacol Ther, 2010. **125**(3): p. 376-93.
9. Finkel, T., *Signal transduction by reactive oxygen species.* J Cell Biol, 2011. **194**(1): p. 7-15.
10. Beckman, K.B. and B.N. Ames, *The free radical theory of aging matures.* Physiol Rev, 1998. **78**(2): p. 547-581.
11. Heitzer, T., et al., *Endothelial dysfunction, oxidative stress, and risk of cardiovascular events in patients with coronary artery disease.* Circulation, 2001. **104**(22): p. 2673-2678.
12. Halliwell, B. and J.M. Gutteridge, *Oxygen free radicals and iron in relation to biology and medicine: some problems and concepts.* Arch Biochem Biophys, 1986. **246**(2): p. 501-14.
13. den Hengst, W.A., et al., *Lung ischemia-reperfusion injury: a molecular and clinical view on a complex pathophysiological process.* Am J Physiol Heart Circ Physiol, 2010. **299**(5): p. H1283-99.
14. Schock, S.C., et al., *Microparticles generated during chronic cerebral ischemia deliver proapoptotic signals to cultured endothelial cells.* Biochem Biophys Res Commun, 2014. **450**(1): p. 912-7.
15. Zeng, M., et al., *Reactive oxygen species contribute to simulated ischemia/reperfusion-induced autophagic cell death in human umbilical vein endothelial cells.* Med Sci Monit, 2014. **20**: p. 1017-23.

16. Laude, K., V. Richard, and C. Thuillez, *Coronary endothelial cells: a target of ischemia reperfusion and its treatment?* Arch Mal Coeur Vaiss, 2004. **97**(3): p. 250-4.
17. Tan, J., et al., *MAPK mediates inflammatory response and cell death in rat pulmonary microvascular endothelial cells in an ischemia-reperfusion model of lung transplantation.* J Heart Lung Transplant, 2013. **32**(8): p. 823-31.
18. Suzuki, Y., N. Nagai, and K. Umemura, *Novel situations of endothelial injury in stroke--mechanisms of stroke and strategy of drug development: intracranial bleeding associated with the treatment of ischemic stroke: thrombolytic treatment of ischemia-affected endothelial cells with tissue-type plasminogen activator.* J Pharmacol Sci, 2011. **116**(1): p. 25-9.
19. Aird, W.C., *Spatial and temporal dynamics of the endothelium.* J Thromb Haemost, 2005. **3**(7): p. 1392-406.
20. Aird, W.C., *Endothelial cell heterogeneity.* Cold Spring Harb Perspect Med, 2012. **2**(1): p. a006429.
21. Warren, M.C., et al., *Oxidative stress-induced apoptosis of endothelial cells.* Free Radic Biol Med, 2000. **29**(6): p. 537-47.
22. Kossenjans, W., et al., *Menadione-induced oxidative stress in bovine heart microvascular endothelial cells.* Microcirculation, 1996. **3**(1): p. 39-47.
23. Lee, J.Y., et al., *Menadione induces endothelial dysfunction mediated by oxidative stress and arylation.* Chem Biol Interact, 2001. **137**(2): p. 169-83.
24. Zhao, Y. and B. Zhao, *Protective effect of natural antioxidants on heart against ischemia-reperfusion damage.* Curr Pharm Biotechnol, 2010. **11**(8): p. 868-74.
25. Dilsiz, N., et al., *Protective effects of various antioxidants during ischemia-reperfusion in the rat retina.* Graefes Arch Clin Exp Ophthalmol, 2006. **244**(5): p. 627-33.
26. Dosluoglu, H.H., et al., *Does preferential use of endovascular interventions by vascular surgeons improve limb salvage, control of symptoms, and survival of patients with critical limb ischemia?* Am J Surg, 2006. **192**(5): p. 572-6.
27. Christophe, M. and S. Nicolas, *Mitochondria: a target for neuroprotective interventions in cerebral ischemia-reperfusion.* Curr Pharm Des, 2006. **12**(6): p. 739-57.
28. Trocciola, S.M., et al., *Comparison of results in endovascular interventions for infrainguinal lesions: claudication versus critical limb ischemia.* Am Surg, 2005. **71**(6): p. 474-9; discussion 479-80.
29. Ko, Y.E., et al., *Mechanism of glutathione depletion during simulated ischemia-reperfusion of H9c2 cardiac myocytes.* Free Radic Res, 2011. **45**(9): p. 1074-82.
30. Forgiarini, L.F., et al., *N-Acetylcysteine administration confers lung protection in different phases of lung ischemia-reperfusion injury.* Interact Cardiovasc Thorac Surg, 2014.
31. Hsieh, C.C., et al., *Protective Effects of N-acetylcysteine and a Prostaglandin E1 Analog, Alprostadil, Against Hepatic Ischemia: Reperfusion Injury in Rats.* J Tradit Complement Med, 2014. **4**(1): p. 64-71.

32. Kilciksiz, S., et al., *The effect of N-acetylcysteine on biomarkers for radiation-induced oxidative damage in a rat model.* Acta Med Okayama, 2008. **62**(6): p. 403-9.
33. Miller, A.C., et al., *Influence of nebulized unfractionated heparin and N-acetylcysteine in acute lung injury after smoke inhalation injury.* J Burn Care Res, 2009. **30**(2): p. 249-56.
34. Cortijo, J., et al., *Attenuation by oral N-acetylcysteine of bleomycin-induced lung injury in rats.* Eur Respir J, 2001. **17**(6): p. 1228-35.
35. Caprio, M., C. Mammi, and G.M. Rosano, *Vitamin D: a novel player in endothelial function and dysfunction.* Arch Med Sci, 2012. **8**(1): p. 4-5.
36. Paolini, M., et al., *The nature of prooxidant activity of vitamin C.* Life Sci, 1999. **64**(23): p. PL 273-8.
37. Dietrich, M., et al., *Vitamin E supplement use and the incidence of cardiovascular disease and all-cause mortality in the Framingham Heart Study: Does the underlying health status play a role?* Atherosclerosis, 2009. **205**(2): p. 549-53.
38. Tavani, A. and C. La Vecchia, *Plasma ascorbic acid and risk of heart disease and cancer.* Lancet, 2001. **357**(9274): p. 2134-5.
39. Maheshwari, R.K., et al., *Multiple biological activities of curcumin: a short review.* Life Sci, 2006. **78**(18): p. 2081-7.
40. Noorafshan, A. and S. Ashkani-Esfahani, *A review of therapeutic effects of curcumin.* Curr Pharm Des, 2013. **19**(11): p. 2032-46.
41. Jurenka, J.S., *Anti-inflammatory properties of curcumin, a major constituent of Curcuma longa: a review of preclinical and clinical research.* Altern Med Rev, 2009. **14**(2): p. 141-53.
42. Moghadamtousi, S.Z., et al., *A review on antibacterial, antiviral, and antifungal activity of curcumin.* Biomed Res Int, 2014. **2014**: p. 186864.
43. Banaganapalli, B., et al., *Synthesis and biological activity of new resveratrol derivative and molecular docking: dynamics studies on NFkB.* Appl Biochem Biotechnol, 2013. **171**(7): p. 1639-57.
44. Sovak, M., *Grape Extract, Resveratrol, and Its Analogs: A Review.* J Med Food, 2001. **4**(2): p. 93-105.
45. Wu, J.M., et al., *Mechanism of cardioprotection by resveratrol, a phenolic antioxidant present in red wine (Review).* Int J Mol Med, 2001. **8**(1): p. 3-17.
46. Wang, Y., et al., *Quercetin postconditioning attenuates myocardial ischemia/reperfusion injury in rats through the PI3K/Akt pathway.* Braz J Med Biol Res, 2013. **46**(10): p. 861-7.
47. Kidd, P.M., *Bioavailability and activity of phytosome complexes from botanical polyphenols: the silymarin, curcumin, green tea, and grape seed extracts.* Altern Med Rev, 2009. **14**(3): p. 226-46.
48. Andriantsitohaina, R., et al., *Systems biology of antioxidants.* Clin Sci (Lond), 2012. **123**(3): p. 173-92.
49. Wang, X., et al., *Structure-activity relationships in the cytoprotective effect of caffeic acid phenethyl ester (CAPE) and fluorinated derivatives: effects on heme*

oxygenase-1 induction and antioxidant activities. Eur J Pharmacol, 2010. **635**(1-3): p. 16-22.
50. Yang, J., et al., *Synthesis of a series of caffeic acid phenethyl amide (CAPA) fluorinated derivatives: comparison of cytoprotective effects to caffeic acid phenethyl ester (CAPE).* Bioorg Med Chem, 2010. **18**(14): p. 5032-8.
51. Parlakpinar, H., et al., *Protective effect of caffeic acid phenethyl ester (CAPE) on myocardial ischemia-reperfusion-induced apoptotic cell death.* Toxicology, 2005. **209**(1): p. 1-14.
52. Ilhan, A., et al., *The effects of caffeic acid phenethyl ester (CAPE) on spinal cord ischemia/reperfusion injury in rabbits.* Eur J Cardiothorac Surg, 1999. **16**(4): p. 458-63.
53. Andrade-Silva, A.R., et al., *Effect of NFkappaB inhibition by CAPE on skeletal muscle ischemia-reperfusion injury.* J Surg Res, 2009. **153**(2): p. 254-62.
54. Saavedra-Lopes, M., et al., *The protective effect of CAPE on hepatic ischemia/reperfusion injury in rats.* J Surg Res, 2008. **150**(2): p. 271-7.
55. Ozyurt, H., et al., *Caffeic acid phenethyl ester (CAPE) protects rat skeletal muscle against ischemia-reperfusion-induced oxidative stress.* Vascul Pharmacol, 2007. **47**(2-3): p. 108-12.
56. Sud'ina, G.F., et al., *Caffeic acid phenethyl ester as a lipoxygenase inhibitor with antioxidant properties.* FEBS Lett, 1993. **329**(1-2): p. 21-4.
57. Deanfield, J.E., et al., *Medical treatment of myocardial ischemia in coronary artery disease: effect of drug regime and irregular dosing in the CAPE II trial.* J Am Coll Cardiol, 2002. **40**(5): p. 917-25.
58. Armagan, A., et al., *Caffeic acid phenethyl ester modulates methotrexate-induced oxidative stress in testes of rat.* Hum Exp Toxicol, 2008. **27**(7): p. 547-52.
59. Akyol, S., et al., *Caffeic acid phenethyl ester as a protective agent against nephrotoxicity and/or oxidative kidney damage: a detailed systematic review.* ScientificWorldJournal, 2014. **2014**: p. 561971.
60. Ulasli, S.S., et al., *Anticancer effects of thymoquinone, caffeic acid phenethyl ester and resveratrol on A549 non-small cell lung cancer cells exposed to benzo(a)pyrene.* Asian Pac J Cancer Prev, 2013. **14**(10): p. 6159-64.
61. Scapagnini, G., et al., *Caffeic acid phenethyl ester and curcumin: a novel class of heme oxygenase-1 inducers.* Mol Pharmacol, 2002. **61**(3): p. 554-61.
62. Ozturk, G., et al., *The anticancer mechanism of caffeic acid phenethyl ester (CAPE): review of melanomas, lung and prostate cancers.* Eur Rev Med Pharmacol Sci, 2012. **16**(15): p. 2064-8.
63. Perez-Alvarez, V., et al., *Dose-regimen dependent caffeic acid prevention of acute liver damage.* Proc West Pharmacol Soc, 1999. **42**: p. 17-8.
64. Uang, Y.S. and K.Y. Hsu, *A dose-dependent pharmacokinetic study on caffeic acid in rabbits after intravenous administration.* Biopharm Drug Dispos, 1997. **18**(8): p. 727-36.
65. Hwang, H.J., et al., *Inhibitory effects of caffeic acid phenethyl ester on cancer cell metastasis mediated by the down-regulation of matrix metalloproteinase*

expression in human HT1080 fibrosarcoma cells. J Nutr Biochem, 2006. **17**(5): p. 356-62.
66. Pramanik, K.C., et al., *Caffeic acid phenethyl ester suppresses melanoma tumor growth by inhibiting PI3K/AKT/XIAP pathway.* Carcinogenesis, 2013. **34**(9): p. 2061-70.
67. Roos, T.U., et al., *Caffeic acid phenethyl ester inhibits PDGF-induced proliferation of vascular smooth muscle cells via activation of p38 MAPK, HIF-1alpha, and heme oxygenase-1.* J Nat Prod, 2011. **74**(3): p. 352-6.
68. Kim, J.K. and H.D. Jang, *Nrf2-mediated HO-1 induction coupled with the ERK signaling pathway contributes to indirect antioxidant capacity of caffeic acid phenethyl ester in HepG2 cells.* Int J Mol Sci, 2014. **15**(7): p. 12149-65.
69. Cho, M.S., et al., *Caffeic acid phenethyl ester promotes anti-inflammatory effects by inhibiting MAPK and NF-kappaB signaling in activated HMC-1 human mast cells.* Pharm Biol, 2014. **52**(7): p. 926-32.
70. Atreya, I., R. Atreya, and M.F. Neurath, *NF-kappaB in inflammatory bowel disease.* J Intern Med, 2008. **263**(6): p. 591-6.
71. Okamoto, T. and A. Tsuchiya, *[NF-kappaB as a therapeutic target of rheumatoid arthritis]*. Nihon Rinsho Meneki Gakkai Kaishi, 2007. **30**(5): p. 383-9.
72. Shen, Y.C., J.C. Yen, and K.T. Liou, *Ameliorative effects of caffeic acid phenethyl ester on an eccentric exercise-induced skeletal muscle injury by down-regulating NF-kappab mediated inflammation.* Pharmacology, 2013. **91**(3-4): p. 219-28.
73. Ang, E.S., et al., *Caffeic acid phenethyl ester, an active component of honeybee propolis attenuates osteoclastogenesis and bone resorption via the suppression of RANKL-induced NF-kappaB and NFAT activity.* J Cell Physiol, 2009. **221**(3): p. 642-9.
74. Demestre, M., et al., *CAPE (caffeic acid phenethyl ester)-based propolis extract (Bio 30) suppresses the growth of human neurofibromatosis (NF) tumor xenografts in mice.* Phytother Res, 2009. **23**(2): p. 226-30.
75. Berger, N., et al., *Cytotoxicity of NF-kappaB inhibitors Bay 11-7085 and caffeic acid phenethyl ester to Ramos and other human B-lymphoma cell lines.* Exp Hematol, 2007. **35**(10): p. 1495-509.
76. Zhang, J., et al., *Synthesis and effects of new caffeic acid derivatives on nitric oxide production in lipopolysaccharide-induced RAW 264.7 macrophages.* Int J Clin Exp Med, 2014. **7**(4): p. 1022-7.
77. Jin, U.H., et al., *Caffeic acid phenethyl ester induces mitochondria-mediated apoptosis in human myeloid leukemia U937 cells.* Mol Cell Biochem, 2008. **310**(1-2): p. 43-8.
78. Fitzpatrick, L.R., J. Wang, and T. Le, *Caffeic acid phenethyl ester, an inhibitor of nuclear factor-kappaB, attenuates bacterial peptidoglycan polysaccharide-induced colitis in rats.* J Pharmacol Exp Ther, 2001. **299**(3): p. 915-20.

79. Son, S. and B.A. Lewis, *Free radical scavenging and antioxidative activity of caffeic acid amide and ester analogues: structure-activity relationship.* J Agric Food Chem, 2002. **50**(3): p. 468-72.
80. Suzuki, K., et al., *Drastic effect of several caffeic acid derivatives on the induction of heme oxygenase-1 expression revealed by quantitative real-time RT-PCR.* Biofactors, 2006. **28**(3-4): p. 151-8.
81. Reuland, D.J., et al., *Upregulation of phase II enzymes through phytochemical activation of Nrf2 protects cardiomyocytes against oxidant stress.* Free Radic Biol Med, 2013. **56**: p. 102-11.
82. Takeda, A., et al., *Increased expression of heme oxygenase mRNA in rat brain following transient forebrain ischemia.* Brain Res, 1994. **666**(1): p. 120-4.
83. Agarwal, A. and S. Bolisetty, *Adaptive responses to tissue injury: role of heme oxygenase-1.* Trans Am Clin Climatol Assoc, 2013. **124**: p. 111-22.
84. Poss, K.D. and S. Tonegawa, *Reduced stress defense in heme oxygenase 1-deficient cells.* Proc Natl Acad Sci U S A, 1997. **94**(20): p. 10925-30.
85. Maines, M.D., *Heme oxygenase: function, multiplicity, regulatory mechanisms, and clinical applications.* FASEB J, 1988. **2**(10): p. 2557-68.
86. Mishra, M. and J.F. Ndisang, *A critical and comprehensive insight on heme oxygenase and related products including carbon monoxide, bilirubin, biliverdin and ferritin in type-1 and type-2 diabetes.* Curr Pharm Des, 2014. **20**(9): p. 1370-91.
87. Hayashi, S., et al., *Characterization of rat heme oxygenase-3 gene. Implication of processed pseudogenes derived from heme oxygenase-2 gene.* Gene, 2004. **336**(2): p. 241-50.
88. Zhou, J.L., et al., *Change and role of heme oxygenase-1 in injured lungs following limb ischemia/reperfusion in rats.* Chin J Traumatol, 2004. **7**(3): p. 131-7.
89. Issan, Y., et al., *Heme oxygenase-1 induction improves cardiac function following myocardial ischemia by reducing oxidative stress.* PLoS One, 2014. **9**(3): p. e92246.
90. Zeng, Z., et al., *Contributions of heme oxygenase-1 in postconditioning-protected ischemia-reperfusion injury in rat liver transplantation.* Transplant Proc, 2011. **43**(7): p. 2517-23.
91. Wu, Y.D., et al., *[Heme oxygenase-1 gene transfer protects rat kidney transplant from ischemia/reperfusion injury].* Zhonghua Wai Ke Za Zhi, 2005. **43**(18): p. 1215-8.
92. Aztatzi-Santillan, E., et al., *The protective role of heme oxygenase-1 in cerebral ischemia.* Cent Nerv Syst Agents Med Chem, 2010. **10**(4): p. 310-6.
93. Fu, R., et al., *Expression of heme oxygenase-1 protein and messenger RNA in permanent cerebral ischemia in rats.* Neurol Res, 2006. **28**(1): p. 38-45.
94. Nakamichi, I., et al., *Hemin-activated macrophages home to the pancreas and protect from acute pancreatitis via heme oxygenase-1 induction.* J Clin Invest, 2005. **115**(11): p. 3007-14.

95. Devadas, K. and S. Dhawan, *Hemin activation ameliorates HIV-1 infection via heme oxygenase-1 induction.* J Immunol, 2006. **176**(7): p. 4252-7.
96. George, E.M., et al., *Induction of heme oxygenase 1 attenuates placental ischemia-induced hypertension.* Hypertension, 2011. **57**(5): p. 941-8.
97. Hsu, H.H., et al., *Simvastatin ameliorates established pulmonary hypertension through a heme oxygenase-1 dependent pathway in rats.* Respir Res, 2009. **10**: p. 32.
98. Botros, F.T., et al., *Induction of heme oxygenase-1 in renovascular hypertension is associated with inhibition of apoptosis.* Cell Mol Biol (Noisy-le-grand), 2007. **53**(4): p. 51-60.
99. Sun, J., et al., *Effects of natural products on ischemic heart diseases and cardiovascular system.* Acta Pharmacol Sin, 2002. **23**(12): p. 1142-51.
100. Huang, L., T. Su, and X. Li, *Natural products as sources of new lead compounds for the treatment of Alzheimer's disease.* Curr Top Med Chem, 2013. **13**(15): p. 1864-78.
101. Zhang, M.J., et al., *Uncarilic acid and secouncarilic acid, two new triterpenoids from Uucaria sessilifructus.* Molecules, 2013. **18**(8): p. 9727-34.
102. Hao, J., et al., *Synthesis and cytotoxicity evaluation of oleanolic acid derivatives.* Bioorg Med Chem Lett, 2013. **23**(7): p. 2074-7.
103. Honda, T., et al., *Design and synthesis of 2-cyano-3,12-dioxoolean-1,9-dien-28-oic acid, a novel and highly active inhibitor of nitric oxide production in mouse macrophages.* Bioorg Med Chem Lett, 1998. **8**(19): p. 2711-4.
104. Honda, T., et al., *Novel synthetic oleanane and ursane triterpenoids with various enone functionalities in ring A as inhibitors of nitric oxide production in mouse macrophages.* J Med Chem, 2000. **43**(9): p. 1866-77.
105. Honda, T., et al., *A novel dicyanotriterpenoid, 2-cyano-3,12-dioxooleana-1,9(11)-dien-28-onitrile, active at picomolar concentrations for inhibition of nitric oxide production.* Bioorg Med Chem Lett, 2002. **12**(7): p. 1027-30.
106. Honda, T., et al., *Synthetic oleanane and ursane triterpenoids with modified rings A and C: a series of highly active inhibitors of nitric oxide production in mouse macrophages.* J Med Chem, 2000. **43**(22): p. 4233-46.
107. Suh, N., et al., *A novel synthetic oleanane triterpenoid, 2-cyano-3,12-dioxoolean-1,9-dien-28-oic acid, with potent differentiating, antiproliferative, and anti-inflammatory activity.* Cancer Res, 1999. **59**(2): p. 336-41.
108. Liby, K., et al., *The synthetic triterpenoids, CDDO and CDDO-imidazolide, are potent inducers of heme oxygenase-1 and Nrf2/ARE signaling.* Cancer Res, 2005. **65**(11): p. 4789-98.
109. Konopleva, M., et al., *Novel triterpenoid CDDO-Me is a potent inducer of apoptosis and differentiation in acute myelogenous leukemia.* Blood, 2002. **99**(1): p. 326-35.
110. Wang, Y., et al., *A synthetic triterpenoid, 2-cyano-3,12-dioxooleana-1,9-dien-28-oic acid (CDDO), is a ligand for the peroxisome proliferator-activated receptor gamma.* Mol Endocrinol, 2000. **14**(10): p. 1550-6.

111. Wust, H.H., B. Janssen, and F. Frickel, *Biological properties and chemistry of some new retinoids.* Biochem Soc Trans, 1986. **14**(5): p. 933-6.
112. Jencks, W.P. and J. Carriuolo, *Imidazole catalysis. III. General base catalysis and the reactions of acetyl imidazole with thiols and amines.* J Biol Chem, 1959. **234**(5): p. 1280-5.
113. Jencks, W.P. and J. Carriuolo, *Imidazole catalysis. II. Acyl transfer and the reactions of acetyl imidazole with water and oxygen anions.* J Biol Chem, 1959. **234**(5): p. 1272-9.
114. Matt, T., *Transcriptional control of the inflammatory response: a role for the CREB-binding protein (CBP).* Acta Med Austriaca, 2002. **29**(3): p. 77-9.
115. Couch, R.D., et al., *Studies on the reactivity of CDDO, a promising new chemopreventive and chemotherapeutic agent: implications for a molecular mechanism of action.* Bioorg Med Chem Lett, 2005. **15**(9): p. 2215-9.
116. Ikeda, T., et al., *Triterpenoid CDDO-Im downregulates PML/RARalpha expression in acute promyelocytic leukemia cells.* Cell Death Differ, 2005. **12**(5): p. 523-31.
117. Ito, Y., et al., *The novel triterpenoid CDDO induces apoptosis and differentiation of human osteosarcoma cells by a caspase-8 dependent mechanism.* Mol Pharmacol, 2001. **59**(5): p. 1094-9.
118. Speranza, G., et al., *Phase I study of the synthetic triterpenoid, 2-cyano-3, 12-dioxoolean-1, 9-dien-28-oic acid (CDDO), in advanced solid tumors.* Cancer Chemother Pharmacol, 2012. **69**(2): p. 431-8.
119. Yang, C., et al., *Blockage of Stat3 with CDDO-Me inhibits tumor cell growth in chordoma.* Spine (Phila Pa 1976), 2010. **35**(18): p. 1668-75.
120. Townson, J.L., et al., *The synthetic triterpenoid CDDO-Imidazolide suppresses experimental liver metastasis.* Clin Exp Metastasis, 2011. **28**(3): p. 309-17.
121. Wang, Y.Y., H. Zhe, and R. Zhao, *Preclinical evidences toward the use of triterpenoid CDDO-Me for solid cancer prevention and treatment.* Mol Cancer, 2014. **13**: p. 30.
122. Deeb, D., et al., *CDDO-Me: A Novel Synthetic Triterpenoid for the Treatment of Pancreatic Cancer.* Cancers (Basel), 2010. **2**(4): p. 1779-93.
123. Kim, E.H., et al., *CDDO-imidazolide induces DNA damage, G2/M arrest and apoptosis in BRCA1-mutated breast cancer cells.* Cancer Prev Res (Phila), 2011. **4**(3): p. 425-34.
124. Sardina, J.L., et al., *CDDO-Im, an antitumor molecule that also improves platetet production.* Leuk Res, 2011. **35**(4): p. 427-8.
125. Reddy, N.M., et al., *The triterpenoid CDDO-imidazolide confers potent protection against hyperoxic acute lung injury in mice.* Am J Respir Crit Care Med, 2009. **180**(9): p. 867-74.
126. Sussan, T.E., et al., *Targeting Nrf2 with the triterpenoid CDDO-imidazolide attenuates cigarette smoke-induced emphysema and cardiac dysfunction in mice.* Proc Natl Acad Sci U S A, 2009. **106**(1): p. 250-5.

127. Eskiocak, U., et al., *CDDO-Me protects against space radiation-induced transformation of human colon epithelial cells.* Radiat Res, 2010. **174**(1): p. 27-36.
128. Pergola, P.E., et al., *Bardoxolone methyl and kidney function in CKD with type 2 diabetes.* N Engl J Med, 2011. **365**(4): p. 327-36.
129. Pergola, P.E., et al., *Effect of bardoxolone methyl on kidney function in patients with T2D and Stage 3b-4 CKD.* Am J Nephrol, 2011. **33**(5): p. 469-76.
130. Wu, Q.Q., et al., *Bardoxolone methyl (BARD) ameliorates ischemic AKI and increases expression of protective genes Nrf2, PPARgamma, and HO-1.* Am J Physiol Renal Physiol, 2011. **300**(5): p. F1180-92.
131. Liu, M., et al., *The Nrf2 triterpenoid activator, CDDO-imidazolide, protects kidneys from ischemia-reperfusion injury in mice.* Kidney Int, 2014. **85**(1): p. 134-41.
132. Gao, X., et al., *Synthetic oleanane triterpenoid, CDDO-Me, induces apoptosis in ovarian cancer cells by inhibiting prosurvival AKT/NF-kappaB/mTOR signaling.* Anticancer Res, 2011. **31**(11): p. 3673-81.
133. Yore, M.M., et al., *Proteomic analysis shows synthetic oleanane triterpenoid binds to mTOR.* PLoS One, 2011. **6**(7): p. e22862.
134. Wang, X., et al., *Cytoprotection of human endothelial cells against oxidative stress by 1-[2-cyano-3,12-dioxooleana-1,9(11)-dien-28-oyl]imidazole (CDDO-Im): application of systems biology to understand the mechanism of action.* Eur J Pharmacol, 2014. **734**: p. 122-31.
135. Nobel, D., *Music of Life: Biology Beyond Genes*. 2008: Oxford University Press.
136. Rothschuh, K.E., *[Rene Descartes and the theory of life phenomena]*. Sudhoffs Arch, 1966. **50**(1): p. 25-42.
137. Smut, J.C., *Holism and Evolution.* New York: Viking Press, 1926.
138. Hood, L., *A personal view of molecular technology and how it has changed biology.* J Proteome Res, 2002. **1**(5): p. 399-409.
139. Hood, L., *Systems biology: integrating technology, biology, and computation.* Mech Ageing Dev, 2003. **124**(1): p. 9-16.
140. Robb, H.J., *Chronic arterial ischemia.* J Mich State Med Soc, 1960. **59**: p. 1698-9.
141. Danforth, W.H., S. Naegle, and R.J. Bing, *Effect of ischemia and reoxygenation on glycolytic reactions and adenosine-triphosphate in heart muscle.* Circ Res, 1960. **8**: p. 965-71.
142. Boyle, E.M., Jr., et al., *Treating myocardial ischemia-reperfusion injury by targeting endothelial cell transcription.* Ann Thorac Surg, 1999. **68**(5): p. 1949-53.
143. Yi, H.Z., W.K. Wu, and C. Hou, *[Progress on research in preventing and treating the myocardial ischemia/reperfussion injury with Chinese herb medicine]*. Zhongguo Zhong Xi Yi Jie He Za Zhi, 1995. **15**(8): p. 509-11.
144. Hager, D. and A.M. Katz, *Treating cardiac ischemia: pathophysiologic guidelines.* Hosp Pract (Off Ed), 1987. **22**(6): p. 213-5, 218, 221-2.

145. Ma'ayan, A., et al., *Network analysis of FDA approved drugs and their targets.* Mt Sinai J Med, 2007. **74**(1): p. 27-32.
146. Visser, S.A., et al., *Implementation of quantitative and systems pharmacology in large pharma.* CPT Pharmacometrics Syst Pharmacol, 2014. **3**: p. e142.
147. Ideker, T., T. Galitski, and L. Hood, *A new approach to decoding life: systems biology.* Annu Rev Genomics Hum Genet, 2001. **2**: p. 343-72.
148. Ideker, T., J. Dutkowski, and L. Hood, *Boosting signal-to-noise in complex biology: prior knowledge is power.* Cell, 2011. **144**(6): p. 860-3.
149. Cowley, A.W., Jr., *The elusive field of systems biology.* Physiol Genomics, 2004. **16**(3): p. 285-6.
150. Barabasi, A.L. and Z.N. Oltvai, *Network biology: understanding the cell's functional organization.* Nat Rev Genet, 2004. **5**(2): p. 101-13.
151. Zhao, S. and S. Li, *Network-based relating pharmacological and genomic spaces for drug target identification.* PLoS One, 2010. **5**(7): p. e11764.
152. Zhao, S. and R. Iyengar, *Systems pharmacology: network analysis to identify multiscale mechanisms of drug action.* Annu Rev Pharmacol Toxicol, 2012. **52**: p. 505-21.
153. Berger, S.I. and R. Iyengar, *Network analyses in systems pharmacology.* Bioinformatics, 2009. **25**(19): p. 2466-72.
154. van der Graaf, P.H. and N. Benson, *Systems pharmacology: bridging systems biology and pharmacokinetics-pharmacodynamics (PKPD) in drug discovery and development.* Pharm Res, 2011. **28**(7): p. 1460-4.
155. Zhang, L., M. Pfister, and B. Meibohm, *Concepts and challenges in quantitative pharmacology and model-based drug development.* AAPS J, 2008. **10**(4): p. 552-9.
156. Van Der Graaf, P.H. and J. Gabrielsson, *Pharmacokinetic-pharmacodynamic reasoning in drug discovery and early development.* Future Med Chem, 2009. **1**(8): p. 1371-4.
157. Rogers, M., P. Lyster, and R. Okita, *NIH Support for the Emergence of Quantitative and Systems Pharmacology.* CPT Pharmacometrics Syst Pharmacol, 2013. **2**: p. e37.
158. Huber, W., et al., *Graphs in molecular biology.* BMC Bioinformatics, 2007. **8 Suppl 6**: p. S8.
159. Baitaluk, M., et al., *PathSys: integrating molecular interaction graphs for systems biology.* BMC Bioinformatics, 2006. **7**: p. 55.
160. Baker, E., et al., *Identifying common components across biological network graphs using a bipartite data model.* BMC Proc, 2014. **8**(Suppl 6 Proceedings of the Great Lakes Bioinformatics Confer): p. S4.
161. Ohta, J., *Connectivity matrix method for analyses of biological networks and its application to atom-level analysis of a model network of carbohydrate metabolism.* Syst Biol (Stevenage), 2006. **153**(5): p. 372-4.

162. Kuhnert, M.T., et al., *Identifying important nodes in weighted functional brain networks: a comparison of different centrality approaches.* Chaos, 2012. **22**(2): p. 023142.
163. Cucurull-Sanchez, L., K.G. Spink, and S.A. Moschos, *Relevance of systems pharmacology in drug discovery.* Drug Discov Today, 2012. **17**(13-14): p. 665-70.
164. Bates, S., *The role of gene expression profiling in drug discovery.* Curr Opin Pharmacol, 2011. **11**(5): p. 549-56.
165. Jenkins, S.L. and A. Ma'ayan, *Systems pharmacology meets predictive, preventive, personalized and participatory medicine.* Pharmacogenomics, 2013. **14**(2): p. 119-22.
166. Melas, I.N., K. Kretsos, and L.G. Alexopoulos, *Leveraging systems biology approaches in clinical pharmacology.* Biopharm Drug Dispos, 2013. **34**(9): p. 477-88.
167. Das, J., J. Mohammed, and H. Yu, *Genome-scale analysis of interaction dynamics reveals organization of biological networks.* Bioinformatics, 2012. **28**(14): p. 1873-8.
168. Sun, M.G. and P.M. Kim, *Evolution of biological interaction networks: from models to real data.* Genome Biol, 2011. **12**(12): p. 235.
169. Talalay, P., *Chemoprotection against cancer by induction of phase 2 enzymes.* Biofactors, 2000. **12**(1-4): p. 5-11.
170. Place, A.E., et al., *The novel synthetic triterpenoid, CDDO-imidazolide, inhibits inflammatory response and tumor growth in vivo.* Clin Cancer Res, 2003. **9**(7): p. 2798-2806.
171. Suh, N., et al., *A novel synthetic oleanane triterpenoid, 2-cyano-3,12-dioxoolean-1,9-dien-28-oic acid, with potent differentiating, antiproliferative, and anti-inflammatory activity.* Cancer Res, 1999. **59**(2): p. 336-341.
172. Ito, Y., et al., *The novel triterpenoid 2-cyano-3,12-dioxoolean-1,9-dien-28-oic acid induces apoptosis of human myeloid leukemia cells by a caspase-8-dependent mechanism.* Cell Growth Differ, 2000. **11**(5): p. 261-267.
173. Kim, K.B., et al., *Identification of a novel synthetic triterpenoid, methyl-2-cyano-3,12-dioxooleana-1,9-dien-28-oate, that potently induces caspase-mediated apoptosis in human lung cancer cells.* Mol Cancer Ther, 2002. **1**(3): p. 177-184.
174. Ma, Q., *Role of nrf2 in oxidative stress and toxicity.* Annu Rev Pharmacol Toxicol, 2013. **53**: p. 401-426.
175. Zhang, Y., et al., *Redox control of the survival of healthy and diseased cells.* Antioxid Redox Signal, 2011. **15**(11): p. 2867-2908.
176. Papaharalambus, C.A. and K.K. Griendling, *Basic mechanisms of oxidative stress and reactive oxygen species in cardiovascular injury.* Trends Cardiovasc Med, 2007. **17**(2): p. 48-54.
177. Salvemini, D. and S. Cuzzocrea, *Superoxide, superoxide dismutase and ischemic injury.* Curr Opin Investig Drugs, 2002. **3**(6): p. 886-895.

178. Uttara, B., et al., *Oxidative stress and neurodegenerative diseases: a review of upstream and downstream antioxidant therapeutic options.* Curr Neuropharmacol, 2009. **7**(1): p. 65-74.
179. Waris, G. and H. Ahsan, *Reactive oxygen species: role in the development of cancer and various chronic conditions.* J Carcinog, 2006. **5**: p. 14-14.
180. Heiss, E.H., et al., *Active NF-E2-related factor (Nrf2) contributes to keep endothelial NO synthase (eNOS) in the coupled state: role of reactive oxygen species (ROS), eNOS, and heme oxygenase (HO-1) levels.* J Biol Chem, 2009. **284**(46): p. 31579-31586.
181. Zhang, F., et al., *Pharmacological induction of heme oxygenase-1 by a triterpenoid protects neurons against ischemic injury.* Stroke, 2012. **43**(5): p. 1390-7.
182. Kalmar, B. and L. Greensmith, *Induction of heat shock proteins for protection against oxidative stress.* Adv Drug Deliv Rev, 2009. **61**(4): p. 310-318.
183. Schroder, M. and R.J. Kaufman, *The mammalian unfolded protein response.* Annu Rev Biochem, 2005. **74**: p. 739-789.
184. Jakob, U., et al., *Chaperone activity with a redox switch.* Cell, 1999. **96**(3): p. 341-352.
185. Calabrese, V., et al., *Redox regulation in neurodegeneration and longevity: role of the heme oxygenase and HSP70 systems in brain stress tolerance.* Antioxid Redox Signal, 2004. **6**(5): p. 895-913.
186. Saleh, A., et al., *Negative regulation of the Apaf-1 apoptosome by Hsp70.* Nat Cell Biol, 2000. **2**(8): p. 476-483.
187. Malhotra, V. and H.R. Wong, *Interactions between the heat shock response and the nuclear factor-kappaB signaling pathway.* Crit Care Med, 2002. **30**(1 Supp): p. 89-89.
188. Wang, X., Bynum, J.A. Stavchansky, S.A. Bowman, P.D., *Cytoprotection of human endothelial cells against oxidative stress by 2-Cyano-3,12-dioxooleana-1,9-dien-28-imidazolide (CDDO-Im): Application of systems biology to understand the mechanism of action.* European Journal of Pharmacology, 2014. **in press**.
189. Kulkarni, A.A., et al., *The triterpenoid CDDO-Me inhibits bleomycin-induced lung inflammation and fibrosis.* PLoS One, 2013. **8**(5): p. e63798.
190. Sussan, T.E., et al., *Targeting Nrf2 with the triterpenoid CDDO-imidazolide attenuates cigarette smoke-induced emphysema and cardiac dysfunction in mice.* 2009. **106**(1): p. 250-255.
191. Reisman, S.A., et al., *CDDO-Im protects from acetaminophen hepatotoxicity through induction of Nrf2-dependent genes.* Toxicol Appl Pharmacol, 2009. **236**(1): p. 109-14.
192. Deeb, D., et al., *Inhibition of Telomerase Activity by Oleanane Triterpenoid CDDO-Me in Pancreatic Cancer Cells is ROS-Dependent.* Molecules, 2013. **18**(3): p. 3250-3265.

193. Kim, E.H., et al., *CDDO-Imidazolide Induces DNA Damage, G2/M Arrest and Apoptosis in BRCA1-Mutated Breast Cancer Cells.* Cancer Prevention Research, 2011. **4**(3): p. 425-434.
194. Speranza, G., et al., *Phase I study of the synthetic triterpenoid, 2-cyano-3, 12-dioxoolean-1, 9-dien-28-oic acid (CDDO), in advanced solid tumors.* Cancer Chemotherapy and Pharmacology, 2011. **69**(2): p. 431-438.
195. Dinkova-Kostova, A.T., et al., *Extremely potent triterpenoid inducers of the phase 2 response: correlations of protection against oxidant and inflammatory stress.* Proc Natl Acad Sci U S A, 2005. **102**(12): p. 4584-9.
196. Graber, D.J., et al., *Synthetic Triterpenoid CDDO Derivatives Modulate Cytoprotective or Immunological Properties in Astrocytes, Neurons, and Microglia.* Journal of Neuroimmune Pharmacology, 2010. **6**(1): p. 107-120.
197. Thimmulappa, R.K., et al., *Preclinical evaluation of targeting the Nrf2 pathway by triterpenoids (CDDO-Im and CDDO-Me) for protection from LPS-induced inflammatory response and reactive oxygen species in human peripheral blood mononuclear cells and neutrophils.* Antioxid Redox Signal, 2007. **9**(11): p. 1963-70.
198. Grosser, M., et al., *Gene expression analysis of HUVEC in response to TF-binding.* Thromb Res, 2011. **127**(3): p. 259-63.
199. Breen, L.T., P.E. McHugh, and B.P. Murphy, *HUVEC ICAM-1 and VCAM-1 synthesis in response to potentially athero-prone and athero-protective mechanical and nicotine chemical stimuli.* Ann Biomed Eng, 2010. **38**(5): p. 1880-92.
200. Miro, X., et al., *Phosphodiesterases 4D and 7A splice variants in the response of HUVEC cells to TNF-alpha(1).* Biochem Biophys Res Commun, 2000. **274**(2): p. 415-21.
201. Marchionatti, A.M., et al., *Mitochondrial dysfunction is responsible for the intestinal calcium absorption inhibition induced by menadione.* Biochim Biophys Acta, 2008. **1780**(2): p. 101-7.
202. Criddle, D.N., et al., *Menadione-induced reactive oxygen species generation via redox cycling promotes apoptosis of murine pancreatic acinar cells.* J Biol Chem, 2006. **281**(52): p. 40485-92.
203. Chen, Q., et al., *Oxidative DNA damage and senescence of human diploid fibroblast cells.* Proc Natl Acad Sci U S A, 1995. **92**(10): p. 4337-41.
204. Packer, L. and K. Fuehr, *Low oxygen concentration extends the lifespan of cultured human diploid cells.* Nature, 1977. **267**(5610): p. 423-5.
205. Anoopkumar-Dukie, S., et al., *Resazurin assay of radiation response in cultured cells.* Br J Radiol, 2005. **78**(934): p. 945-7.
206. Gao, X., A.T. Dinkova-Kostova, and P. Talalay, *Powerful and prolonged protection of human retinal pigment epithelial cells, keratinocytes, and mouse leukemia cells against oxidative damage: the indirect antioxidant effects of sulforaphane.* Proc Natl Acad Sci U S A, 2001. **98**(26): p. 15221-6.

207. Nieminen, A.L., et al., *A novel cytotoxicity screening assay using a multiwell fluorescence scanner.* Toxicol Appl Pharmacol, 1992. **115**(2): p. 147-55.
208. Fleige, S., et al., *Comparison of relative mRNA quantification models and the impact of RNA integrity in quantitative real-time RT-PCR.* Biotechnol Lett, 2006. **28**(19): p. 1601-13.
209. Simon, R., et al., *Analysis of gene expression data using BRB-ArrayTools.* Cancer Inform, 2007. **3**: p. 11-7.
210. Eisen, M.B., et al., *Cluster analysis and display of genome-wide expression patterns.* Proc Natl Acad Sci U S A, 1998. **95**(25): p. 14863-8.
211. Saldanha, A.J., *Java Treeview--extensible visualization of microarray data.* Bioinformatics, 2004. **20**(17): p. 3246-8.
212. Montojo, J., et al., *GeneMANIA Cytoscape plugin: fast gene function predictions on the desktop.* Bioinformatics, 2010. **26**(22): p. 2927-8.
213. Mostafavi, S., et al., *GeneMANIA: a real-time multiple association network integration algorithm for predicting gene function.* Genome Biol, 2008. **9 Suppl 1**: p. S4.
214. Zuberi, K., et al., *GeneMANIA prediction server 2013 update.* Nucleic Acids Res, 2013. **41**(Web Server issue): p. W115-22.
215. Anderson, K.E., et al., *Tissue distribution and disposition of tin-protoporphyrin, a potent competitive inhibitor of heme oxygenase.* The Journal of pharmacology and experimental therapeutics, 1984. **228**(2): p. 327-333.
216. Drummond, G.S. and A. Kappas, *Prevention of neonatal hyperbilirubinemia by tin protoporphyrin IX, a potent competitive inhibitor of heme oxidation.* Proceedings of the National Academy of Sciences of the United States of America, 1981. **78**(10): p. 6466-6470.
217. Baker, G.L., R.J. Corry, and A.P. Autor, *Oxygen free radical induced damage in kidneys subjected to warm ischemia and reperfusion. Protective effect of superoxide dismutase.* Ann Surg, 1985. **202**(5): p. 628-41.
218. Walker, L.M., et al., *Oxidative stress and reactive nitrogen species generation during renal ischemia.* Toxicol Sci, 2001. **63**(1): p. 143-8.
219. Honda, T., et al., *A novel dicyanotriterpenoid, 2-cyano-3,12-dioxooleana-1,9(11)-dien-28-onitrile, active at picomolar concentrations for inhibition of nitric oxide production.* Bioorganic & Medicinal Chemistry Letters, 2002. **12**(7): p. 1027-1030.
220. Honda, T., et al., *Novel synthetic oleanane triterpenoids: a series of highly active inhibitors of nitric oxide production in mouse macrophages.* Bioorganic & Medicinal Chemistry Letters, 1999. **9**(24): p. 3429-3434.
221. Honda, T., et al., *Design and synthesis of 2-cyano-3,12-dioxoolean-1,9-dien-28-oic acid, a novel and highly active inhibitor of nitric oxide production in mouse macrophages.* Bioorganic & Medicinal Chemistry Letters, 1998. **8**(19): p. 2711-2714.

222. Place, A.E., et al., *The novel synthetic triterpenoid, CDDO-imidazolide, inhibits inflammatory response and tumor growth in vivo.* Clin Cancer Res, 2003. **9**(7): p. 2798-806.
223. Kim, E.H., et al., *CDDO-methyl ester delays breast cancer development in BRCA1-mutated mice.* Cancer Prev Res (Phila), 2012. **5**(1): p. 89-97.
224. Liu, M., et al., *Transcription factor Nrf2 is protective during ischemic and nephrotoxic acute kidney injury in mice.* Kidney Int, 2009. **76**(3): p. 277-85.
225. Ma'ayan, A., *Introduction to network analysis in systems biology.* Sci Signal, 2011. **4**(190): p. tr5.
226. Yates, M.S., et al., *Pharmacodynamic characterization of chemopreventive triterpenoids as exceptionally potent inducers of Nrf2-regulated genes.* Mol Cancer Ther, 2007. **6**(1): p. 154-62.
227. Lee, S.C., et al., *Induction of heme oxygenase-1 protects against podocyte apoptosis under diabetic conditions.* Kidney Int, 2009. **76**(8): p. 838-48.
228. Liang, O.D., et al., *Mesenchymal stromal cells expressing heme oxygenase-1 reverse pulmonary hypertension.* Stem Cells, 2011. **29**(1): p. 99-107.
229. Liby, K., et al., *The synthetic triterpenoids, CDDO and CDDO-imidazolide, are potent inducers of heme oxygenase-1 and Nrf2/ARE signaling.* Cancer Research, 2005. **65**(11): p. 4789-4798.
230. Liu, J., et al., *Nrf2 protection against liver injury produced by various hepatotoxicants.* Oxid Med Cell Longev, 2013. **2013**: p. 305861.
231. Chin, M., et al., *Bardoxolone methyl analogs RTA 405 and dh404 are well tolerated and exhibit efficacy in rodent models of Type 2 diabetes and obesity.* AJP: Renal Physiology, 2013. **304**(12): p. F1438-F1446.
232. Wasserberg, N., et al., *Heme oxygenase-1 upregulation protects against intestinal ischemia/reperfusion injury: a laboratory based study.* Int J Surg, 2007. **5**(4): p. 216-24.
233. Jozkowicz, A., et al., *Heme oxygenase and angiogenic activity of endothelial cells: stimulation by carbon monoxide and inhibition by tin protoporphyrin-IX.* Antioxid Redox Signal, 2003. **5**(2): p. 155-62.
234. Sardana, M.K. and A. Kappas, *Dual control mechanism for heme oxygenase: tin(IV)-protoporphyrin potently inhibits enzyme activity while markedly increasing content of enzyme protein in liver.* Proc Natl Acad Sci U S A, 1987. **84**(8): p. 2464-8.
235. Xing, Y., et al., *Triterpenoid dihydro-CDDO-trifluoroethyl amide protects against maladaptive cardiac remodeling and dysfunction in mice: a critical role of Nrf2.* PLoS One, 2012. **7**(9): p. e44899.
236. Hensen, S.M., et al., *Activation of the antioxidant response in methionine deprived human cells results in an HSF1-independent increase in HSPA1A mRNA levels.* Biochimie, 2013. **95**(6): p. 1245-51.
237. Sasi, B.K., et al., *Coordinated transcriptional regulation of Hspa1a gene by multiple transcription factors: crucial roles for HSF-1, NF-Y, NF-kappaB, and CREB.* J Mol Biol, 2014. **426**(1): p. 116-35.

238. Han, J., et al., *Expression of bbc3, a pro-apoptotic BH3-only gene, is regulated by diverse cell death and survival signals.* Proc Natl Acad Sci U S A, 2001. **98**(20): p. 11318-23.
239. Reimertz, C., et al., *Gene expression during ER stress-induced apoptosis in neurons: induction of the BH3-only protein Bbc3/PUMA and activation of the mitochondrial apoptosis pathway.* J Cell Biol, 2003. **162**(4): p. 587-97.
240. Hopkins, A.L., *Network pharmacology: the next paradigm in drug discovery.* Nat Chem Biol, 2008. **4**(11): p. 682-90.
241. Wist, A.D., S.I. Berger, and R. Iyengar, *Systems pharmacology and genome medicine: a future perspective.* Genome Med, 2009. **1**(1): p. 11.
242. Bynum, J.A., Rastogi, Ashish, Stavchansky, Salomon A., Bowman, Phillip D., *Cytoprotection of Human Endothelial Cells from Oxidant Stress with CDDO Derivatives:*
Network Analysis of Genes Responsible for Cytoprotection and Differences in Mechanism of Action. European Journal of Pharmacology, 2014.
243. Bynum, J.A., Rastogi, Ashish, Stavchansky, Salomon A., Bowman, Phillip D, *Cytoprotection of Human Endothelial Cells from Oxidant Stress with CDDO Derivatives: Network Analysis of Genes Responsible for Cytoprotection and Differences in Mechanism of Action.* . European Journal of Pharmacology, In Press.
244. Pronk, T.E., et al., *Comparison of the molecular topologies of stress-activated transcription factors HSF1, AP-1, NRF2, and NF-kappaB in their induction kinetics of HMOX1.* Biosystems, 2014. **124C**: p. 75-85.
245. Chen, E.Y., et al., *Expression2Kinases: mRNA profiling linked to multiple upstream regulatory layers.* Bioinformatics, 2012. **28**(1): p. 105-11.
246. Bai, J.P., et al., *Strategic applications of gene expression: from drug discovery/development to bedside.* AAPS J, 2013. **15**(2): p. 427-37.
247. Rowell, J., et al., *Dynamic Gene Expression Patterns in Animal Models of Early and Late Heart Failure Reveal Biphasic-Bidirectional Transcriptional Activation of Signaling Pathways.* Physiol Genomics, 2014.
248. Iyer, V.R., et al., *The transcriptional program in the response of human fibroblasts to serum.* Science, 1999. **283**(5398): p. 83-7.
249. Huang, S., *Gene expression profiling, genetic networks, and cellular states: an integrating concept for tumorigenesis and drug discovery.* J Mol Med (Berl), 1999. **77**(6): p. 469-80.
250. Dave, S., et al., *Nuclear MEK1 sequesters PPARgamma and bisects MEK1/ERK signaling: a non-canonical pathway of retinoic acid inhibition of adipocyte differentiation.* PLoS One, 2014. **9**(6): p. e100862.
251. Greulich, H. and R.L. Erikson, *An analysis of Mek1 signaling in cell proliferation and transformation.* J Biol Chem, 1998. **273**(21): p. 13280-8.
252. Pearson, G., et al., *Uncoupling Raf1 from MEK1/2 impairs only a subset of cellular responses to Raf activation.* J Biol Chem, 2000. **275**(48): p. 37303-6.

253. Kidambi, S., et al., *Propofol induces MAPK/ERK cascade dependant expression of cFos and Egr-1 in rat hippocampal slices.* BMC Res Notes, 2010. **3**: p. 201.
254. Zhang, L., et al., *Curcumin produces antidepressant effects via activating MAPK/ERK-dependent brain-derived neurotrophic factor expression in the amygdala of mice.* Behav Brain Res, 2012. **235**(1): p. 67-72.
255. Besnard, A., S. Laroche, and J. Caboche, *Comparative dynamics of MAPK/ERK signalling components and immediate early genes in the hippocampus and amygdala following contextual fear conditioning and retrieval.* Brain Struct Funct, 2014. **219**(1): p. 415-30.
256. Fischer, A., et al., *Glucocorticoids regulate barrier function and claudin expression in intestinal epithelial cells via MKP-1.* Am J Physiol Gastrointest Liver Physiol, 2014. **306**(3): p. G218-28.
257. Chi, H., et al., *Dynamic regulation of pro- and anti-inflammatory cytokines by MAPK phosphatase 1 (MKP-1) in innate immune responses.* Proc Natl Acad Sci U S A, 2006. **103**(7): p. 2274-9.
258. Casteel, M., et al., *Impact of DUSP1 on the apoptotic potential of deoxynivalenol in the epithelial cell line HepG2.* Toxicol Lett, 2010. **199**(1): p. 43-50.
259. Hammer, M., et al., *Dual specificity phosphatase 1 (DUSP1) regulates a subset of LPS-induced genes and protects mice from lethal endotoxin shock.* J Exp Med, 2006. **203**(1): p. 15-20.
260. Hammer, M., et al., *Control of dual-specificity phosphatase-1 expression in activated macrophages by IL-10.* Eur J Immunol, 2005. **35**(10): p. 2991-3001.
261. Rastogi, R., et al., *Rapamycin induces mitogen-activated protein (MAP) kinase phosphatase-1 (MKP-1) expression through activation of protein kinase B and mitogen-activated protein kinase kinase pathways.* J Biol Chem, 2013. **288**(47): p. 33966-77.
262. Xiao, Y.Q., et al., *Cross-talk between ERK and p38 MAPK mediates selective suppression of pro-inflammatory cytokines by transforming growth factor-beta.* J Biol Chem, 2002. **277**(17): p. 14884-93.

VITA

Jim enrolled at the University of Texas A&M shortly after graduating high school in 1992. In 1995, he transferred to the University of Texas at San Antonio where he received the degree of Bachelor of Science in Biology in 1998. During the following years, Jim was employed in various research positions including research associate at the Southwest Foundation for Biomedical Research and Lab Manager at the Audie L. Murphy Veterans Hospital. In April 2003, he joined the US Army-Institute of Surgical Reseach (now Battlefield Health and Trauma Center) at San Antonio Military Medical Center (SAMMC) as a research biologist under the supervision of Dr. Phillip Bowman. During his time at SAMMC he has been involved in molecular and cell biology projects focused on battlefield-related trauma. Throughout his years in research he has been an author of several publications and presented his research at different regional and international conferences. He has collaborated on numerous projects including work with Dr. Salomon Stavchansky at the University of Texas at Austin College of Pharmacy in the area of drug discovery and development for treatment of ischemia/reperfusion injury. In 2012, Jim entered the Ph.D. program in the pharmaceutics division of the College of Pharmacy at the University of Texas at Austin under the supervision of Dr. Salomon Stavchansky. He has been awarded graduate fellowships from the College of Pharmacy since 2012. During his graduate studies, Jim has presented work at several national scientific meetings, has published two manuscripts and has an additional manuscript submitted for publication.

Email contact – james.bynum@utexas.edu

This dissertation was typed by the author